CALIFORNIA STATE POLYTECHNIC UNIVERSITY, POMONA
THESIS ELECTRONIC SIGNATURE PAGE

Submitted: Term Fall Year 2021
Bronco ID: 010418369
Email Address: alyoung@cpp.edu

THESIS INFORMATION

THESIS TITLE	Investigation of Anomalous Sulfate Concentrations Within the San Antonio Canyon
AUTHOR	Alyssa Young
PROGRAM	Geology, M.S.

SIGNATURES

Jonathan Nourse
Committee Chair Name
Thesis Committee Chair
Position
Geological Sciences
Department
Organization

DocuSigned by: Jonathan Nourse 562E96F6E80E44B...
Signature 12/14/2021
janourse@cpp.edu
Email

Stephen Osborn
Committee Member 2 Name
Thesis Committee Member
Position
Geological Sciences
Department
Organization

DocuSigned by: Stephen Osborn B1E6BFB18441457...
Signature 12/14/2021
sgosborn@cpp.edu
Email

Nicholas Van Buer
Committee Member 3 Name
Thesis Committee Member
Position
Geological Sciences
Department
Organization

DocuSigned by: ED2E989A7B2A47B...
Signature 12/14/2021
njvanbuer@cpp.edu
Email

Upload Thesis Attachment:

INVESTIGATION OF ANOMALOUS SULFATE CONCENTRATIONS WITHIN THE SAN ANTONIO CANYON WATERSHED, SAN GABRIEL MOUNTAINS, CALIFORNIA

A Thesis

Presented to the

Faculty of

California State Polytechnic University, Pomona

In Partial Fulfillment

Of the Requirements for the Degree

Master of Science

In

Geological Sciences

By

Alyssa L. Young

2021

Signature Page

Thesis:	INVESTIGATION OF ANOMALOUS SULFATE CONCENTRATIONS WITHIN THE SAN ANTONIO CANYON WATERSHED OF THE SAN GABRIEL MOUNTAINS, CALIFORNIA
Author:	Alyssa L. Young
Date Submitted:	Fall 2021
	Department of Geological Sciences

Dr. Jon Nourse
Thesis Committee Chair
Department Chair of Geological Sciences _____

Dr. Stephen Osborn
Professor of Geological Sciences _____

Dr. Nick Van Buer
Associate Professor of Geological Sciences _____

ACKNOWLEDGMENTS

I would like to thank my advisors, Dr. Jon Nourse, Dr. Stephen Osborn, and Dr. Nick Van Buer, for giving me this opportunity to work on this project and for providing their knowledge and advice. We would like to thank Dr. Osborn for the use of his hydrogeology lab and IC, UCR for the use of their hydrogeology lab and ICP-OES, CPP for the use of their geology lab, and WSU for the use of their GeoAnalytical Lab and XRF. We would also like to thank past and present Cal Poly students, faculty, the Los Angeles Department of Public Works, and the San Bernardino County Department of Public Works for their assistance and for providing the much-needed data, research, and maps. I would like to thank my mom, Stephanie, for driving me everywhere I needed to go and for assisting in my fieldwork by taking pictures, GPS coordinates, and providing advice. I would also like to thank the residents in the Mt. Baldy area and the Barrett-Stoddard cabin community for their knowledge of the area.

ABSTRACT

The objective of this research is to analyze various streams and springs, as well as local rocks, to deduce the source of these anomalous concentrations of sulfate in surface waters of San Antonio Canyon Watershed of the eastern San Gabriel Mountains. Canyons of interest include the main San Antonio Canyon, along with some of its tributaries: Evey Canyon, North and South forks of Barrett Canyon, and Cascade Canyon. In the past, sulfate has been as high as 1,706 mg/L in Cascade Canyon (Yaralian, 2017).

Water samples were collected bi-weekly from November 2018 to August 2019, although some sites were intermittent or ephemeral, flowing only during the wet season or right after a storm event. Water samples were analyzed for alkalinity, pH, oxidation-reduction potential, and concentrations of anions (IC, at CPP) and cations (ICP-OES, at UC Riverside). Current results show sulfate as high as 836 mg/L in Cascade Canyon, with elevated values of 164 mg/L and 58 mg/L in Barrett and Evey canyons, respectively, which exceeds background values of 25 - 30mg/L. Water quality data from past research by alumni and faculty are also included in this study, as well as precipitation records from 2017 to 2020. Most samples appear to exhibit seasonal fluctuations in sulfate concentration, with a decrease during the wet season and an increase during the dry season.

Sulfate in water systems has three potential sources: the decomposition of organic matter via microbes, precipitation from environmentally impacted areas, and groundwater interaction with local geology. The latter source is hypothesized to play a more significant role, due to the abundance of hematite- and limonite-stained, hydrothermally

altered, and mineralized sulfur-odorous bedrock in the headwaters of Cascade and Barrett canyons. Spring Hill landslide is of special interest as it contributes groundwater to the Barrett and Cascade watersheds, and sulfur-bearing horizons are locally exposed. The most ubiquitous sulfide mineral present in the area is pyrite, which releases high amounts of sulfate and iron as it weathers.

We analyzed local rock samples on the XRF to supplement the water data and narrow down the sulfate source to a specific area or rock unit. Although the water supply is regularly tested by cabin owners in North Fork Barrett Canyon, this study is imperative to the residents who tap directly from the local streams and springs, and recreation visitors or animals that drink from the water.

TABLE OF CONTENTS

LIST OF TABLES

LIST OF FIGURES

INTRODUCTION

Purpose and Objectives

Sulfate concentrations in most natural waters range from about 3 - 30 mg/L, with concentrations of about 10mg/L or more possibly correlating with environmentally impacted areas (EPA, 2003). The secondary drinking water standard for sulfate in California is 250 mg/L (EPA, 2019). Past sulfate concentrations measured in San Antonio Canyon watershed ranged from about 25 - 38 mg/L (Soto, 2017) to 1,706 mg/L (Yaralian, 2017). The purpose of this project is to identify the source of elevated sulfate within the watershed; more specifically, the general source location, and if the sulfate anomaly is associated with a specific rock unit or group of units or an anthropogenic contaminant source. The amount of publicly available water quality and geochemical data concerning the San Antonio Canyon Watershed is insufficient to fully understand the sources and concentrations of sulfur as sulfate in the area. To fill this knowledge gap, my project has the following objectives: 1) Systematically collect surface water samples over a large area during wet and dry seasons; 2) Measure sulfate concentrations and other important water quality parameters within the water samples, 3) Collect representative rock samples for XRF analysis, and 4) Analyze the spatial and temporal distribution of the results.

Location of Study Area

The San Antonio Canyon Watershed lies in the eastern San Gabriel Mountains, with Claremont and Rancho Cucamonga to the south and Mt. San Antonio (also called Mt. Baldy) to the north (Figures 1 and 2). The watershed is about sixty-six km^2 (26 mi^2) and the main trunk stream is San Antonio Creek, which is about 31 km (19 mi) long and is one of several major streams in Las Angeles County. It discharges into the Chino Creek and then into the Santa Ana River. Many residents live within the watershed, either in Icehouse Canyon, Mt. Baldy Village, Barrett Canyon cabin community, or near the base of the watershed.

The San Antonio Canyon is the largest drainage in the watershed and includes many smaller tributary canyons, including Icehouse Canyon, North Fork Barrett Canyon, South Fork Barrett Canyon, Cascade Canyon, Spruce Canyon, and Evey Canyon (Figures 3-4). For ease of analysis and discussion, three smaller areas of investigation were sectioned off within the entire study area, labeled as Area 1, Area 2, and Area 3 (Figure 2). This allows us to view the sulfate concentrations across various parts of the watershed and to observe any possible seasonal fluctuations throughout the year.

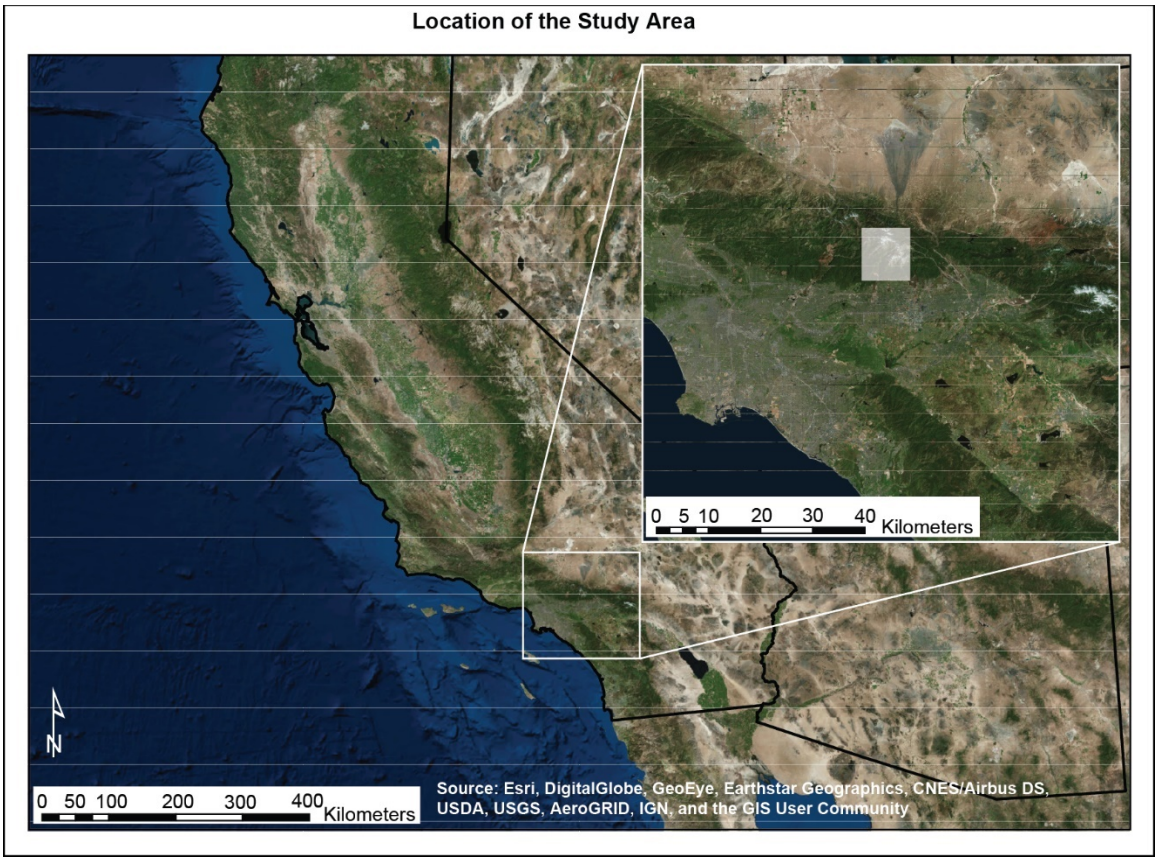

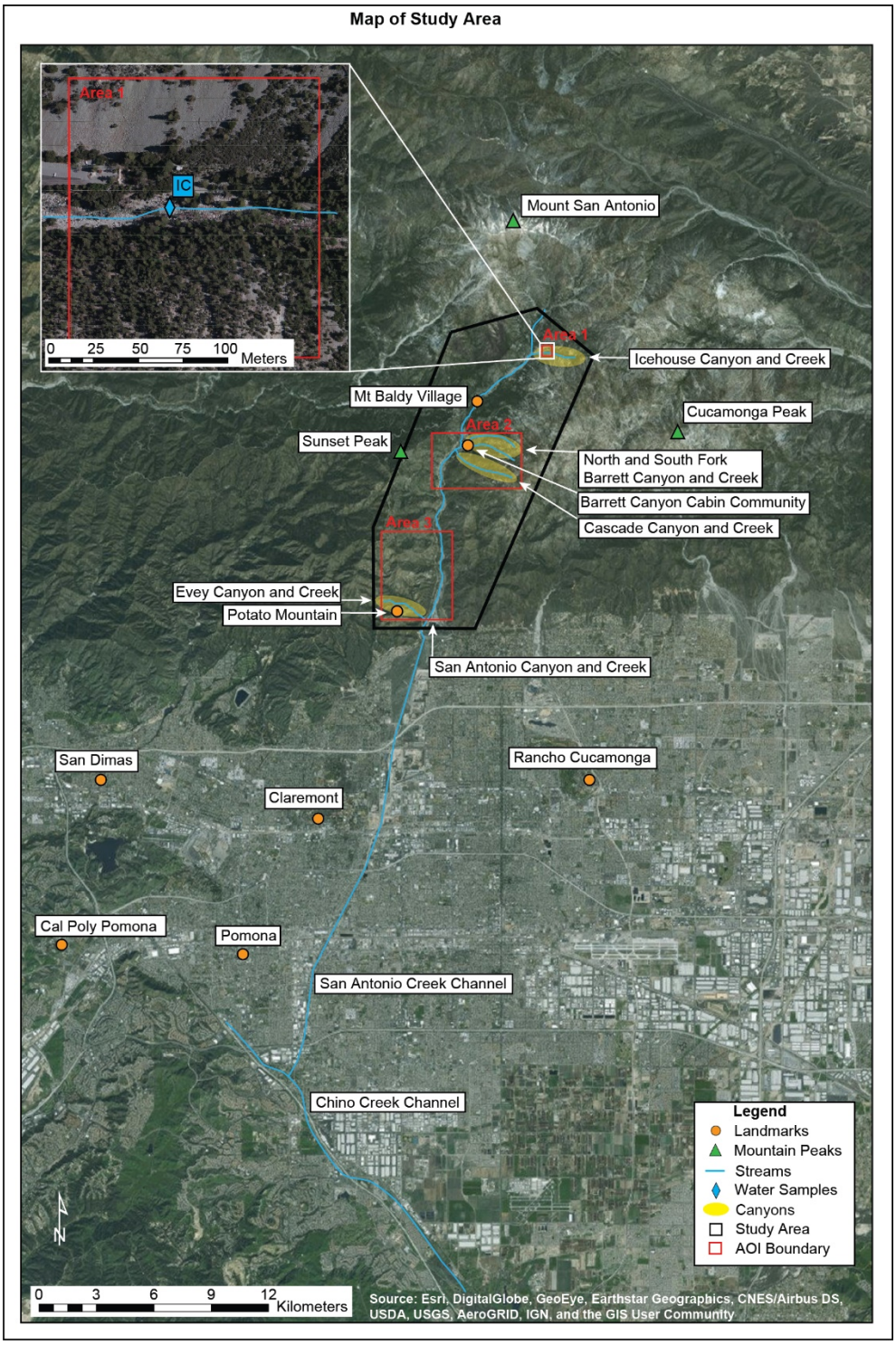

Figure 2: *Map of the study area (opaque white box from Figure 1) with boundary (black polygon), three areas of investigation or AOI (red rectangles), landmarks (orange circles), mountain peaks (green triangles), streams and channels (green lines), water samples (blue diamonds), rock samples (yellow diamonds), and canyons (yellow ellipses). San Antonio Canyon is labeled but does not have a yellow marker as it would interfere visually with the other canyon markers. An inset of Area 1 is included due to its small size. See Appendix G for an additional figure showing the Santa Ana River Drainage Basin.*

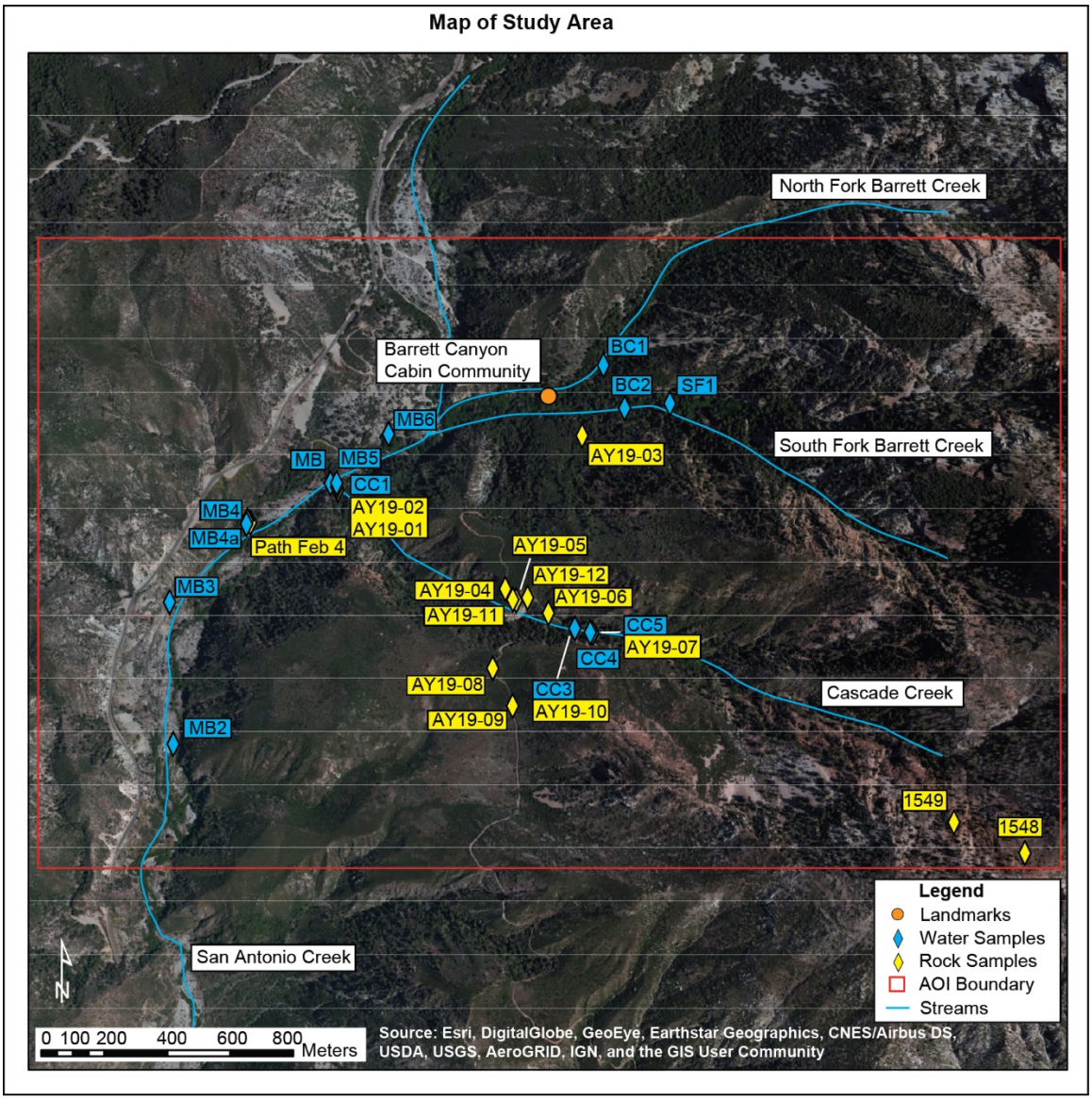

Figure 3: *Map of Area 2 showing landmarks (orange circles), streams (blue lines), water samples (blue diamonds), rock samples (yellow diamonds).*

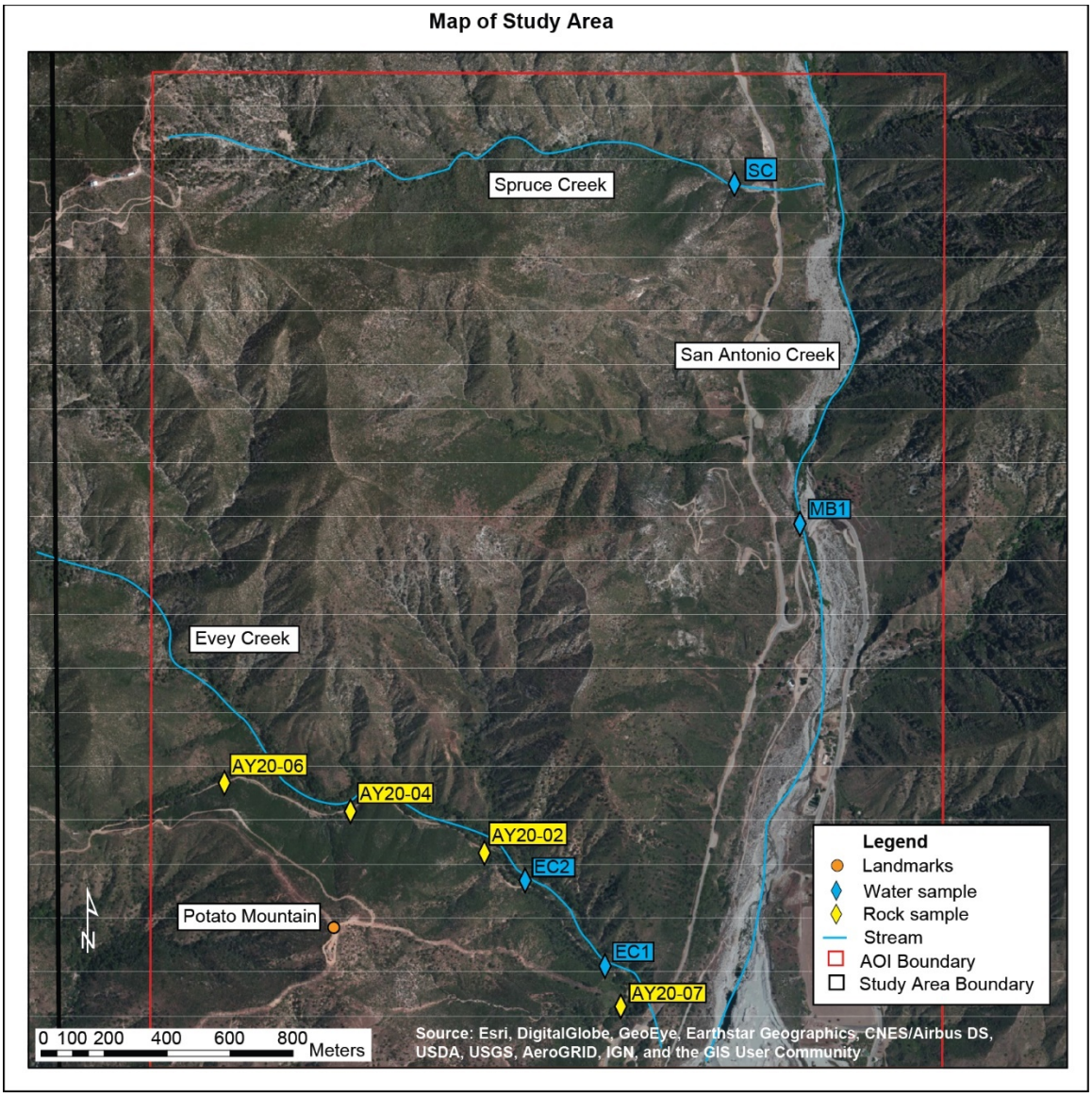

Figure 4: *Map of Area 3 showing landmarks (orange circles), streams (blue lines) water samples (blue diamonds), rock samples (yellow diamonds). Use blue line to show Evey creek and San Antonio creek. Potato Mountain.*

As shown in Figure 2, Area 1 is located in the uppermost watershed and includes Icehouse Canyon (IC) sample sites. Area 2 is located in the mid-upper watershed and includes sample sites at Silver Falls (SF), North Fork Barrett Canyon (BC1), South Fork Barrett Canyon (BC2), Hogback Spring (MB6), north of the Gaging Station U15-R (MB), Gaging Station U15R (MB5), Cascade Canyon mouth (CC1), upper Cascade Canyon (CC3, CC4, and CC5), the pond and nearby stream (MB4 and MB4a, respectively), the spring south of the pond (MB3), and Sierra Powerhouse (MB2) along the San Antonio Creek. Area 3 is located in the lower watershed and includes the Spruce Canyon (SC), San Antonio Stream/Shinn Rd. (MB1), and lower and upper Evey Canyon (EC2 and EC1, respectively) samples. For ease of communication, the common sample site names (e.g., Hogback Spring, upper Cascade Canyon, Sierra Powerhouse, etc.) will be used, unless exact names are required.

Importance of Water Quality Study in San Antonio Canyon

Understanding the source of the elevated sulfate or other dissolved constituents within the watershed may also impact water resource management. The area is used extensively for residential and recreational uses, with several different hiking trails and campgrounds to choose from. Nearby streams and springs are a source of water for visitors, residents, and the local biota. Many hikers will also refrain from picking up after their pets, which can introduce bacteria or other waste products into the water supply.

Access to clean water is an essential need, and due to its frequency of use, is imperative to not only to those who live within the study area, but also everyone

downgradient within the Santa Ana drainage basin. Water quality is important because the quality of one area may potentially impact the water downgradient.

The main residential areas within the San Antonio Canyon Watershed include lower Icehouse Canyon, Barrett Canyon Cabin Community, Mt. Baldy Village, and the lower watershed area. There are about 36 cabins within the Barrett Canyon Cabin Community (Gray, 2000), many of which obtain their water directly from local streams via pipes or buckets. Because of this, it is always advisable to understand the quality of the local waters. As per the residents of the Barrett Canyon cabin community, many have installed filters and/or boil water before consuming it to avoid illness. Boiling the water kills bacteria and pathogens but may not always remove all dissolved substances. With respect to sulfate, concentrations of sulfate above 250 mg/L are not immediately harmful to people, aside from a possible laxative effect, bitter taste, or an unpleasant sulfurous odor, like that of a rotten egg (EPA, 2019 and EPA, 2003).

Research Questions

This project will address the following research questions: 1) What are the sulfate concentrations within the watershed? 2) Is there a seasonal effect on sulfate concentrations? 3) What is the source of the elevated sulfate, and if geologically related, which unit is the likely contributor? 4) Is there measurable down-gradient leaching from the bedrock, landslide deposits, or stream sediments? 5) Are there potential health hazards associated with the elevated sulfate concentrations within the study area?

WATERSHED CHARACTERISTICS AND PREVIOUS STUDIES

To better understand the sources of sulfur as sulfate in the San Antonio Canyon Watershed, results will be compared with previous studies both in the study area and in areas with similar geography and geology. Previous research by Cal Poly Pomona alumni and faculty provides a significant contribution to this project, as it gives insight into the current state of knowledge concerning sulfate within the San Antonio Canyon Watershed. The first indication of a sulfate anomaly was first recognized during the initial calibration of Dr. Osborn's ion chromatograph instrument during winter 2014 (Nourse, unpub. data, 2013). A water sample collected by Dr. Nourse form the mouth of Cascade Canyon ran about 400 mg/L sulfate while samples from nearby reaches of San Antonio Creek ran <50 mg/L sulfate.

Geology

The geology of the study area is complex and includes mostly granitic, intrusive, metasedimentary, and alluvial/colluvial/talus rock types (Nourse, 1998, Nourse, 2003, Heaton, 2008, and Zylstra, 2017). The deformation and tectonic history of this area is equally complex, resulting in numerous fault zones, intrusive units, and variable lithology (Figure 5). See Figure 6 for various field photos.

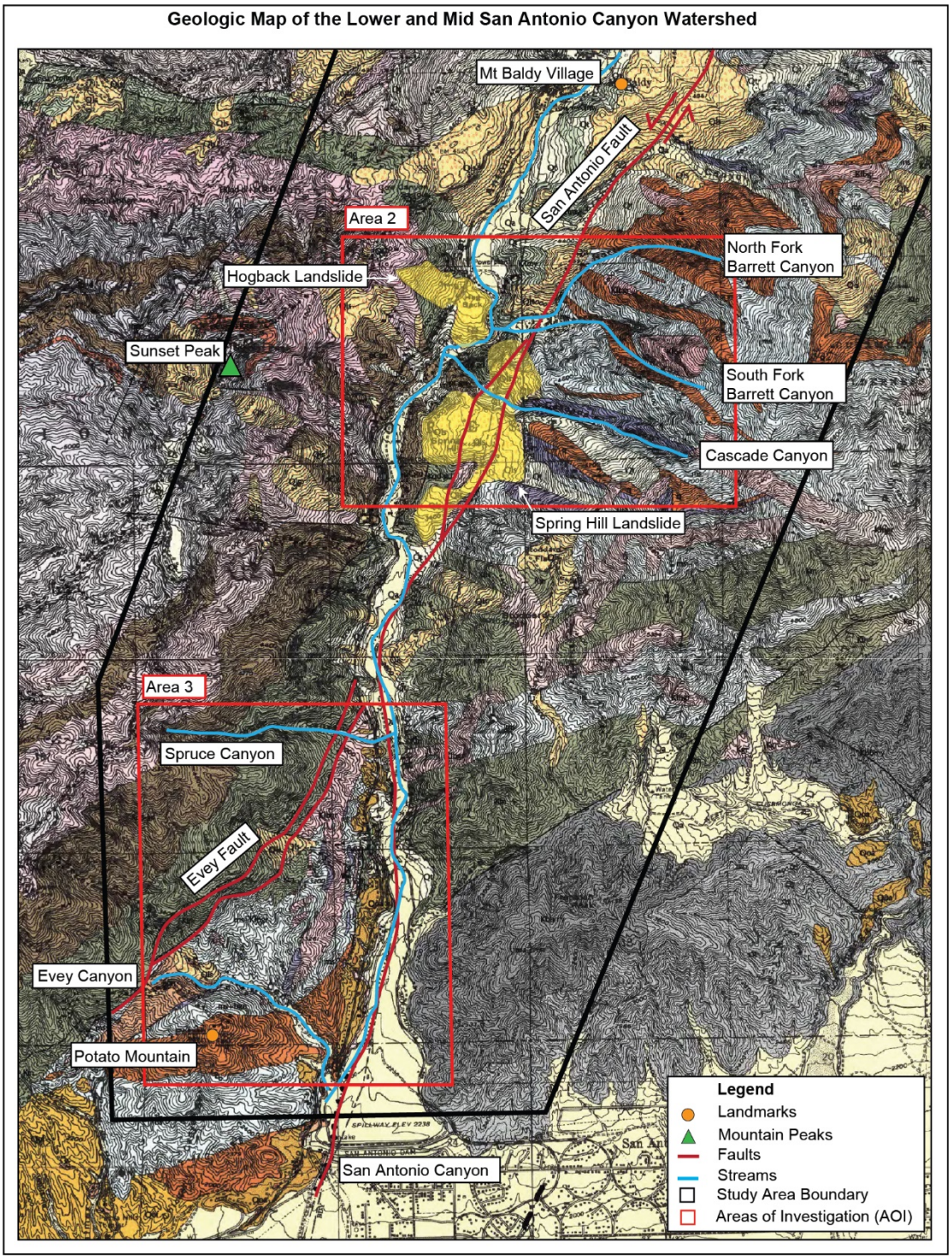

Figure 5: *Geologic map of the Mount Baldy area, modified from (Nourse et al., 1998). Major units include Quaternary sediments (shades of yellow), Cretaceous granitoids (pink), Mesozoic quartz diorite (green), Jurassic-Triassic plutonic rocks (purple), undifferentiated metasediments (light blue), quartzite (orange), Precambrian gneiss (brown and gray), and marble/calcsilicate gneiss (darker blue).*

Field Photos: Barrett-Cascade Area

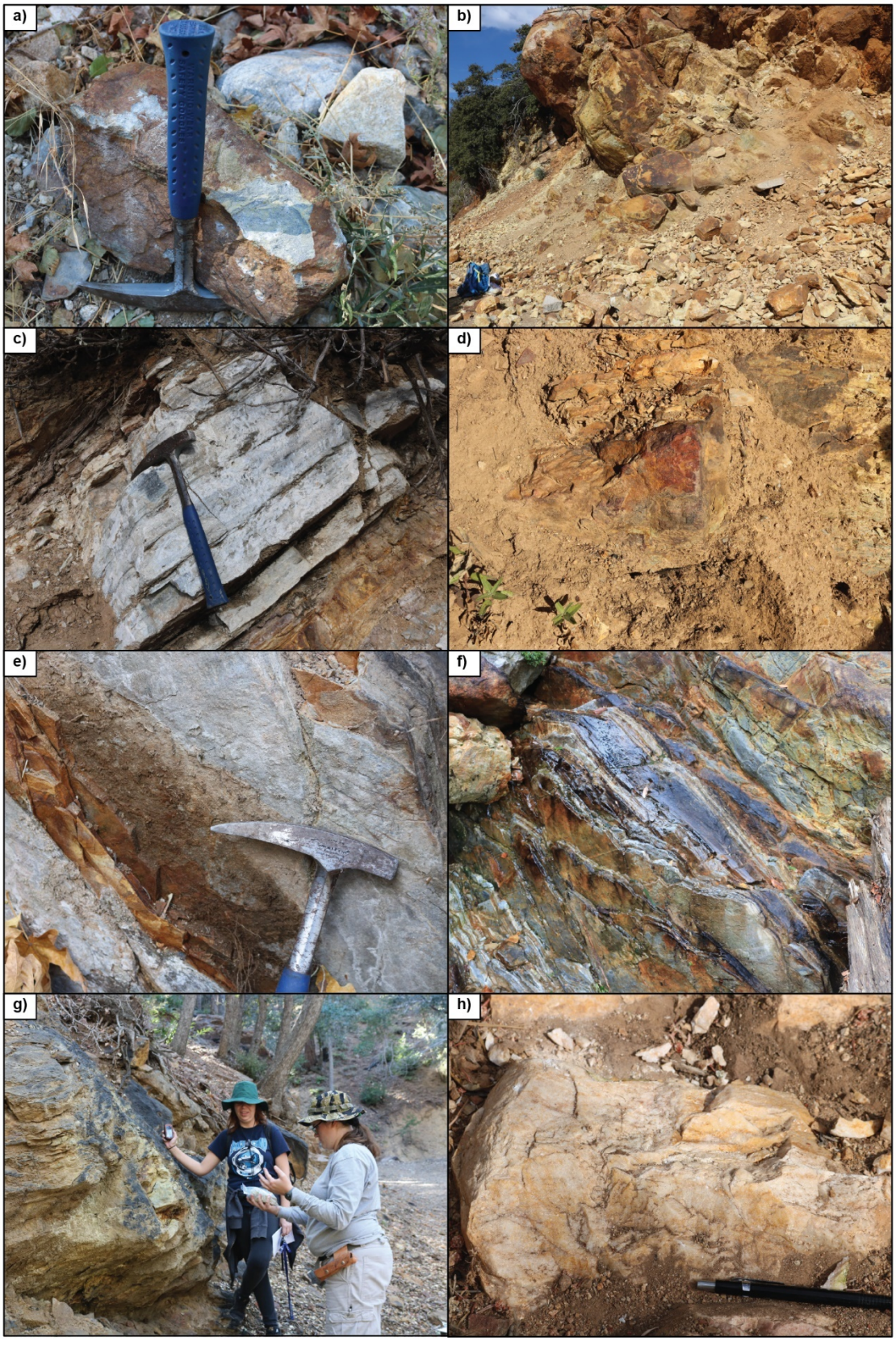

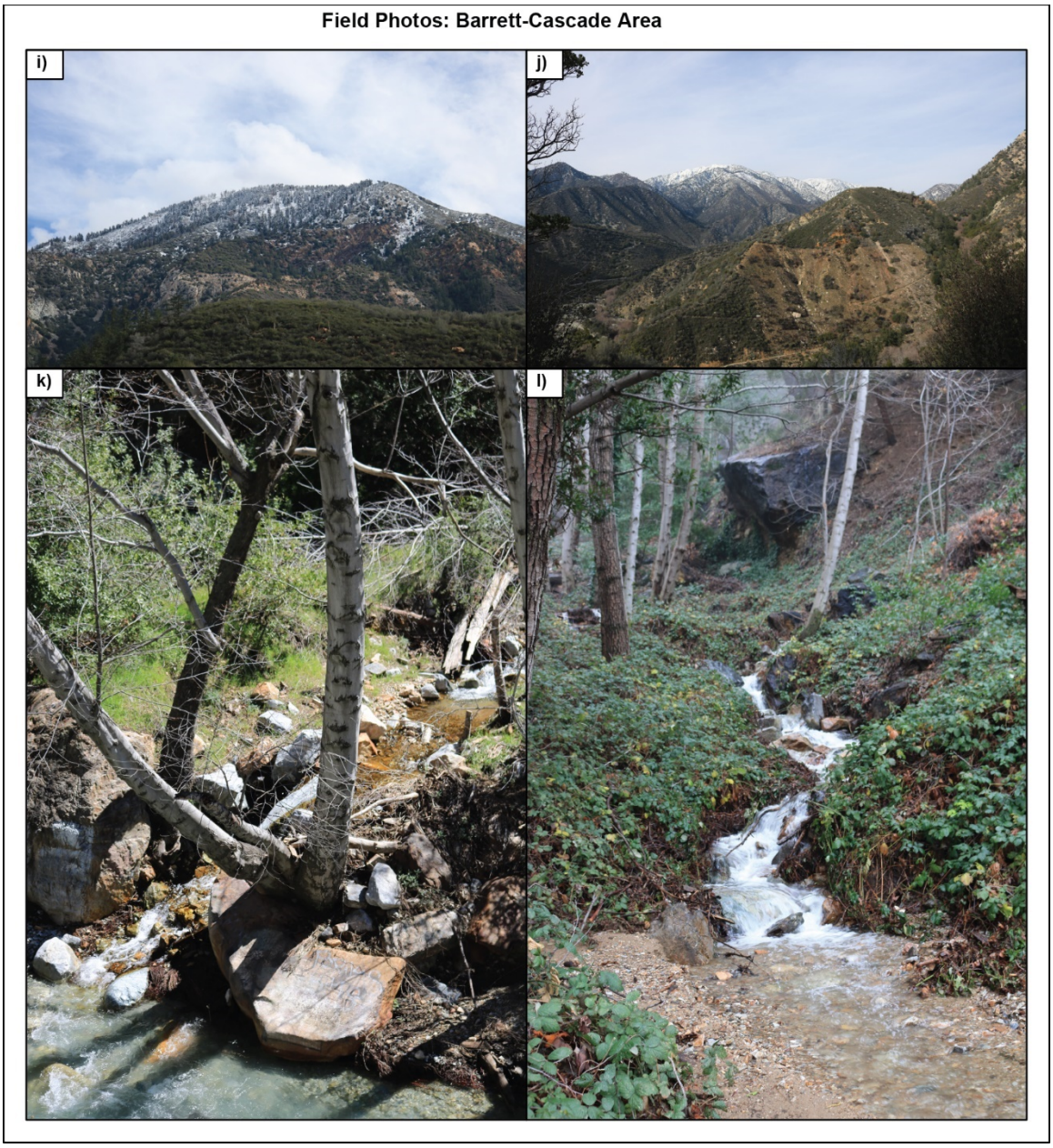

Figure 6a-l: *Field photos from the Barrett-Cascade area. Photos include a representation of rock samples a) AY19-01, b) AY19-05, c) AY19-06, d) alluvial samples AY19-10 and AY19-11, e-f) NW-dipping AY19-07, g) AY19-03 along with GPS logging and rock sample collection, and h) AY19-08. The second half shows i-j) a snowy Mount San Antonio in the background with part of the red-colored Spring Hill landslide in the foreground, k) the mouth of Cascade Canyon, and l) the South Fork Barrett Creek.*

The oldest rocks are Proterozoic-age gneisses, augen-gneisses, and metasediments. The gneisses and augen gneisses are generally light-colored and medium to fine-grained. The "San Gabriel" type gneiss recrystallized under the upper amphibolite facies and may be derived from igneous and/or immature sedimentary protoliths with felsic to mafic ranges. It is the oldest basement recognized in the western San Gabriel Mountains (Silver, 1971; Barth et al., 1995). In some areas, k-spar augen-gneiss can also be observed. These units appear to outcrop more on the western side of the canyon as well as at the center. During fieldwork, these units were observed as outcrops along the trails as well as boulders in the San Antonio Creek streambed. The metasediments are largely undifferentiated and strongly foliated and isoclinally folded at the upper amphibolite facies (Nourse, 1998). This is locally subdivided into marble/calcsilicate gneiss, quartzite, and gneiss/schist/phyllite. The marble/calcsilicate gneiss is fine-grained and gray-blue with strong foliations and isoclinal folding. Hematite- and limonite-staining along with hydrothermally altered bedrock was observed in Cascade Canyon. The quartzite units are generally light gray in color with orange staining on weathered surfaces. The gneiss/schist/phyllite units are typically seen near Evey Canyon and Potato Mountain. They commonly have well-developed mm-cm scale folding and are intruded and deformed by biotite granitoid or pegmatite dikes or veins. Outcrops west of Potato Mountain are interfolded with Precambrian augen gneiss.

The Mesozoic-age rocks are mostly granitoids and can include diorite, granodiorite, or tonalite. These units are generally medium- to fine-grained with poor to moderate foliation and variable proportions of biotite and/or hornblende (Nourse, 1998). K-spar phenocrysts or sills can be observed in the upper part of the canyon. The Triassic diorite is associated with the Mount Lowe intrusive unit. The Cretaceous granitics are

fine to medium-grained, weakly foliated, and mylonized in some spots due to some shearing from the Vincent Thrust.

An additional unit that exists here is the corundum granofels/schist, which appears to be late Cretaceous (Wire, 2021) in age, about 72±1.5 Ma. This unit is light colored and medium-grained with small corundum crystals ranging from a few mm to cm long. It may also contain accessory minerals like sillimanite, rutile, phlogopite, muscovite, pyrite, and graphite (Wire, 2021). The unit has a yellow-orange limonite coating, and in some areas of Barrett Canyon, is blackened by wildfire. It also has a distinct sulfurous odor, especially when samples are broken apart. Regionally, it can be found as blocks within a landslide deposit in the Barrett and Cascade canyon area and as outcrops near the upper part of Cascade Canyon as well.

It is important to include previous fieldwork by Dr. Van Buer in August 2015. Samples NVB-1548 and NVB-1549 were collected in the upper cascade canyon area. "I parked at the base of the Barrett Stoddard Road and walked up that road to where it intersects the ridge south of Cascade Canyon...I bushwhacked up that ridge to Peak 6857. The ridge there is held up by north-dipping quartzite, and its north face is basically a dip slope of the red-weathering corundum-bearing unit (sample 1548) that overlies the quartzite. I believe there were also some granite dikes in the area. Although the map outcrop is broader due to the dip slope, I doubt the corundum unit was over 10 m thick. Stratigraphically above the corundum unit (but downslope) is the crenulated biotite gneiss (sample 1549)." He hypothesizes that, since dip slopes are known to be prone to landslides, the origin of the Spring Hill landslide may be near there.

The youngest units include Cenozoic-age mylonized orthogneiss, which is associated with chlorite-epidote alteration and is intruded by Tertiary volcanics, typically as sills. It has also undergone some shearing from the Vincent Thrust and overlies the Pelona schist. The most recent includes alluvium and colluvium/talus from numerous landslides. Two main landslides in the area are Hogback and Spring Hill landslide, which lie in the Barrett-Cascade area next to the San Antonio Creek. The latter can be identified by its red-colored sediments, and in some areas, blocks of the corundum granofels unit.

Although water-rock interactions are pertinent to this study, soils should be considered, as they can affect the composition of water as it percolates through the soil column. This is because soils contain not only sediment from the parent rock, but microbes and other biota as well as plants and organic matter. The soils in the watershed are dominantly loam, 1 - 5 ft. thick, with grain sizes ranging from coarse sand to gravels and cobbles. There also exists talus and streamflow deposits, ranging from about 4 in. to 5 ft. thick, with high permeability, and variable parent material. The Spring Hill landslide is of interest to this study, as it may supply some sulfate to the system.

With respect to water flow, faults and joints should be considered, as they can either hinder flow or act as conductors. Faults can also deform and fracture rocks, often bringing them to the surface to be exposed to erosion. The main ones that exist locally include the San Andreas Fault, the San Gabriel Fault, the San Antonio Fault which runs N/S down the length of the San Antonio Canyon, the Vincent Thrust, and the Cucamonga Fault. An additional fault in the study area is the Evey Fault, which runs NE/SW along the top of Evey Canyon. The deformation and tectonic history of this area is complex, as much of the area has been faulted, metamorphosed, and folded. During field work, this

was most apparent in the tilted Cascade Canyon units as well as slicken lines present in many outcrops and fallen rocks.

There is also abundant deformation in the area, as metamorphic rocks and folding is commonly seen. Metamorphic rocks that are often associated with sulfur include those that formed in reduced environments, such as organic-rich black shales and some limestones. Although there are no black shales observed in the area, their metamorphosed versions (e.g., phyllite, schist, and gneiss) are common, with some units in the upper watershed area containing graphite. Similarly, there are no limestones observed in the watershed, but marbles are present within the northeast and southwest areas.

Mining History

The Gold Rush was an integral part of Californian history. Thousands of prospectors, farmers, and businessmen flocked to California to try and strike it rich. Sutter's Mill was the main site of the Gold Rush in 1848, but a lesser-known discovery site was the western foothills of the San Gabriel Mountains in 1842. Although less plentiful than Sutter's Mill, prospectors continued to arrive. The East Fork of the San Gabriel Canyon became the site of a population boom (Angeles Adventures, 2019, Rare Gold Nuggets, 2017, and Parra, 2013). Placerita Canyon included a small town the prospectors called "Eldoradoville". The settlement was soon abandoned after being destroyed in a flood in 1859 (Parra, 2013).

Most of the gold found was in the form of nuggets, called placer gold. These were found in streambeds and were extracted using the panning method. The 1870s marked the age of hydraulic mining in the East Fork. The placer gold was nearly depleted from the

river, which led to prospectors searching the hillsides for gold deposits called “lode gold”. This appeared to be common in quartz veins within the gneisses and schists as well as pyrite-rich rock. They extracted the gold using both dredging and hydraulic mining, which involves breaking rock using high-pressure water cannons. Eventually, most major mining operations ceased in the 1930s and prospecting is forbidden in many areas of the San Gabriels. However, numerous claims have been made in the Mount Baldy and Lytle Creek Mining Districts throughout the 1900s and 2000s, with a boom in the 1970s and 1980s (The Diggings). Most mines are currently closed, but some have remained open.

In the upper watershed area near Thunder Mountain (Figure 7), there are 16 closed claims and 1 open claim. Most of these claims were originally filed in the 1970s and 1980s, with one in 2004. The single open claim here is called the Blue Diamond Mine #1, which was originally filed in 1977. It has tungsten as its primary commodity and gold and silver as its secondary commodity. There are several closed Blue Diamond claims in the area as well, but exact commodities of all closed claims are unlisted (The Diggings). Near Mt. San Antonio, there are 6 closed claims originally filed in the 1980s. In the middle part of the watershed north of Kirkoff Canyon, there are 4 closed claims originally filed in the 1980s. In the upper Barrett and Cascade Canyon area, there are 8 closed claims originally filed in the 1970s and 1980s.

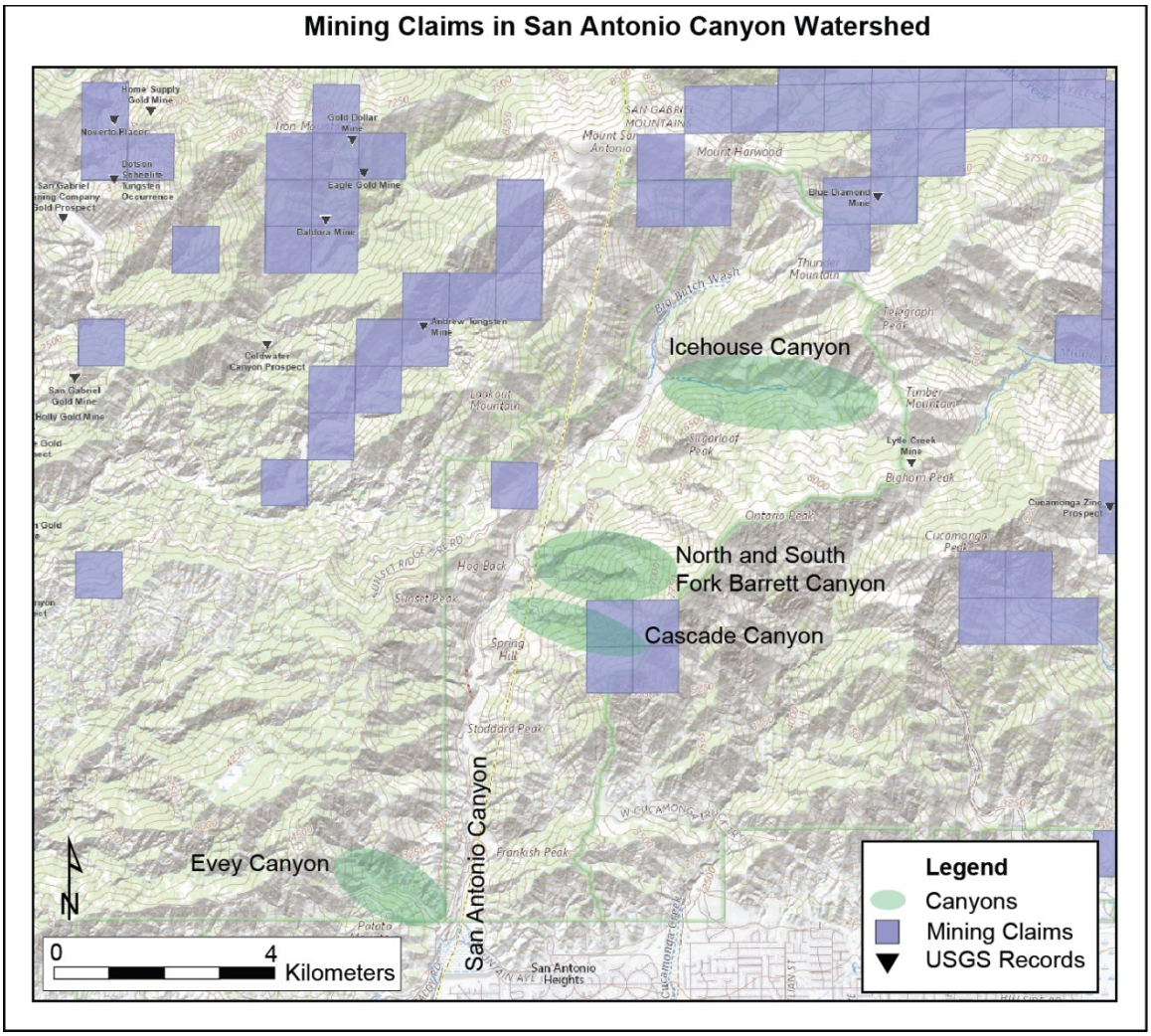

Figure 7*: Maps of mining claims (purple boxes) and USGS records (small black triangles with labels) from (The Diggings.com).*

Studies Within the San Antonio Canyon Watershed

Most streams in the area have perennial flow and are continuously fed by groundwater via springs, while others have ephemeral flow and are fed by meteoric waters. As mentioned in pH and Alkalinity, the differences in water quality can help distinguish between the two sources.

Water quality at the middle and upper reaches of the San Antonio Canyon has been studied with higher frequency that that of the lower reaches. Previous analysis was done by (Kurashige, 2012), (Bloom, 2012), (Osborn, unpub. data, 2012), (Nourse, unpub. data, 2013), (Wicks, 2014), (Osborn, unpub. data, 2015), (Lenhert and Soto, 2015), (Soto, 2015), (Soto and Lenhert, 2015), and (Yaralian, 2017). On average, sulfate concentrations here are higher than those in the lower reaches. See Table 1 for sulfate concentration ranges and associated references.

Location	Sulfate Concentration (mg/L)	Reference
Area 1		
Icehouse/Upper Watershed	13.96 - 30.90	Wicks, 2014 and Soto, 2015
Area 2		
Barrett Canyon Area	13.95 (averaged) 35.56 - 59.01 96.68 - 650.43	Osborn, unpub. data, 2012 Nourse, unpub. data, 2013 Yaralian, 2018
Hogback Spring	16.83 83.20 - 223.78	Nourse, unpub. data, 2013 Yaralian, 2018
Cascade Canyon	320.52 - 393.56 1609.82 - 1706.33	Nourse, unpub. data, 2013 Yaralian, 2018
Pond and S. Spring Area	25.93 (averaged)	Osborn, unpub. data, 2012
Sierra Powerhouse	30.12 (averaged)	Osborn, unpub. data, 2012
Area 3		
Lower SA Creek	30.83 (averaged)	Osborn, unpub. data, 2012
Evey Canyon Area	24.78 - 38.14	Wicks, 2014, Soto, 2015, Lenhert and Soto, 2015, and Soto and Lenhert, 2015

Table 1: *Sulfate concentration ranges of water samples in the San Antonio Creek watershed for previous studies, along with their associated references. Datasets obtained through IC analysis.*

Based on baseflow studies in the upper watershed areas (Nourse, 2010), (Perez, 2015), and (Miranda, 2018), Icehouse Canyon shows flow of 0.0 cfs - about 30.0 cfs with gaining and losing segments. The former is likely from tributary inflow or indicates the locations of significant springs, while the latter likely shows where the stream infiltrates into the ground. This gaining and losing trend appears to be seen in reaches of the Cascade Creek, where the losing reaches exist where the creek crosses the fire trail.

Seasonal fluctuations in pH and dissolved ions were observed in (Kurashige, 2012)'s thesis, but more study is needed to confirm this, since there may have been corrupted data due to some technical difficulties with the pHmV meter. Dissolved oxygen (DO) is important, as it tells us how much oxygen is in the water. When streams have less flow and energy, less oxygen is becoming incorporated into the water. Dissolved Oxygen also showed some seasonal fluctuations, decreasing slightly in warmer months. This could be due to the increase in evaporation as well as loss of water volume due to decreased precipitation or a lower water table. Oxidation-Reduction Potential (ORP) shows no visible trend, and further study is needed. Both (Yaralian, 2017) and (Kurashige, 2012) observed elevated sulfate concentrations in the Cascade-Barrett Canyon area, with (Kurashige, 2012) observing elevated concentrations of dissolved ions at the base of Cascade Canyon. Both concluded that the elevated sulfate may result from groundwater interacting with a sulfide-rich rock unit. Adding to this, (Yaralian, 2017) concludes that sulfate concentrations may have been higher due to the drought present at the time of the study. There could also be some dilution by groundwater or precipitation, but further data analysis is needed to confirm this.

Water quality of the lower reaches of the San Antonio Canyon was studied mainly by (Osborn, unpub. data, 2015), (Lenhert and Soto, 2015), (Soto, 2015), (Soto and Lenhert, 2015), and (Osborn, unpub. data, 2012). Sulfate concentrations here are lower compared to the upper reaches, ranging from about 24 mg/L - 38 mg/L in Evey Canyon (Soto, 2015). Earlier samples collected in the area in spring 2012 by Dr. Osborn lie within this range. Based on Tritium analysis, (Soto, 2015, Lenhert and Soto, 2015, and Soto and Lenhert, 2015) found that the waters supplying Evey Canyon are recent, about 10-30 years in age. Since concentrations of bromide, chloride, and nitrate were all < 10 mg/L, she concluded that sulfate was not being introduced via brine mixing or gypsum weathering. She also concluded that the likely source of the sulfate is from groundwater interaction with a fractured metasediment unit low in oxidized pyrite in addition to some leaching from the soils. (Lenhert and Soto, 2015) also found that the Evey Canyon fault is dipping about 60 degrees upgradient to the NW and is likely an important groundwater source to the local streams.

Studies from Other Comparison Areas

It is important to investigate areas with similar geology, geography, and elevated sulfate, as it provides additional clues to the sulfur cycle in a generic watershed system. This section will summarize papers representing the current state of knowledge, from the last 5 to 10 years, and the historical state of knowledge, from the last 10 to 50 years, to try and bridge the knowledge gap.

Elevated sulfate concentrations in Vermont streams were observed across several years in addition to wet years following the 2001 drought (Meyer et al. 2010). During summer 2001, sulfate concentrations peaked over 550 μeq/L before returning to below 200 μeq/L. In general, sulfate concentrations appeared to increase after large rain events following a drought in addition to s the seasonal cycles. To supplement this, total sulfur content was analyzed within metamorphic rocks. Their results show that quartzites and granitic units were low to moderate, ranging from 70 μg/g - 530 μg/g, while the schists and phyllites were much higher, ranging from 1,930 μg/g - 13,010 μg/g. They concluded that sulfate in the streams appeared to have three main sources, with soil providing sulfate during times of snowmelt in addition to a secondary, oxidized form during the re-wetting phase, and the weathering of local rocks providing sulfate during baseflow conditions in the dry season. Due to the presence of similar rocks in the study area, similar values may be possible.

(Johnson, 1977) found that sulfate's mobility is strongly pH-dependent, increasing with higher pH values. This may result from positively charged surfaces and a reduced concentration of OH^- ions. Certain soil horizons, such as A and B, can show

considerable changes in sulfate with changes in pH. Overall, in most soils, when acid was added, sulfate appeared to increase, unless local pH was variable.

(Garrels and Mackenzie, 1966) studied various springs and lakes in the Sierra Nevada Mountain region. The local geology includes granitic rocks ranging from quartz diorite to quartz microcline gneiss. Traces of kaolinite was commonly observed, due to the weathering of feldspars. Using water quality parameters to reconstruct the parent rock, and assuming a closed system, they found that "kaolinite" controls the composition of waters it interacts with, and that plagioclase weathering can account for about 80% of the geologically derived constituents in the ephemeral springs. When compared to ephemeral springs, perennial springs appear to run deeper with higher pH values and concentrations of constituents. With respect to sulfate, the mean concentrations within perennial springs were also slightly higher than that of ephemeral springs.

Evaporation in surface water systems should also be considered, as it can increase the pH of a water body (Garrels and Mackenzie, 1966). Elements like calcium and magnesium precipitate out as calcite, thus increasing the concentrations of carbonate and OH-. Sodium, potassium, chloride, and sulfate become concentrated without precipitating out, which further increases the pH. This provides the system with a buffer. The pH remains constant until all insoluble carbonates that formed during evaporation have been removed. Overall, they concluded that "waters maintained in equilibrium with the atmosphere and separated from decomposition products, with univalent ions originally derived from the incongruent solution of silicates will inevitably become highly alkaline if concentrated greatly" (Garrels and Mackenzie, 1966).

In Minnesota, the maximum contaminant level (MCL) is 500 mg/L (MPCA, 1999). According to this study, this limit was exceeded in 73 of the 954 groundwater wells, although the median was about 19 mg/L. Sulfate concentrations varied throughout the state, but Cretaceous aquifers appeared to have relatively higher values at about 420 mg/L. Other areas of high concentrations included those with large amounts of organic matter, oxidizing sulfur-bearing minerals, and industrial deposition.

RELEVANT ASPECTS OF AQUEOUS GEOCHEMISTRY

pH and Alkalinity

The chemistry of water largely depends on the mineralogy and type of geologic material that it has interacted with (e.g., rock, soil, or other unconsolidated material) as well as the age of the water. Rocks are composed of various minerals, which are made of various elements and ions. When geologic bodies weather, the elements that were locked within the rock become free to move about. Depending on the properties of the water, many ions will remain in solution for a certain time, while others prefer to precipitate out of solution. Each geologic body will impart certain ions into the water, so its chemistry can help determine which type of geologic body it was interacting with. The number of ions in solution typically increases with time, so older waters are expected to have higher concentrations of certain ions as opposed to younger waters. The chemistry of water can be measured using a wide variety of methods, including pH and alkalinity.

The pH is a measure of the activity of hydrogen ions is in the water, basically the number of acidic H^+ ions present. pH is measured from 1 to 12, with 1 being acidic and 12 being basic or alkaline. When an acid is added to a water sample, the pH will decrease

towards 1. Rainwater is somewhat acidic, often with a pH of about 5.6 (Hem, 1985 and USGS, 2021), due to the carbonic acid produced when carbon dioxide in the atmosphere reacts with water vapor. Ground and surface water pH will vary depending on the composition of the local rocks, but in general, ranges from about 6.0 - 8.0 (USGS, 2021). For groundwater, this is due to prolonged interaction with the bedrock, which typically acts as a buffer and prevents any acidic input to the system (American Groundwater Trust, 2003). For reference, the average pH of the ocean is currently about 8.1 (Boyd, 2020).

Alkalinity is a measure of the carbonate and bicarbonate levels in the water. It provides important information about the type of geologic material it has interacted with and whether it is relatively young or old. The longer a water body is in contact with a geologic material, the more ions it picks up and carries in solution. Meteoric waters, like rain and snow, come directly from the atmosphere and have no alkalinity. Younger groundwaters or surface waters typically have alkalinities <100 mg/L due to their brief interactions with geologic materials. Older groundwaters and brines typically have alkalinities >100 mg/L due to their prolonged interaction with geologic materials. Because springs are fed by groundwater, their alkalinities are typically closer to that range, although values can vary. Alkalinities can also vary depending on the source rock, soil chemistry, durations of flow, and the presence of nearby faults or fractures.

Prior to weathering, the local sulfur is held within a body of rock in the form of iron sulfide, or pyrite. Along with igneous rocks, Pyrite often occurs in many sedimentary rocks and often is associated with biogenic deposits. Such deposits typically form in strongly reducing environments and can be associated with mining (Hem, 1985 and

Bowell, 2004). Mining in the presence of pyrite typically results in acid mine drainage. This is due to the oxidation of pyrite in tailings, which releases sulfur as well as other metals into the local waters. This drainage typically has a low pH and can have high concentrations of other metals. Sulfate reduction is important to remediating the mine drainage. The production of sulfide from sulfate can reduce the heavy metals into metal-sulfide precipitates, which, along with the bicarbonate created from oxidizing organic matter, acts as a buffer to lower the pH (Miao, 2012). Most of the mines in the area are abandoned or nearly inaccessible, so information may be difficult to obtain. According to (Hem, 1985), organic-rich waters typically have a pH lower than 4.5. This is unlikely to exist in the study areas, due to the pH of local waters being much more basic.

Typically, the outer surfaces of a rock body are most susceptible to weathering, however, this can be altered by both natural and tectonic forces. The more faulted and fractured a rock body is, the more surface area the rock has, and thus, more of the rock body is susceptible to weathering. Such fractures may also allow water to permeate through the rock, which further increases the potential weathering and transport of sulfur as sulfate. As water interacts with the rock, the minerals are weathered away, often by dissolution. Post-weathering, the pH of the water takes over as a mobility control. This pH change depends not only on the ions present from the rock, but mainly on the mobility of such ions. In other words, a mobile ion will stay in solution longer, while an immobile ion will attach, or sorb, to a surrounding body of geologic material.

Previous Studies on Dissolved Sulfate

Sulfur is ubiquitous in most natural waters (Hem, 1985, Morse et al, 1987, Miao, 2012, and EPA, 2003). Concentrations generally range from about 3 to 30 mg/L in most ground and surface waters, and about 2,700 mg/L in seawater (EPA, 2003). However, some locations have been found to have >1,000 mg/L (EPA, 2003). Sulfate has three main sources: the decomposition of organic matter via microbes, precipitation from environmentally impacted areas, and local geology (Hem, 1985, Morse et al, 1987, and EPA, 2003). Elevated concentrations can be due to either natural or anthropogenic causes and can also result in acidification of the local waters and soils.

Sulfur can have either organic or inorganic forms and often cycles between the two "via mobilization, immobilization, mineralization, oxidation, and reduction processes" (Edwards, 1998). The inorganic forms tend to be more mobile than the organic forms, with sulfate being the most mobile. Sulfate's mobility is often dependent upon the pH, concentrations of sulfate and other dissolved ions, and the redox conditions of the surrounding area. Sulfate's mobility appears to decrease with pH, according to (Edwards, 1998, Johnson, 1977, Harrison et al. 1989, and Hem, 1985).

Paired with its high mobility, sulfur is also redox-sensitive, so it can become one of several species, depending on the environmental conditions that are present. Within an oxidizing environment, it can become sulfate or hydrogen sulfate by attaching itself to available oxygen in the water (Hem, 1985 and Miao, 2012). Within a reducing environment, sulfur can become sulfide, hydrogen sulfide or bisulfide, or hydrosulfuric acid (Hem, 1985). Sulfate reduction can vary by location, but in general, occurs

extensively in most natural waters (Hem, 1985 and Miao, 2012). From the data and the pH-Eh graph from (Hem, 1985), sulfate should be the dominant ion within the study area.

According to (Hem, 1985), in areas where mining is common, sulfate concentrations can range from 1,000 mg/L to 6,000 mg/L in surface waters and about 10 mg/L to 100 mg/L in groundwater. In some areas, very low pH ranges of about 1 to 4 were observed, which (Hem, 1985) hypothesizes may be due to pyrite oxidation. In major mining areas, the effects of the drainage may continue long after mining operations have ceased. In western Pennsylvania, many water samples in areas of bituminous and anthracite coal mining showed elevated sulfate with a pH range of about 2.7 to 7.3, although a range of less than 5 is observed (Cravotta C.A, 2006 and Hem, 1985). To maintain such low pH, a large amount of acid is needed to counteract any geological or environmental buffers.

Environmental conditions may include atmospheric temperature, pH, and amount of organic matter. Since chemical reactions tend to occur more often or more quickly in warmer environments, one can predict higher sulfate concentrations and higher alkalinity during periods of warmer weather. During the dry season (June to September), increased Electrical Conductivity (likely derived from Sulfates) and pH have been observed (Kurashige, 2012). A similar decrease has been observed during the wet season (November to March). This increase may indicate that the sulfates become more concentrated when locked up in the rock. During the wet seasons, the sulfates are then flushed out and diluted. Since reduced sulfur tends to lower pH, one can predict to see lower pH ranges in waters with higher concentrations.

Previous Studies on Iron

This study focuses on sulfur, but iron is another useful element to discuss, as iron in the form of pyrite (FeS_2) can be used to determine if the source of the elevated sulfate is geologic in nature. Although iron is the second most abundant element in the Earth's crust, concentrations in natural waters are typically low to nondetect due to its low mobility (Hem, 1985 and Hem and Cropper, 1959). For this reason, samples collected during this study are unlikely to show any significant concentrations of iron. To counter this issue, rock samples are analyzed as well.

In natural waters, iron is commonly seen in two states, ferrous Fe(II) or ferric Fe(III). Fe(II) is the reduced state and forms in reduced to moderately oxidized waters, commonly groundwater, and is more soluble than its other state. Fe(III) is the oxidized state, forms in oxidized waters, is insoluble when the pH lies between 5.0 to 8.0 (Hem, 1985 and Hem and Cropper, 1959). Because of Fe(III)'s insolubility, any iron observed in surface waters, especially those within the 5.0 to 8.0 pH range, is likely to be the Fe(II) state.

The solubility of iron largely depends on both pH and oxidation intensity of the environment (Hem, 1985). According to (Hem, 1985), there are two conditions where iron solubility is low. The first is a strongly reducing environment in the presence of sulfur with a wide pH range. The second is a moderately oxidizing environment with a pH higher than 5.0 and is in the ferric hydroxide ($FeOH_3$) stability region. At very low pH ranges, iron is soluble, but most natural waters are well outside that range. According to (Santos, 2019), in aqueous and oxygen-rich environments, the oxidizing reactions on the surface of pyrite can fall into two categories: Type I and Type II. Type I is a redox

reaction in which the iron oxidizes from Fe(II) to Fe(III) and consumes the Fe(II)-H_2O groups. Type II is a redox reaction in which the iron reduces from Fe(III) to Fe(II) and generates the Fe(II)-H_2O groups.

Redox reactions are catalyzed by water and because they are reversable, ions will go back and forth between states. The oxidation process of iron is outlined by the formula below (Hem and Cropper, 1959).

$$Fe^{3+} + H_20 \leftrightarrow Fe(OH)^{2+} + H^+ + H_20 \leftrightarrow Fe(OH)_2^+ + H^+ + H_20 \leftrightarrow Fe(OH)_3 + H^+$$

As pyrite is one of the more common sulfide minerals, its redox reaction should be discussed. When pyrite interacts with water and weathers, it breaks down into its component ions. The sulfide oxidizes to sulfate and Fe(II) is released, in addition to some H^+ ions. The oxidation process is outlined by the formula below.

$$2\,FeS_2 + 7\,O_2 + 2\,H_2O \rightarrow 2\,Fe^{2+} + 4\,SO_4^{2-} + 4\,H^+$$

Ferrous compounds can also take place in biological processes, such as photosynthesis (Hem, 1985). Many of these organic iron compounds are also more resistant to oxidation than free ions. Although the study area is home to numerous plants, including trees, bushes, aquatic plants, and algae, the amount of iron they take in is unknown.

With respect to rocks, iron can be found in many minerals, including biotite, hematite, limonite, and pyrite. The San Antonio Canyon Watershed includes an abundant amount of these in the form of biotite gneisses, granitoids, hematite and/or limonite-coated rocks, and pyrite-bearing rock. As the pyrite-rich rocks weather, the mineral becomes exposed to the air. Under oxygen-rich environments, pyrite is unstable and will typically weather more easily than the surrounding minerals. Evidence of pyrite

weathering can be observed in coatings of limonite (iron oxide), which can be yellow-orange or brown. Such coatings can be observed on the rocks within the Barrett-Cascade Canyon area, mainly the marble and corundum granofels/schist units, indicating a significant amount of iron.

METHODS

Field Methods: Water Samples

Sampling was conducted bi-weekly, starting from November 2018, and ending in August 2019, with two spot samples collected in July 2020. Water samples were collected from various streams and springs, at strategic locations. Sample sites were divided between me and another colleague, Laura Estenssoro. These data were combined into one dataset for us both to use. There are 19 sample sites, including 3 spring sites, 1 pond site, and 15 stream sites. A few spot samples were collected and labeled as such. More sample sites are ideal, but accessibility and flow are highly variable, especially in the dry season. Poison oak is also common in the area, along with areas of difficult terrain.

The sites were chosen to try and determine the area with the highest sulfate concentrations and, if possible, which rock unit it is originating from. Springs are the most valuable sampling sites since the groundwater generally has more time to interact with the rocks as opposed to quickly flowing across them. Streams are the second most important sampling sites since areas of elevated concentrations can help determine approximate locations of the source. Stream samples were collected at the bottom, middle, and upper reaches of the streams. This is to help determine where along the

stream the sulfate is being introduced. During the dry months, the perennial streams in the watershed are spring-fed. Springs are fairly numerous, but this project covered only a few of them.

Prior to sampling, the bottles must be prepared. The bottles were cleaned and labeled with colored tape (red, yellow, and blue) to indicate which test is to be performed upon the sample. The red-labeled bottles are to be tested for anions using the ICP-OES (Inductively Coupled Plasma Optical Emission Spectrometer) at UCR. The Blue-labeled bottles are to be tested for anions using the IC (Ion Chromatograph) in Dr. Osborn's lab at CPP. The yellow-labeled bottles were titrated for alkalinity in the CPP laboratory as well.

The red-labeled bottles were acidified by adding 2-3 drops of optima-grade nitric acid. For ease of sampling, sample kits were made up, with each kit indicating a single sample site. In each kit includes a pair of nitrile gloves, a syringe, a 0.45-micron syringe filter, and three bottles with different colored tape. Extra supplies were brought in case of an issue.

When sampling in the field, gloves must always be worn to avoid any cross-contamination between the sample and collector as well as protect the collector from any bacteria or contamination within the sample. Contamination of the sample by bodily fluids (e.g., sweat or saliva) or bacteria can skew laboratory results for that sample. Although the syringes are sterile, they were rinsed out three times by drawing in water and squirting it out downstream. If using a container to collect or transport the water, it must be similarly rinsed before sampling to prevent cross-contamination between any possible remnants from the previous test or any debris in the container that could interfere

with the analysis. After the syringe is filled, the filter was screwed on the end. Care must be taken to keep the syringe and filters as sterile as possible by laying them back in their containers when not in use. To avoid contamination from sweat or dirt, keep the face to the side of the bottle, rather than above it. Keep the filter top from touching the bottles as well. The blue and yellow-labeled bottles were filled with no air bubbles. This is done by letting the water dome up above the bottle's mouth and doing the same to the lid. After setting the filter and syringe down, carefully hold the bottle and cap so that the cap is next to the bottle's mouth. In one swift motion, screw on the lid. The acidified bottles were filled until about halfway up the neck of the bottle before being closed.

After sampling, notes were made about water properties (e.g., clarity, scent, color) as well as surrounding rock, nearby canyons, or other features. GPS coordinates were taken at each site and again only if the sample site changed. The time of sampling was included with any relevant weather or storm activity. The bottles were labeled with a sample ID (e.g., EC1-110918-01), indicating the location name, the date, and the sample number. The bottles were put into a plastic bag, which was labeled as a secondary precaution. Samples must be kept in a cool place, so a cooler was used to store them in the field prior to storage in the laboratory refrigerator. See Appendix G for field photos outlining the collection process.

Field Methods: Rock Samples

After water sampling was completed, rock samples were collected. A total of 19 samples were collected and analyzed on the XRF at WSU for full-elemental analysis. Rock samples were collected from the Cascade and Barrett Canyon areas as well as the Evey canyon area in the upper and lower watershed, respectively. The collection process goes as follows.

Collecting samples from outcrops or roadcuts is ideal to avoid collecting rocks where the original location is unknown. However, for this project, some red-stained stream and alluvial samples were collected to measure the iron content. Several stream samples were coated in hematite due to surficial chemical alteration from pyrite-weathering. These samples were analyzed to see if any sulfate is leaching from the stream channel rocks. The core of the rocks can be tested against the outer surface to see if any sulfate is being lost. Once at the outcrop, a rock hammer was used to break loose a hand sample. The hammer was then used to break off any areas with weathering rinds or graffiti to get a clean fresh face. This is to ensure that we are getting a pure sample of the rock unit. To get a representative sampling, two samples were collected from each outcrop or location. After the sample has been collected, notes and GPs coordinates were taken at the sample site. The samples were bagged individually, with the sample ID labeled on the bag. For the alluvial samples, a representative and random sampling of loose material was collected and labeled in the same manner.

Based on the IC results previously obtained and the complex nature of the local geology, the areas of interest included the South fork of Barrett Canyon, Cascade Canyon, and Evey Canyon. See Table N for the rock sample data.

Laboratory Methods: Water Samples

Once the sample bottles were taken to the laboratory, the yellow samples were tested for alkalinity using titration. HCl with a normality of 0.1 was used to titrate the samples. Gloves must also be worn in the laboratory to avoid contamination of either the sample or collector as well as protect the collector from harsh chemicals. After each sample is weighed in a clean dry beaker, acid is added until the pH reaches equivalence, about 4.5. Record the pH of the sample and the amount of acid added in mL. Alkalinity was determined using the following formula.

$$Alkalinity = \frac{Acid\ added\ (in\ mL) \times Normality \times 50{,}000}{Weight\ of\ Sample\ (in\ g)}$$

The red sample bottles were analyzed using Ion Chromatography (IC) for cation analysis and the high-sulfate water samples were sent to UCR for cation analysis using Inductively Coupled Plasma - Optical Emission Spectrometry (ICP-OES). For a more detailed process of the IC, see Appendices A-C. Data from these analyses helps determine where the high ionic concentrations are originating from and how it changes over time. The main ions of interest are sulfate from the IC, and iron from the ICP-OES, since pyrite is composed of iron and sulfur.

Laboratory Methods: Rock Samples

X-ray Fluorescence (XRF) was used to analyze the rock samples, as it provides us with whole rock geochemistry. Data from this analysis helps determine if the elevated sulfate is geologic in origin, and if it is originating from a specific rock unit or other geologic feature, such as a landslide.

To prepare the rock samples, they need to be crushed to about 0.5 cm. About 50g to 100g of sample was crushed to account for any lab errors. The crushed sample is then powdered by a mill and then dried to ensure that no water is inside the sample. For a more detailed process, see Appendix D. Some XRF machines analyze pellets, which use cellulose to bind the rock powder and a hydraulic press to make the pellet, while others analyze glass beads made from the rock powder. The latter process was used to analyze the samples at the Peter Hooper GeoAnalytical Lab at WSU.

The corundum-bearing unit had a sulfurous odor in the field, especially when a fresh face is exposed. When preparing the samples for XRF analysis, most crushed rock samples produced a mild sulfurous odor, except quartzites.

RESULTS

Overview

Water and rock samples were collected in strategic locations to get an accurate representation of the water quality and hydrogeologic interactions within the San Antonio Watershed (Figures 2 - 4). Due to their lengthy format, essential information is provided in Data Tables 2 - 6. Raw data for water and rock samples are included in Appendices E and F, respectively. Tables 2 and 3 provide a summary of the water and rock sample sites, respectively. Tables 4 and 5 provide a summary of anion and cation data for water samples, respectively. Table 6 provides whole rock XRF analysis. Additional figures can be found in Appendix F.

The hydrograph (Figure 8) provides important weather information, such as storm events and the duration of wet and dry seasons. Figures 9 through 14 show locational averages and seasonal trends for pH, alkalinity, and sulfate. Figure 13 isolates “MB” samples (MB-MB6) to better show relationships and seasonal trends. In each of the following sections, the Icehouse Canyon, Barrett-Cascade area, and Evey Canyon areas will be discussed.

Locality	Sample ID	Sample Location (UTM)		Description
		Easting	*Northing*	
Area 1				
	IC	441597	3789826	Lower Icehouse Canyon stream, spot sample
Area 2				
	SF1	439445	3786373	Lower Silver Falls stream area, up the canyon from BC2
	BC1	439237	3786446	N. Fork Barrett Canyon stream, near road
	BC2	439164	3785671	S. Fork Barrett Canyon stream, near road
	MB6	438612	3786270	Hogback Spring
	MB	438463	3786118	San Antonio Stream stream just above MB5 and CC1
	CC5	439223	3785649	Upper Cascade Canyon stream, above CC4
	CC4	439190	3785659	Upper Cascade Canyon stream, above trail
	CC3	439164	3785671	Upper Cascade Canyon stream, at trail
	CC1	438445	3786101	Mouth of Cascade Canyon stream
	MB5	436732	3780961	San Antonio Stream at USGS Gaging Station (U15R)
	MB4	438456	3786119	Pond near trail
	MB4a	438139	3875941	Small stream just south of the pond along trail, spot sample
	MB3	437921	3785731	Spring south of the pond, along trail
	MB2	438184	3785989	Sierra Powerhouse Station spring/SAC at small dam
Area 3				
	SC	437752	3785766	Spruce Canyon stream, spot sample
	MB1	437965	3785292	San Antonio Stream near fire/rangers station (Shinn Rd.)
	EC2	438174	3785275	Upper Evey Canyon stream
	EC1	437949	3785275	Lower Evey Canyon stream

Table 2: *Locations and descriptions of water sampling sites.*

Locality	Sample ID	Sample Location (UTM)		Description
		Easting	*Northing*	
Area 1				
				No rock samples collected.
Area 2				
Barrett Canyon	AY19-03	439217	3786213	Corundum granofels. Fine to medium-grained, light colored, corundum (ruby)-bearing granitoid, with black and yellow-orange coating, likely from combustion and other alteration. Rock not in-situ (landslide). Sulfurous odor.
Pond	Path	438456	3786119	Biotite gneiss. Fine-to medium-grained, distinct banding, and decently weathered. Sample is in-situ. Collected by Laura Estenssoro.
Cascade Canyon	1548	440528	3785070	Corundum granofels. Fine-to medium-grained, light colored, corundum (ruby)-bearing granitoid, with yellow coating. collected by Dr. Van Buer.
Cascade Canyon	1549	440526	3785046	Biotite gneiss. Fine-to medium-grained, distinct banding, and decently weathered. Sample is in-situ. Collected by Dr. Van Buer.
Cascade Canyon	AY19-01	438441	3786100	Marble or undifferentiated metasediment. Fine-grained, blue-gray, finely-laminated metasediment with red-orange coating (limonite). Sample not in-situ (streambed). Sulfurous odor.
Cascade Canyon	AY19-02	438444	3786115	Quartzite. Medium-grained, light-colored, quartzite with some flecks of biotite/mica, some orange coating. Sample not in-situ (streambed).
Cascade Canyon	AY19-04	438848	3785992	Granodiorite. Medium-grained, light-colored, qtz-feldspar-mica rich granodiorite. Sample is in-situ.
Cascade Canyon	AY19-05	438996	3785759	Corundum granofels. Fine-to medium-grained, light colored, corundum (ruby)-bearing granitoid, with yellow coating. Rock not in-situ (landslide). Sulfurous odor.
Cascade Canyon	AY19-06	439116	3785702	Marble or undifferentiated metasediment. Fine-grained, light-colored (white and gray), finely laminated marble. Sample is in-situ.

Table 3: *Locations and descriptions of rock samples.*

Locality	Sample ID	Sample Location (UTM)		Description
		Easting	*Northing*	
Area 2				
Cascade Canyon	AY19-07	439206	3785659	Marble or undifferentiated metasediment. Fine-grained, light-colored (white and gray), finely laminated marble, with yellow and orange coating (limonite?). Sample is in-situ.
Cascade Canyon	AY19-08	438993	3785526	Quarzite. Medium to coarse-grained, light-colored quartzite, with white and yellow staining. Sample is in-situ.
Cascade Canyon	AY19-09	438994	3785444	Gniess. Fine-grained, gray/white and slightly blue-green (chlorite?), mica-rich, with distinct lamination. Looks shiny and smooth on the outside. Likely heavily weathered due to being friable when crushed.
Cascade Canyon	AY19-10	439166	3785665	Gravel/Alluvium. Red-brown stream channel gravels and alluvium. Sample is not in-situ.
Cascade Canyon	AY19-11	438988	3785776	Gravel/Alluvium. Red-brown landslide gravels and alluvium. Sample is not in-situ.
Cascade Canyon	AY19-12	439062	3785746	Granodiorite. Coarse-grained, light color (white), qtz-plag-mica rich granitoid, heavily eroded, breaks off easy. Sample is in-situ.
Area 3				
Evey Canyon	AY20 #2	436745	3780893	Biotite gneiss. Fine-to medium-grained, distinct banding, and decently weathered. Sample is in-situ.
Evey Canyon	AY20 #4	436311	3780979	Marble or undifferentiated metasediment. Coarse-grained and slightly blue-white in color. Sample is in-situ.
Evey Canyon	AY20 #6	435894	3781054	Biotite gneiss. Fine-to medium-grained, distinct banding, and decently weathered. Sample is in-situ. Sample is in-situ.
Evey Canyon	AY20 #7	437240	3781386	Quartzite from the potato mountain unit. Medium-grained and light in color with an orange weathering rind. Sample is in-situ.

Table 3 (cont.)

Locality	Sample ID	F	Cl	NO3	Br	SO4
		mg/L	*mg/L*	*mg/L*	*mg/L*	*mg/L*
Area 1						
	IC	0.17 - 0.23	0.74 - 0.94	0.23 - 0.56	0.09 - 0.11	11.94 - 15.05
Area 2						
	SF1	0.50	1.14	0.74	0.07	88.23
	BC1	0.30 - 0.43	0.86 - 1.36	0.06 - 1.22	0.01 - 0.25	35.15 - 53.53
	BC2	0.35 - 0.52	0.96 - 1.60	0.36 - 2.14	0.02 - 0.38	86.66 - 164.13
	MB6	0.26 - 0.36	1.16 - 2.76	1.03 - 3.63	0.03 - 0.16	19.86 - 26.85
	MB	0.33 - 0.45	1.05 - 0.62	0.18 - 1.47	0.03 - 0.10	64.06 - 77.76
	CC5	0.47	2.20	0.68	0.10	492.28
	CC4	0.42 - 0.64	2.12 - 3.58	0.04 - 5.37	0.02 - 0.08	365.54 - 836.23
	CC3	0.37 - 0.63	1.63 - 3.12	0.01 - 1.32	0.01 - 0.23	229.99 - 615.24
	CC1	0.65 - 0.86	2.31 - 3.35	0.06 - 0.99	0.04 - 0.11	463.40 - 663.02
	MB5	0.21 - 0.44	1.09 - 1.95	0.11 - 4.10*	n.a. - 0.45	18.96 - 78.08
	MB4	0.35 - 0.46	1.53 - 1.92	2.28 - 2.20	0.02 - 0.20	24.42 - 32.70
	MB4a	0.37	4.33	34.94*	0.11	16.65
	MB3	0.36 - 0.45	3.28 - 3.77	2.51 - 4.67*	0.04 - 0.16	22.24 - 30.79
	MB2	0.25 - 0.39	0.25 - 2.12*	0.31 - 2.97	n.a. - 0.32	25.33 - 75.40
Area 3						
	SC	0.39	3.77	1.46	0.05	33.32
	MB1	0.31 - 0.45	1.38 - 1.95	0.85 - 2.89	0.07 - 0.27	23.28 - 37.96
	EC2	1.39 - 1.86	5.31 - 9.15	0.06 - 5.09	0.03 - 0.35	30.02 - 50.98
	EC1	1.37 - 1.81	5.95 - 10.48	0.05 - 2.69	0.02 - 0.19	32.80 - 52.28

Table 4: *Summary of anion concentrations for water samples. Ranges with * indicate a possible error in the dataset with the value disregarded.*

Sample ID	Ca	Mg	Na	K	Sr
	mg/L	*mg/L*	*mg/L*	*mg/L*	*mg/L*
BC2	55.08 - 76.55	22.85 - 29.95	0.45 - 5.22	1.11 - 3.94	0.20 - 031
CC5	96.65	61.04	25.25	8.21	0.72
CC4	87.90 - 166.96	43.34 - 90.79	1.19 - 39.90	0.88 - 11.51	0.64 - 1.48
CC3	71.75 - 196.98	38.69 - 77.07	2.26 - 27.56	2.80 - 9.65	0.46 - 1.21
CC1	116.19 - 209.19	68.83 - 82.43	3.38 - 28.52	3.61 - 8.75	0.82 - 1.17
	As	**B**	**Ba**	**Bi**	**Cd**
	mg/L	*mg/L*	*mg/L*	*mg/L*	*mg/L*
BC2	0.00	0.04 - 0.05	0.00 - 0.06	0.03 - 0.04	0.00
CC5	0.00	0.07	0.02	0.04	0.00
CC4	0.00	0.04 - 0.08	0.00 - 0.04	0.03 - 0.05	0.00
CC3	0.00	0.04 - 0.11	0.00 - 0.03	0.03 - 0.08	0.00
CC1	0.00	0.05 - 0.09	0.00 - 0.03	0.03 - 0.05	0.00
	Co	**Cu**	**Fe**	**Mn**	**Mo**
	mg/L	*mg/L*	*mg/L*	*mg/L*	*mg/L*
BC2	0.00	0.00	0.00 - 0.05	0.00	0.03
CC5	0.00	0.00	0.00	0.00	0.03
CC4	0.00	0.00	0.00 - 0.12	0.00	0.03
CC3	0.00	0.00	0.00 - 0.06	0.00	0.03 - 0.06
CC1	0.00	0.00	0.00 - 0.16	0.00	0.03
	Ni	**Pb**	**Pd**	**Rb**	**Si**
	mg/L	*mg/L*	*mg/L*	*mg/L*	*mg/L*
BC2	0.00	0.00	0.00 - 0.01	0.00	9.50 - 11.20
CC5	0.00	0.00	0.00	0.00	15.26
CC4	0.00	0.00	0.00	0.00	13.92 - 20.07
CC3	0.00	0.00	0.00 - 0.01	0.00	12.10 - 27.71
CC1	0.00	0.00	0.00	0.00	15.25 - 17.95
	Ti	**V**	**W**	**Zn**	**Zr**
	mg/L	*mg/L*	*mg/L*	*mg/L*	*mg/L*
BC2	0.02 - 0.03	0.01 - 0.04	0.03 - 0.07	0.00 - 0.02	0.03
CC5	0.02	0.02	0.03	0.00	0.04
CC4	0.02 - 0.03	0.03 - 0.09	0.03 - 0.07	0.00	0.03 - 0.04
CC3	0.02 - 0.05	0.02 - 0.07	0.03 - 0.07	0.00 - 0.01	0.03 - 0.07
CC1	0.02 - 0.03	0.03 - 0.08	0.02 - 0.07	0.00	0.03 - 0.04

Table 5: *Summary of cation concentrations for water samples collected from Area 2.*

Sample ID	**AY19 - 01**	**AY19 - 02**	**AY19 - 03**	**AY19 - 04**	**AY19 - 05**	**AY19 - 06**	**AY19 - 07**
Rock Type	*Marble*	*Qtzite*	*Crn Gfels*	*Grdiorite*	*Crn Gfels*	*Marble*	*Marble*
SO3 >/=	0.082	0.000	0.000	0.000	0.191	0.118	0.072
Cl >/=	0.000	0.000	0.000	0.000	0.000	0.000	0.000
Normalized Major Elements (Weight %):							
SiO2	70.094	97.001	62.715	65.670	58.663	26.382	60.816
TiO2	0.787	0.103	1.065	0.074	0.921	0.158	0.739
Al2O3	14.826	1.823	25.411	19.777	26.120	4.079	14.799
FeO*	2.488	0.180	1.946	0.701	1.135	1.680	4.980
MnO	0.026	0.001	0.028	0.025	0.014	0.056	0.060
MgO	3.372	0.087	1.056	0.583	1.141	28.123	6.587
CaO	1.307	0.087	0.159	2.502	1.728	38.885	2.815
Na2O	3.105	0.527	1.902	10.026	7.103	0.382	8.176
K2O	3.865	0.173	5.610	0.523	2.934	0.155	0.944
P2O5	0.131	0.018	0.107	0.120	0.241	0.099	0.086
Major elements are normalized on a volatile-free basis, with total Fe expressed as FeO.							
NiO	15.550	2.624	3.164	2.974	2.217	8.554	39.096
Cr2O3	93.947	11.209	144.203	9.731	153.415	19.502	92.977
Sc2O3	24.309	0.770	38.384	7.867	34.204	6.205	21.588
V2O3	190.075	10.837	236.557	24.530	305.275	42.988	164.880
BaO	639.998	10.691	370.728	515.080	266.467	37.114	262.624
Rb2O	107.375	3.246	247.995	7.817	87.662	8.606	36.414
SrO	229.859	8.478	155.221	1154.041	164.408	1646.481	189.905
ZrO2	377.866	327.298	266.154	413.833	233.556	31.267	288.505
Y2O3	68.611	8.976	95.850	7.204	63.022	17.788	40.651
Nb2O5	22.082	2.080	32.132	3.316	26.916	2.764	19.745
Ga2O3	27.659	2.578	42.623	28.677	40.480	5.883	26.019
CuO	39.678	2.571	32.206	3.891	4.860	14.511	52.781
ZnO	8.800	0.125	1.814	20.505	9.170	28.032	8.173
PbO	12.312	2.268	4.601	9.457	29.222	2.601	10.561
La2O3	59.215	9.872	94.055	15.159	94.860	16.073	49.785
CeO2	124.931	9.494	208.474	23.401	186.311	36.960	105.707
ThO2	18.168	1.311	23.043	2.357	23.562	5.084	16.868
Nd2O3	55.388	5.558	95.595	9.090	71.641	14.859	45.061
U2O3	8.367	0.993	9.625	1.032	6.356	2.858	3.983
As2O5	11.477	11.988	0.000	9.306	12.749	12.039	18.487
sum tr.	2135.668	432.967	2102.424	2269.267	1816.353	1960.168	1493.812
in %	0.214	0.043	0.210	0.227	0.182	0.196	0.149

Table 6: *Whole rock XRF data for rock samples.*

Sample ID	**AY19 - 08**	**AY19 - 09**	**AY19 - 10**	**AY19 - 11**	**AY19 - 12**	**AY20 - 2**	**AY20 - 4**
Rock Type	*Qtzite*	*BioGneiss*	*Alluv*	*Alluv*	*Grdiorite*	*BioGneiss*	*Marble*
SO3 >/=	0.000	0.000	0.109	0.000	0.000	0.001	0.000
Cl >/=	0.000	0.000	0.000	0.000	0.000	0.000	0.000
Normalized Major Elements (Weight %):							
SiO2	95.911	56.674	60.343	63.638	70.821	67.272	57.936
TiO2	0.065	1.700	0.556	0.772	0.197	1.427	0.335
Al2O3	2.462	31.669	12.027	17.863	16.516	14.881	6.512
FeO*	0.085	2.342	3.558	5.962	1.311	7.633	2.560
MnO	0.001	0.022	0.060	0.057	0.036	0.051	0.060
MgO	0.218	0.992	10.732	3.323	0.351	2.058	2.683
CaO	0.122	0.039	7.117	1.416	2.283	0.931	26.900
Na2O	0.938	0.334	3.808	3.516	4.837	1.997	0.694
K2O	0.186	6.158	1.667	3.290	3.585	3.586	2.246
P2O5	0.012	0.071	0.133	0.163	0.064	0.164	0.073
Major elements are normalized on a volatile-free basis, with total Fe expressed as FeO.							
NiO	2.340	68.192	26.093	38.822	1.756	40.421	22.750
Cr2O3	9.598	195.203	63.811	100.924	6.876	95.806	38.315
Sc2O3	1.602	40.877	16.047	20.837	4.299	25.999	9.423
V2O3	11.344	340.933	128.977	168.232	17.964	140.639	49.260
BaO	49.462	369.822	758.274	676.729	1457.316	897.827	738.268
Rb2O	9.069	197.836	63.889	117.698	105.673	145.118	66.319
SrO	18.886	51.089	444.412	241.757	709.917	190.400	368.504
ZrO2	129.852	415.830	234.454	314.733	182.559	468.973	238.560
Y2O3	6.823	129.789	31.045	52.551	15.954	62.418	32.966
Nb2O5	1.352	49.568	14.535	22.405	13.173	39.340	9.229
Ga2O3	3.587	57.936	20.631	30.126	28.951	29.956	11.702
CuO	2.616	58.208	37.904	46.977	9.837	24.097	4.614
ZnO	0.000	4.108	31.995	38.710	53.765	114.145	53.727
PbO	0.911	3.016	7.802	15.012	22.428	13.304	9.431
La2O3	10.152	134.165	38.993	60.767	37.153	56.293	44.191
CeO2	16.084	301.966	78.647	127.566	61.155	138.291	76.975
ThO2	1.585	41.647	12.076	18.278	7.575	15.988	9.846
Nd2O3	8.240	132.852	34.732	53.195	22.708	58.669	31.412
U2O3	1.150	8.311	3.710	5.729	2.369	3.468	4.171
As2O5	7.784	0.077	15.119	14.507	15.121	13.498	10.288
sum tr.	292.438	2601.426	2063.145	2165.553	2776.550	2574.649	1829.952
in %	0.029	0.260	0.206	0.217	0.278	0.257	0.183

Table 6 (cont.)

Sample ID	**AY20 - 6**	**AY20 - 7**	**1548**	**1549**	**Path**
Rock Type	*Biogneiss*	*Qtzite*	*Crn Gfels*	*Biogneiss*	*Biogneiss*
SO3 >/=	0.0000	0.0000	0.2294	0.0000	0.1554
Cl >/=	0.0000	0.0000	0.0000	0.0000	0.0000
Normalized Major Elements (Weight %):					
SiO2	74.6217	98.3052	56.2490	58.0283	64.7893
TiO2	0.4089	0.0509	1.0269	1.2256	0.7684
Al2O3	11.5787	0.9721	29.7914	28.3154	17.5825
FeO*	2.6610	0.1449	1.4935	1.0254	7.4263
MnO	0.0447	0.0023	0.0049	0.0044	0.2883
MgO	1.6996	0.0586	0.8185	1.0765	4.7007
CaO	3.4653	0.0606	0.5349	0.3127	0.3599
Na2O	1.6700	0.0602	6.1079	3.8485	0.3228
K2O	3.7548	0.3307	3.6776	6.0445	3.4925
P2O5	0.0953	0.0145	0.2952	0.1187	0.2693
Major elements are normalized on a volatile-free basis, with total Fe expressed as FeO.					
NiO	14.2415	2.7653	1.4634	4.9033	21.5824
Cr2O3	34.1349	7.8623	190.0752	243.4172	132.2839
Sc2O3	12.1718	0.6170	31.7508	43.9553	31.1236
V2O3	63.2475	7.7653	291.2090	306.1959	135.5828
BaO	1128.7559	39.6439	490.4995	696.7852	394.0978
Rb2O	128.4127	13.4314	80.4114	138.7668	200.7759
SrO	380.5530	5.6483	138.0693	110.9440	21.1451
ZrO2	376.7414	242.8898	246.6983	510.5639	208.3319
Y2O3	44.7123	5.8101	82.6103	90.5347	64.3573
Nb2O5	13.5075	0.4314	31.9011	41.1383	19.6146
Ga2O3	20.3777	1.9923	48.7957	50.1455	33.0562
CuO	8.5504	2.3286	3.4424	4.4054	24.7088
ZnO	60.7675	0.0000	2.4895	6.8214	36.8853
PbO	16.1232	2.8161	13.0344	19.9300	1.8393
La2O3	59.7873	5.1875	100.0376	115.4468	62.4372
CeO2	128.4171	10.6901	210.6325	244.9164	136.1975
ThO2	19.7745	1.3159	26.5133	31.1785	20.6318
Nd2O3	49.5600	4.2807	89.9286	103.5583	58.4068
U2O3	1.7144	0.8301	7.4306	5.9220	3.8146
As2O5	12.9439	13.2632	14.5719	5.0125	12.9426
sum tr.	2574.4946	369.5694	2101.5650	2774.5416	1619.8154
in %	0.2574	0.0370	0.2102	0.2775	0.1620

Table 6 (cont.)

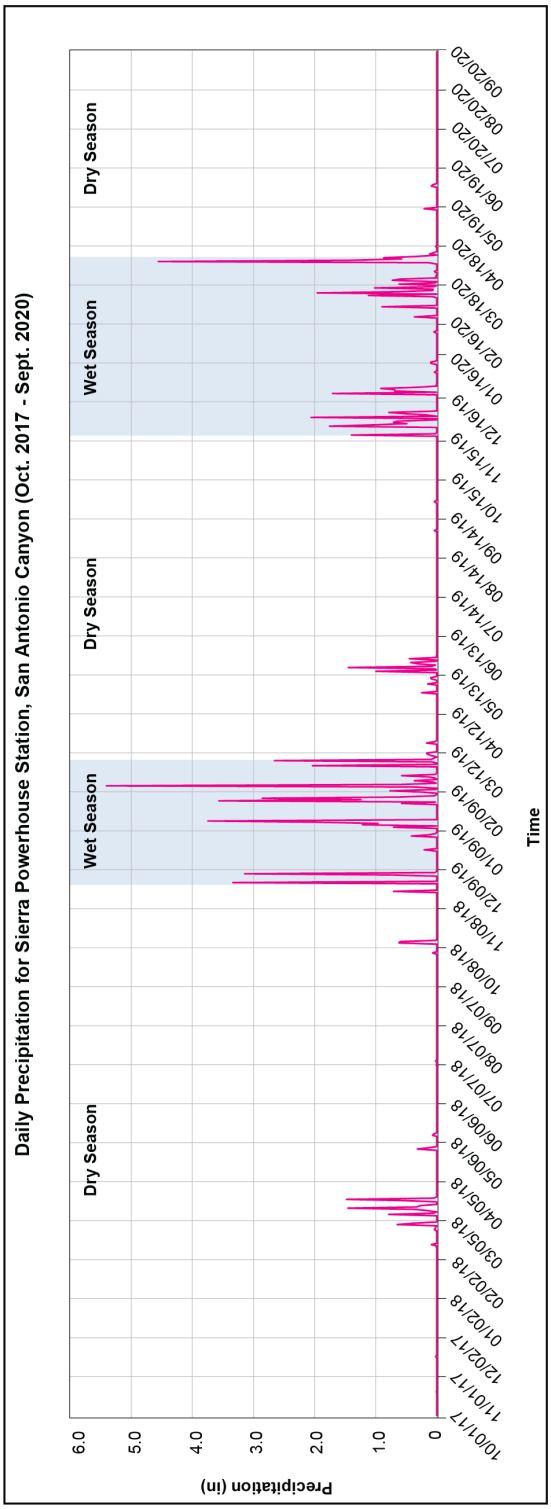

Figure 8: *Hydrograph showing daily precipitation from October 2017 to September 2020, collected at the Sierra Powerhouse station within the San Antonio Canyon Watershed. Wet seasons (shaded blue) and dry seasons (white) were arbitrarily chosen based on precipitation patterns.*

pH and Alkalinity

The pH of waters analyzed ranges from 6.6 to 8.7, with most lying within the 7.5 to 8.5 range (figure 9a). Generally, pH should decrease in the presence of elevated sulfate, but this is not seen in figure 9a. The pH should also decrease in some degree in the wet season due to sulfuric acid formation in the atmosphere and excess sulfur input, which can be seen in Figure 9a as well. However, the pH appears to be higher than expected, especially in areas with the elevated sulfate. See Figures 10a-14a for seasonal trends in pH for water samples.

Most streams here are perennial and spring-fed, so alkalinities >100 mg/L was predicted. Water samples with alkalinity <100 mg/L indicates younger waters, such as precipitation or very recent groundwater. The alkalinity of waters analyzed ranges from 69.63 mg/L to 269.56 mg/L, with most samples lying >100 mg/L (Figure 9b). Alkalinity also increases downstream along the San Antonio Creek, which is to be expected due to a trunk stream's cumulative effect. See Figures 10b-14b for seasonal trends in alkalinity for water samples.

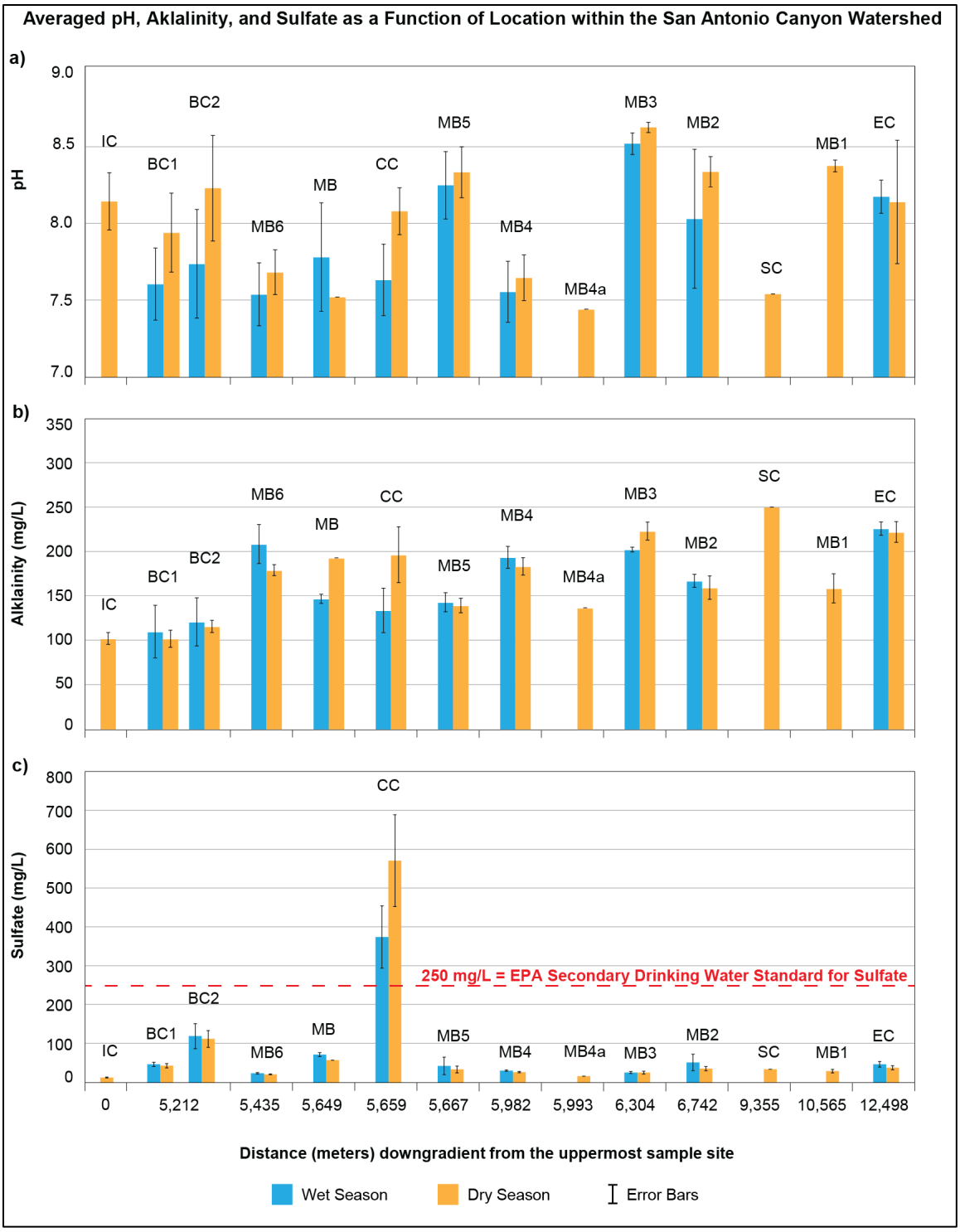

Figure 9a-c: *Averaged a) pH, b) alkalinity, and c) sulfate of sample sites, plotted as a function of sample site location along the San Antonio Creek, with 0m representing the highest elevation sample site (Icehouse Canyon, labeled as IC), and 12,498m representing the lowest elevation sample sites (Evey Canyon, labelled as EC). For sample sites not directly along the trunk stream, distance was determined by where it would discharge into the trunk stream.*

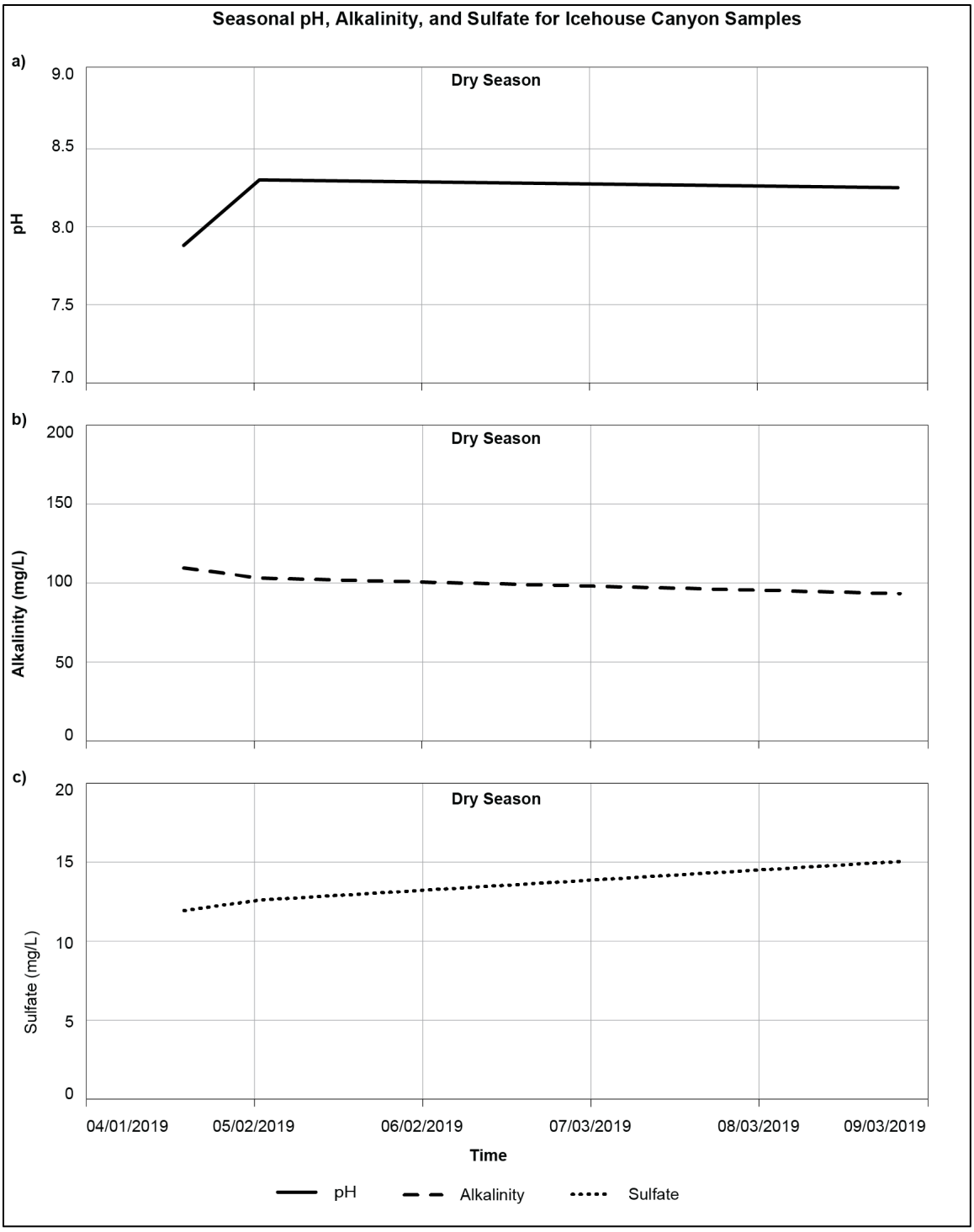

Figure 10a-c: *Seasonal a) pH vs. sulfate and b) alkalinity vs. sulfate trends for Icehouse Canyon*

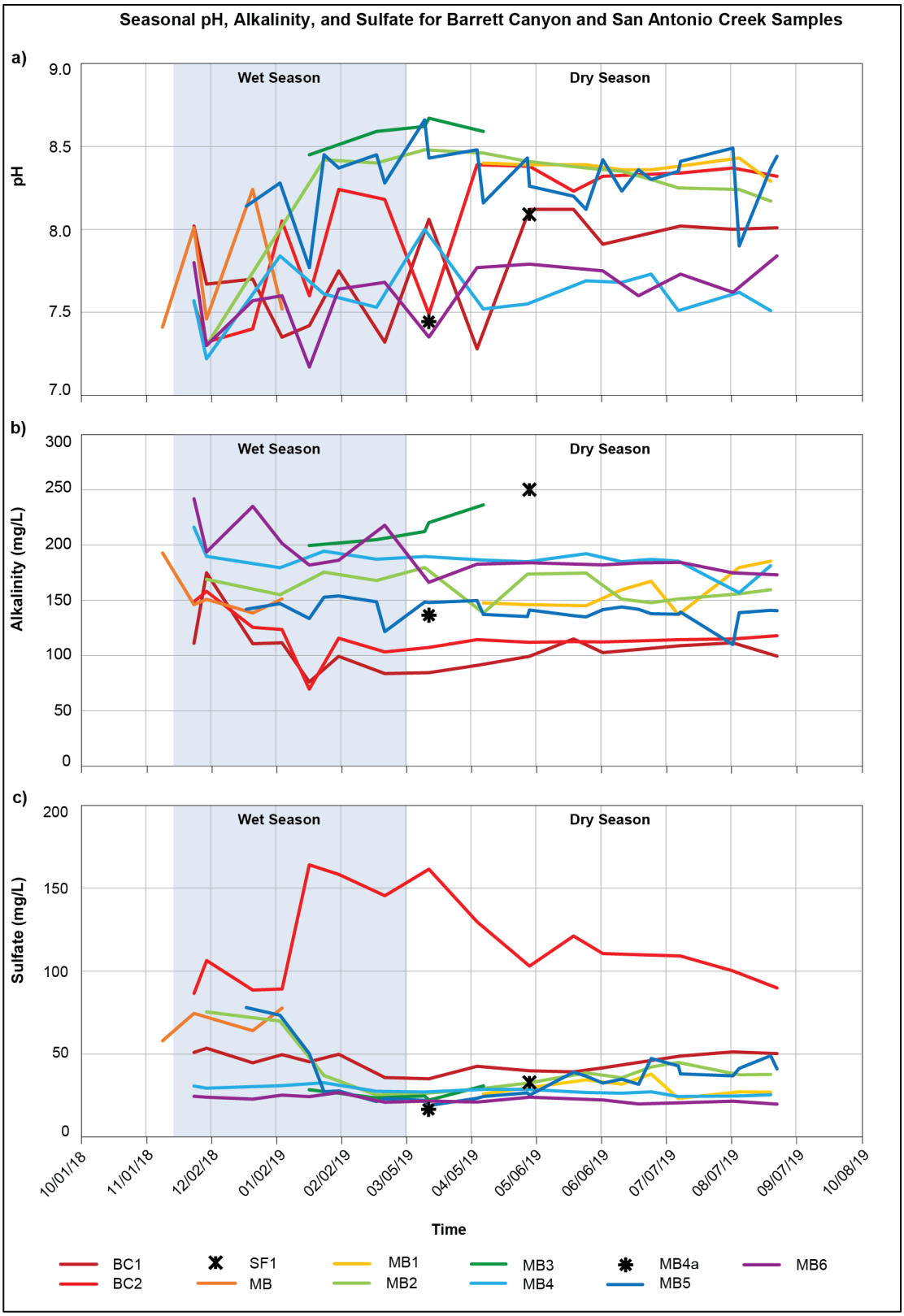

Figure 11a-c: *Seasonal a) pH, b) alkalinity, and c) sulfate trends for the Barrett Canyon area and San Antonio Creek*

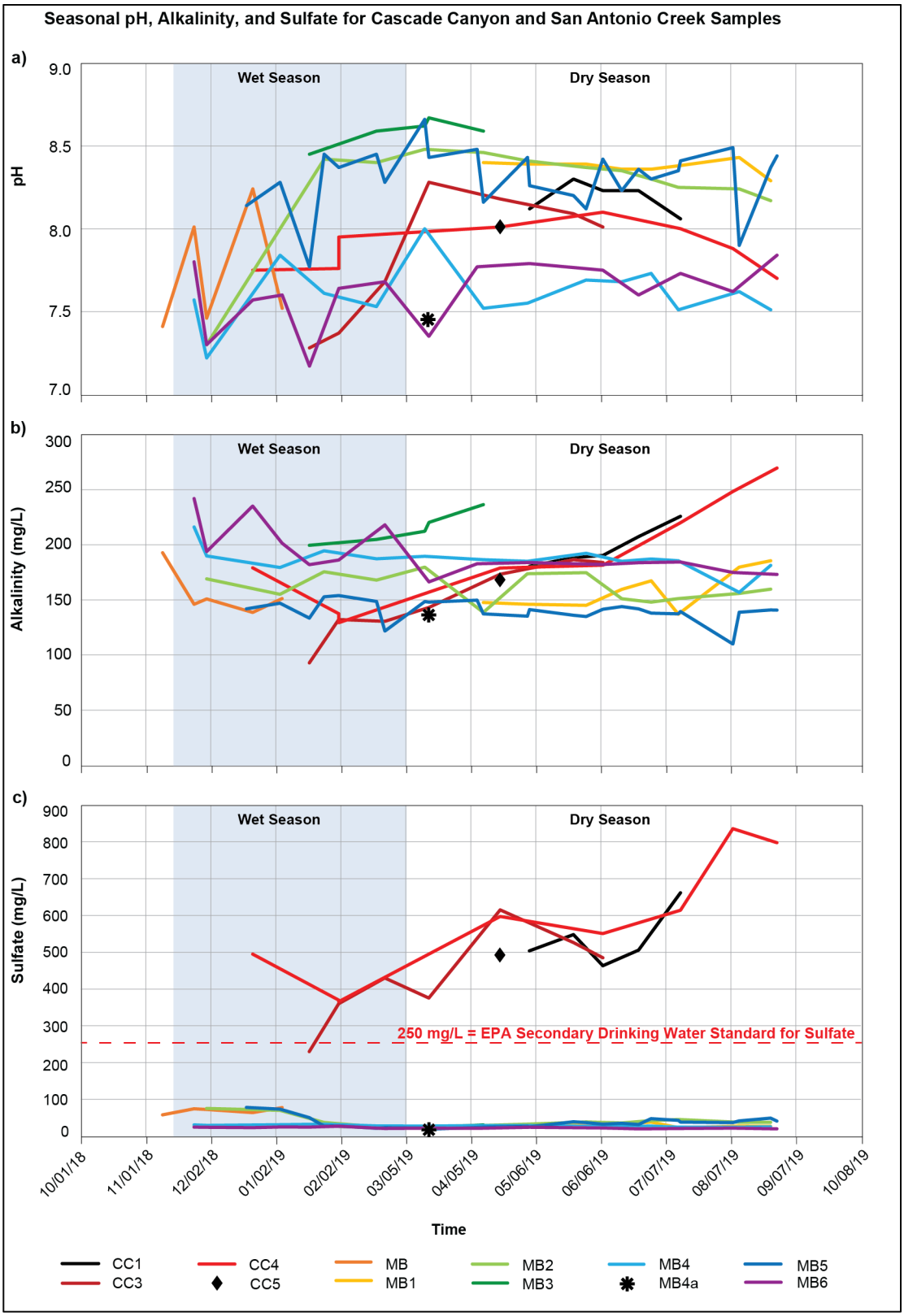

Figure 12a-c: *Seasonal a) pH, b) alkalinity, and c) sulfate trends for the Cascade Canyon area and San Antonio Creek*

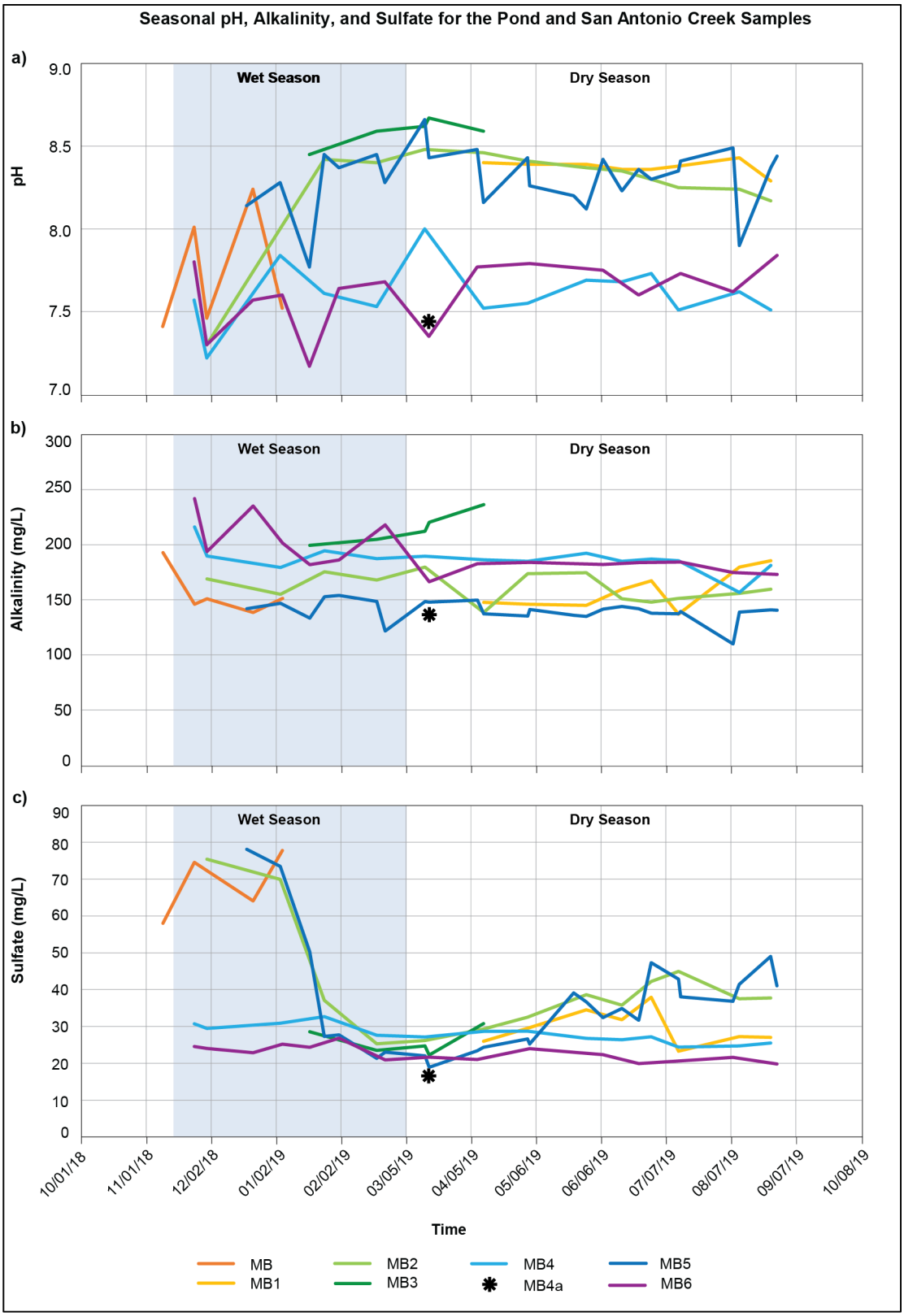

Figure 13a-c: *Seasonal a) pH, b) alkalinity, and c) sulfate trends for the pond, Sierra Powerhouse area, and San Antonio Creek. MB samples isolated to show trends.*

Figure 14a-c: *Seasonal a) pH, b) alkalinity, and c) sulfate trends for the Evey Canyon area and lower San Antonio Creek.*

Icehouse Canyon has the lowest alkalinity compared to most sample sites (Figures 9b and 10b). Water samples were collected away from both significant human population and the zone of elevated sulfate. The waters here are a good indication of both relatively younger waters, and a baseline showing clean groundwater. The alkalinity within the Barrett-Cascade area (Figures 11b and 12b) is higher than the baseline waters in Icehouse Canyon. On average, most sites in Area 2 have elevated alkalinity during the wet season, except for the gaging station (U15-R), Cascade Canyon, and MB3 (Figure 9b). The alkalinity within the Evey Canyon area (Figures 9b and 14b) is on the higher end of the total range and samples are also slightly higher in the wet season. Overall, the wet season increase could be due to natural causes, frequency of sampling, human or mechanical error, or other unknown sources of error.

Anion Analysis

Sulfate concentrations across all samples in the watershed ranges from 11.94 mg/L to 836.23 mg/L. Values will be compared to previous studies, as shown in Table 1. Icehouse Canyon has the lowest sulfate concentrations in the watershed, ranging from 11.94 mg/L to 15.48 mg/L (Figure 9c and 10c), which agrees with the 13.96 mg/L to 30.90 mg/L range provided by (Wicks, 2014 and Soto, 2015). This area provides an average sample of clean groundwater with very little impact from the elevated sulfate.

The Barrett-Cascade area has the highest sulfate concentrations in the watershed, ranging from 35.15 mg/L to 836.23 mg/L (Figures 11c and 12c), which agrees with the 13.95 mg/L to 1706.33 mg/L range provided by (Osborn, unpub. data, 2012, Nourse, unpub. data, 2013, and Yaralian, 2018). When compared to other nearby samples, such as Hogback Spring (labelled MB6), Gaging Station (labelled MB and MB5), and the pond (labelled MB4 and MB4a), the Barrett-Cascade canyon samples (labelled BC and CC) show a dramatic increase (Figure 9c). San Antonio Creek samples collected just upstream of both the Gaging Station and Cascade Canyon's mouth (labelled MB) have a decent amount of sulfate, about 60 mg/L to 70 mg/L.

An interesting finding was that the South Fork Barrett has higher sulfate concentrations than its North Fork (Figure 11c). The mouth of Cascade Canyon (CC1) was dry for most of the sampling duration, but farther up the canyon (sites CC3, CC4, and CC5), the stream experienced low flow. It is likely that the water table is closer to the surface near the top of the canyon than at the bottom. Another interesting finding from fieldwork was that the Cascade Canyon Creek appeared to go underground at or near the

trail intersection (CC3 site), and during times of moderate flow, would surface somewhere downgradient in the mid-canyon.

Sulfate concentrations in the Evey canyon area is fairly low, ranging from 25.98 mg/L to 58.28 mg/L, similar to North Fork Barrett samples (Figure 8c and 14c). This agrees with the 24.78 mg/L to 38.14 mg/L range provided by (Wicks, 2014 and Soto, 2015). See Figures 9c-14c for locational averages and seasonal trends in sulfate concentrations in water samples. Figure 13 isolates "MB" samples (MB-MB6) to better show relationships and seasonal trends.

The pond and Sierra Powerhouse samples are fed by waters unrelated to the Cascade Canyon area. The pond is fed from the Hogback Landslide, represented by the Hogback Spring (labelled MB6) samples. A previous study of Hogback Landslide indicates that, because of the interconnected fracture network, the Hogback Spring likely originated from here (Agunwah, 2020). The Sierra Powerhouse is fed by surface waters of San Antonio Creek, which in turn are derived from farther upstream.

Thin Section Analysis

The NVB-1548 and NVB-1549 rock units, a corundum granofels and a biotite gneiss respectively, were previously collected near the top of Cascade Canyon (Figure 3). Two thin sections were made from each sample and compared to two previous thin sections made from the corundum granofels unit collected from the Spring Hill landslide in the Barrett-Cascade area.

The Spring Hill and 1548 thin sections all show an abundance of altered alkali feldspars, a decent amount of mica (muscovite, sillimanite, and biotite or stilpnomelane), a few corundum crystals a few mm in size, variable amounts of iron oxides (hematite/limonite), and very little quartz. The latter was expected, as corundum forms in rocks with very little silicates, since the two tend to create sillimanite. With respect to iron oxides, the Spring Hill thin sections had very small amounts of hematite/limonite and mostly on the rind of the thin section itself, whereas the 1548A-B thin sections had more iron oxides in veins or fractures (Figures 15 and 16). The 1549A-B thin sections had a decent amount of iron oxides, also as veins or rinds. 1549A shows folding while 1549B shows straight foliation. No pyrite was observed in any of the thin sections, but that doesn’t mean it wasn’t there to begin with. It may have all oxidized away by this point in time.

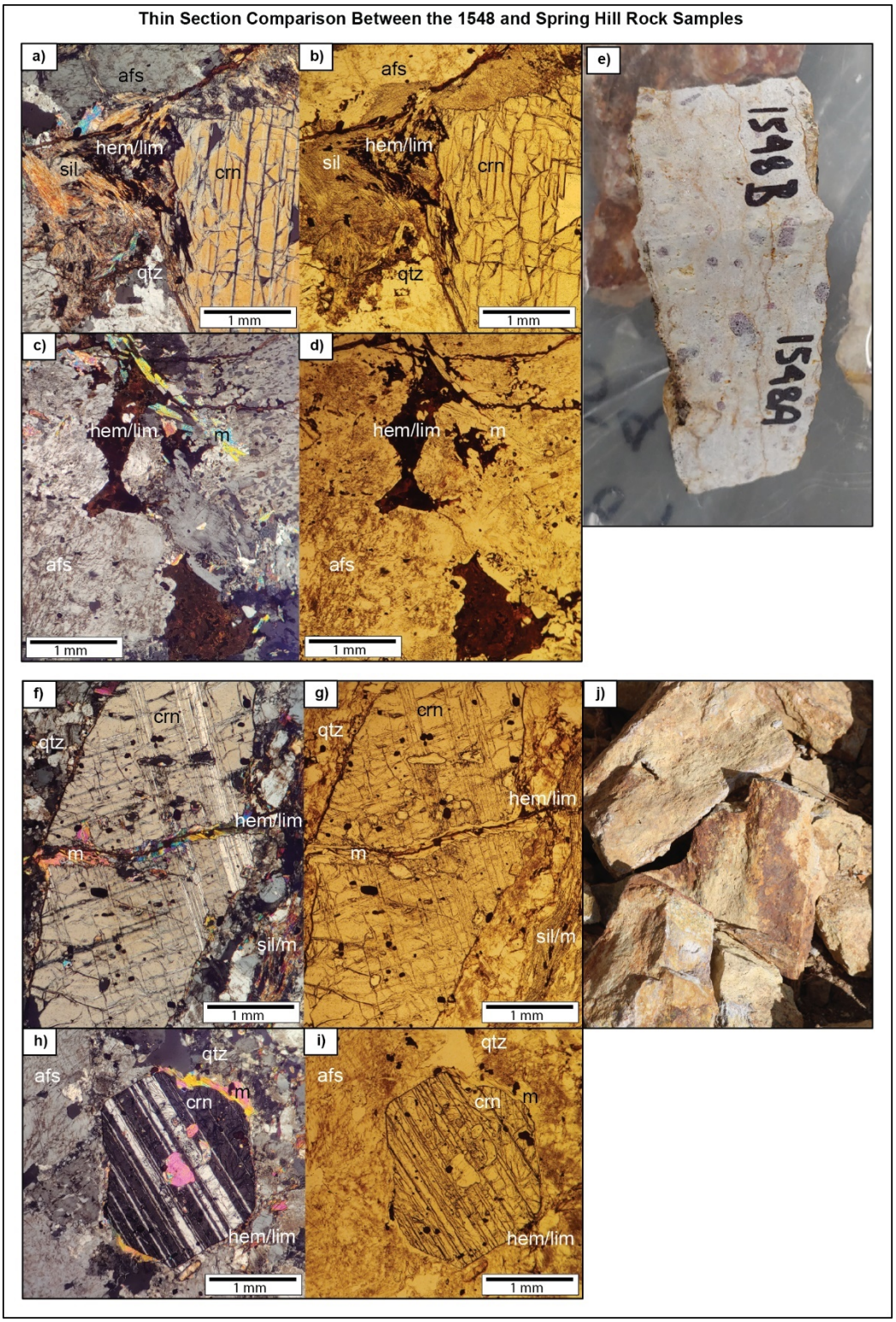

Figure 15: *Images of thin sections showing XPL on the lefthand side, PPL in the middle, and representative rock sample images of each on the far right. Images a-e) show thin sections and an image of the 1549 rock sample. Images f-j) show thin sections and a representative image of the Spring Hill rock sample. Mineralogy is labelled as corundum (crn), altered feldspar (afs), hematite/limonite (hem/lim), sillimanite (sil), muscovite or other micas (m), and quartz (q). The thin sections were viewed under 4x magnification.*

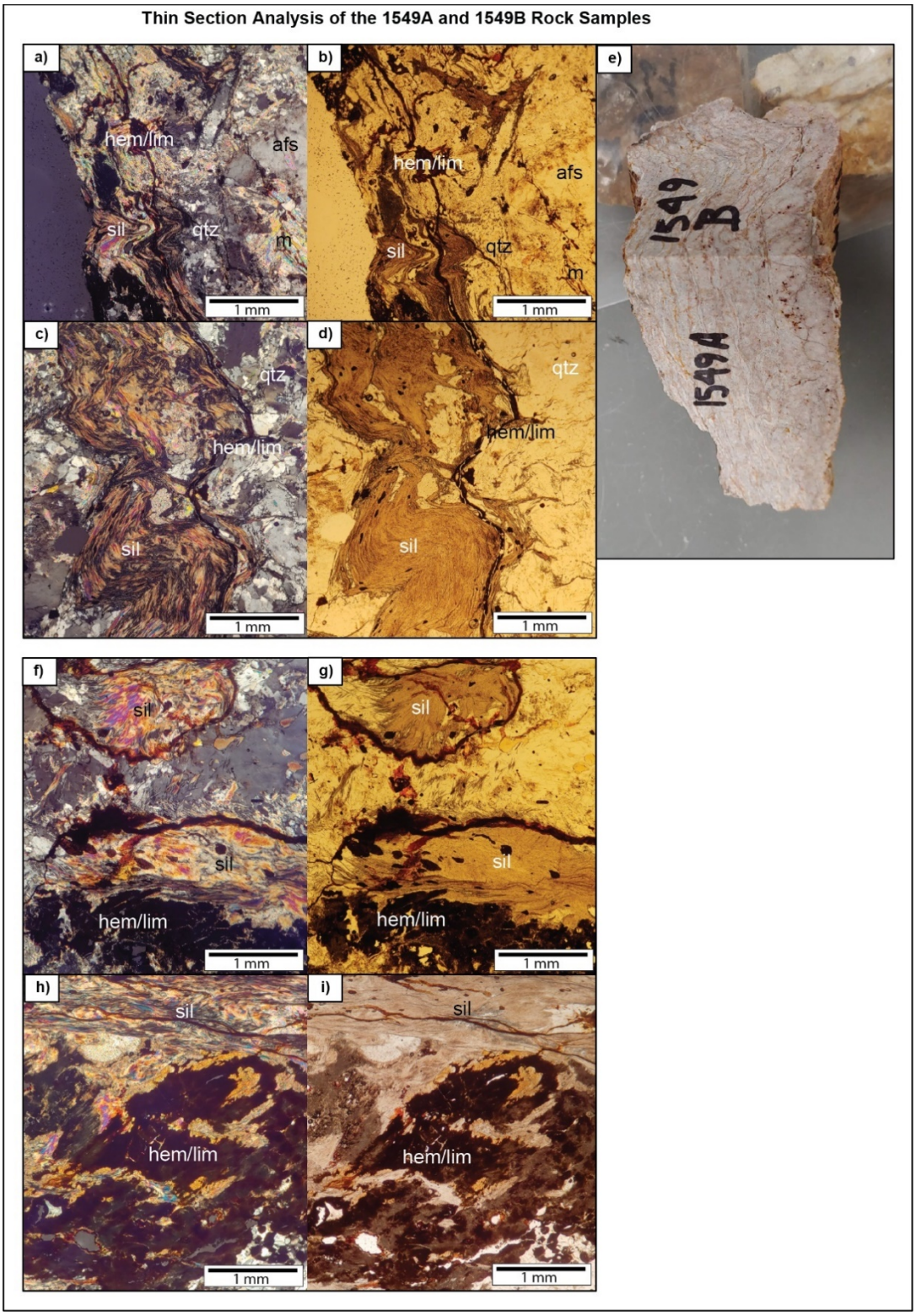

Figure 16: *Images of thin sections showing XPL on the lefthand side, PPL in the middle, and representative rock sample images on the far right. Images a-i) show thin sections and an image of the 1548 rock sample, with a-e being 1549A and f-i being 15489. Mineralogy is labelled as corundum (crn), altered feldspar (afs), hematite/limonite (hem/lim), sillimanite (sil), muscovite or other micas (m), and quartz (q). The thin sections were viewed under 4x magnification.*

Whole Rock XRF Analyses

Based on water quality results, rock samples were collected at strategic points within the San Antonio Canyon Watershed (Figures 2-4 and Table 2). The rock samples were then analyzed using X-Ray Fluorescence (XRF) to provide whole rock geochemistry (Figures 17 and 18). For reference, "sulfur" is reported as SO_3 and "iron" as FeO. Based on these results, sulfur ranges from nondetect to 0.23 wt%, and iron ranges from 0.08 wt% to 7.42 wt% across all rock samples.

Most samples from the same rock type are fairly consistent with each other, although it is more apparent with respect to iron than sulfur (Figures 17 and 18). Samples from some rock types, like the corundum granofels, marble, and alluvium, are more consistent in iron content than in sulfur content. As expected, the quartzites have no detected sulfur, but have a consistently small amount of iron. The unit that varied the most was the biotite gneisses. Both granodiorite samples are consistent in both sulfur and iron and is also similar in iron content to the corundum granofels unit. Many samples, especially the corundum granofels, smelled of sulfur both in the field and during the rock crushing process in the laboratory. The "path" sample was a cobble collected at the pond area, likely derived from Ontario Ridge to the east. I was included for being an example of a weathered and hematite-coated biotite gneiss.

The rock units with the most sulfur include the corundum granofels, followed by the marbles and one alluvial sample, all collected in the Barrett-Cascade area (Figure 17). Samples collected in the Evey Canyon area are mostly nondetect. The rock units with the most iron include the biotite gneisses, followed by the marbles and both alluvial samples

(Figure 18). Samples collected in the Evey Canyon have similar iron concentrations to other samples of the same rock type collected in the upper watershed.

During fieldwork, none of the outcropping units or streambed rocks in the Evey Canyon area exhibited a sulfurous odor, although a decent amount of iron oxide staining was seen on the latter. Many of the Potato Mountain quartzite outcrops have an orange oxidation rind, although an abundance of sulfate is not expected in these samples due to the lack of varied mineralogy in most quartzites. Due to the lack of sulfurous odor in rock samples, as well as the lower concentrations of sulfate in water samples, the Evey Canyon area is not expected to be the source of the elevated sulfate.

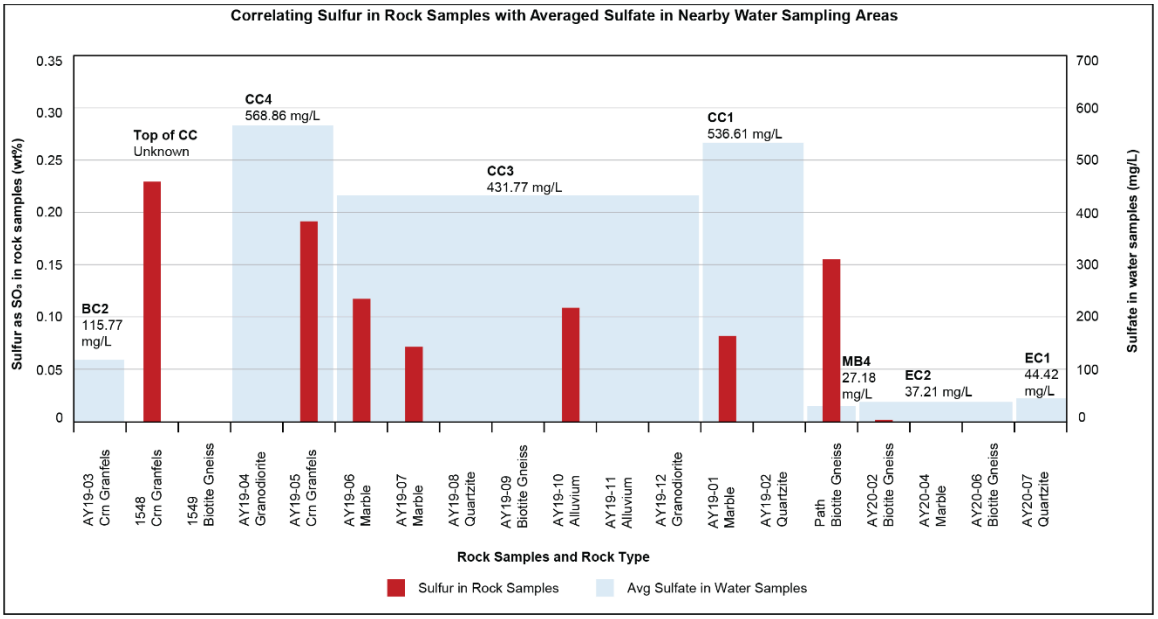

Figure 17: *Sulfur concentrations in rock samples compared to average sulfate concentrations from nearby water sample sites.*

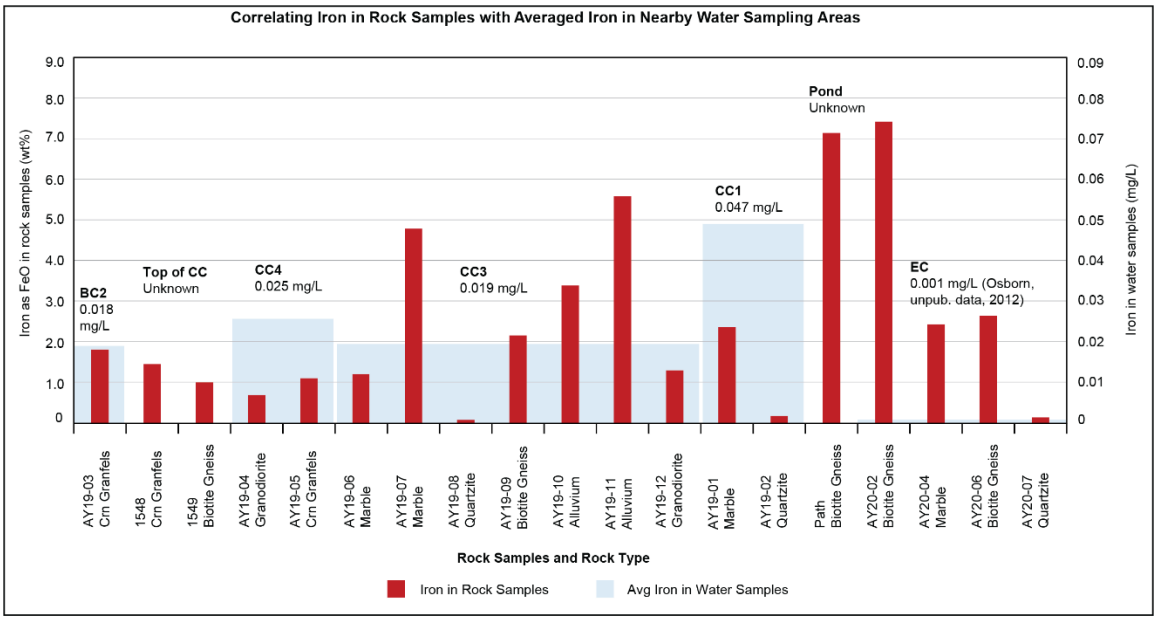

Figure 18: *Iron concentrations in rock samples compared to average iron concentrations from nearby water sample sites.*

Cation Analyses from the Barrett-Cascade Area Water Samples

Most samples were intended to be analyzed at UCR for anion analysis on the ICP-OES, but due to unforeseen circumstances, only the first round of samples was sent. This included the South Fork Barrett Canyon and Cascade Canyon samples, due to their elevated sulfate concentrations relative to the other areas. For reference, iron is reported as total iron, as the ICP-OES does not differentiate between Fe(II) and Fe(III). However, given the latter is nearly insoluble, the iron within the water samples is more likely to be Fe(II)

Iron in the South Fork Barrett samples range from nondetect to 0.05 mg/L. Iron in the Cascade Canyon ranges from nondetect to 0.16 mg/L (Figure 19). Areas with the highest iron content includes the upper Cascade (labeled CC5) and lower Cascade (labelled CC1). Compared to Barrett Canyon samples, the Cascade Canyon samples have higher concentrations of other cations, including Ca, Mg, Na, K, Si, and Sr (Table 5). Unfortunately, no Icehouse Canyon samples were sent to get a good baseline for cations, but we suspect the waters to reflect the clean groundwater source.

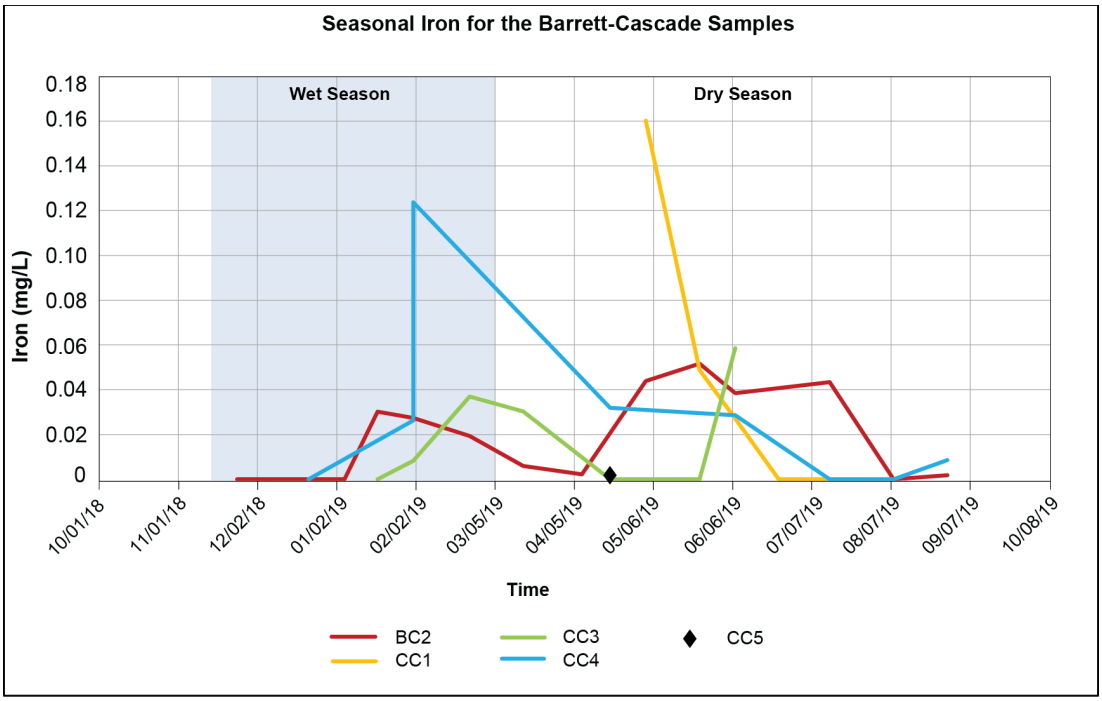

Figure 19: *Seasonal iron trends for the South Fork Barrett Canyon and Cascade Canyon area. The wet season is represented by the semi-transparent blue box.*

DISCUSSION AND INTERPRETATION

Hydrogen sulfide typically has a rotten-egg odor that can be detected in waters with just a few tenths of a mg/L (Hem, 1985). The geologic units in the Barrett-Cascade area, specifically the marble and corundum granofels/schist units, were found to have a light to moderately strong “rotten egg” odor, indicating a significant presence of sulfur.

Sulfate concentrations are highest when geochemical conditions are most favorable. This typically includes 1) a reducing fluvial environment, 2) a moderately to highly fractured metasedimentary or intrusive bedrock rich in sulfides, and 3) ideal environmental conditions (Hem, 1985). In a reducing environment, elevated sulfate may be due to microbial activity and decaying organic matter rather than local geology. However, the study area appears to be mostly oxidizing, so the local rocks are likely to have a greater effect. The rocks that typically contain pyrite include sedimentary, metasedimentary, or intrusive. High concentrations of sulfate can be found in groundwater if the local rocks are heavily fractured. Deeper groundwater can migrate up these fractures and either mix with the local shallow groundwater or precipitate out as mineral deposits. Such mixing typically causes a sharp increase in alkalinity, often much higher than that of ocean water. However, such mixing is not expected in this location (Soto, 2015). Based on preliminary alkalinity data, much of the water has been underground at some point, but not seemingly enough to become a deep brine. Mineral deposits can be of interest to mining, as certain minerals or metals can precipitate out in certain areas.

Sulfate Concentrations Throughout the Watershed

In a typical watershed system, the concentration of dissolved ions in the trunk stream will typically increase downgradient, since the trunk stream is an accumulation of waters from all the tributaries that feed into it. By observing the concentrations of sulfate, or other dissolved substances, we can get a good idea of where the source of the substance is. If there is a localized area with elevated ion concentrations, the source likely originates from that area.

To compare samples, a baseline of clean groundwater is needed. Icehouse Canyon is one of the uppermost canyons in the watershed, and across all samples, the ones collected here have the lowest sulfate concentrations and alkalinities. This indicates that the groundwater here is relatively young and clean, away from the zone of elevated sulfate. The local geology consists of mostly granitoids, mylonites, and gneisses, which are unlikely to contain significant pyrite.

Sulfate concentrations in the Barrett-Cascade area are anomalously high compared to the rest of the watershed, even compared to other surface waters nearby. Results from this study show a high of 836.23 mg/L in this area, while previous studies show a high of 1,706.33 mg/L (Yaralian, 2017). This indicates that the source of the sulfate lies in this localized elevated zone. More specifically, in the upper reaches of the Cascade Canyon Creek (Figure 12c), where the sulfate concentrations are highest. The local geology in the Barrett-Cascade area consists largely of metasediments and intrusive units, which can contain significant pyrite. MB samples are slightly higher than MB5. Although both are close to one another, the increase is likely from MB being downgradient, and a little closer to, Barrett Canyon. Downstream, the values are

unusually low, given Cascade Canyon's elevated values. This is likely due to dilution from the other tributary streams which are relatively clean.

Both the Hogback Spring and Evey Canyon area shows moderately low sulfate concentrations, >80 mg/L (Figures 11c, 13c, and 14c). The Hogback Spring is sourced from the Hogback Landslide, which is the likely sulfate contributor to the pond waters. However, there may also be some anthropogenic sources since the spring lies along a popular hiking trail. Hikers often bring their dogs or horses, and waste can be a source of sulfate. Foot traffic can also carry substances to other areas or waterways. The geology of the Hogback Landslide includes mostly blocks of granitoids and gneisses. Although the Evey Canyon samples have moderately low sulfate concentrations, a downstream increase in sulfate is observed in this study as well as (Soto, 2015). This could be due to sulfate-rich groundwater feeding in from rocks to the west of the Evey Canyon Fault, which are similar to rocks in the Barrett-Cascade area. Rocks exposed upstream of the fault yielded clean waters about 15.9 - 32.1 years old (Lenhert and Soto, 2015 and Soto and Lenhert, 2015). The local soils could also be contributing some sulfate to the system, although more study is needed to confirm this. Evey Canyon geology is vastly different from that of the rest of the watershed due to the Evey Canyon fault and the San Antonio Canyon Fault.

Seasonal Effects of Sulfate

Meteoric and groundwater are the two main sources of water in the area. Many streams within the San Antonio Canyon Watershed appear to have continuous flow, indicating that they are fed by groundwater, via springs, with an additional volume of meteoric water during the wet season. There may be more than one body of groundwater present, but more study is needed to provide a definitive answer.

When observing the seasonal effects of sulfate, it is important to also observe trends in other water quality parameters to provide insight into any hydrogeochemical reactions taking place. In this section the seasonal trends shown in Figures 8-13 will be discussed. Icehouse Creek has only three samples in the dry season, so no significant trends can be interpreted here.

The Barrett-Cascade samples show a distinct seasonal trend. Both forks of Barrett Canyon, show an increase in sulfate during the wet season, albeit more pronounced in the South Fork. Cascade samples increase in sulfate in the dry season. This increase in sulfate could indicate an abundance of redox reactions, like the ones shown below, taking place due to increased rainfall and infiltration into the subsurface. There could also be some "flushing out" of sulfates that accumulated during the dry season.

Pyrite Oxidation: *sulfur is oxidized to sulfate and Fe(II) is released*

$$2\ FeS_2 + 7\ O_2 + 2\ H_2O \Rightarrow 2\ Fe^{2+} + 4\ SO_4^{2-} + 4\ H^+$$

The upper Cascade Creek was flowing year-round, so it is likely that the water table is always higher there. If the corundum granofels unit exists at depth and is constantly interacting with the groundwater near the surface, it could explain the increase in sulfate

during the dry season. In addition to this, the warm weather could initiate more chemical reactions.

An interesting trend can be found in Barrett Canyon's pH, where it transitions from erratic in the wet season to more static in the dry season. This saw-toothed trend could likely show pulses of meteoric waters to the area, from large storm events and possibly snowmelt. This erratic to linear trend shows a transition from mixed groundwater and meteoric waters in the wet season to a pure groundwater source in the dry season. This relationship can be seen in other areas as well, such as Hogback Spring, much of the main San Antonio Canyon samples (labeled MB), and Evey Canyon.

The Hogback Spring and pond area samples (labeled MB6 and MB4/MB4a, respectively) are from the same source and are expected to have similar trends. However, we see inverse relationships in sulfate, pH, and alkalinities between these sites (Figure 12). These samples show a slight increase in sulfate during the wet season as well as a similar pH trend to other areas. The pond has decent inflow and outflow, so it is likely to have more groundwater than meteoric waters, much like many of the perennial streams in the watershed. The pond also has an abundance of aquatic plant and animal life, which has its own nutrient cycles.

The Gaging Station area (labeled MB and MB5) samples have no apparent seasonal trend, likely because water from other canyons upstream drowns out any local signature. These samples also have a slight sawtooth pattern which could also indicate pulses of meteoric waters to the system.

Similar to the Barrett Canyon samples, the Evey Canyon and lower San Antonio Creek samples also show the same distinct increase in sulfate during the wet season,

which could also be the result of increased redox reactions in the subsurface. A similar interesting trend to the one discussed above can be seen in the pH (Figure 13a), where it increases in the wet season into the dry season, after which it levels off. The lower pH could be due to abundant redox reaction staking place and creating enough sulfuric acid to counteract any buffers taking place as a result of the granitic and/or metamorphic rocks.

Source of Anomalous Sulfate

There are three possible sources of sulfur in the environment. The first is decomposing organic matter. This involves the chemical breakdown of organic matter by bacteria, generally in reducing environments, which then releases hydrogen sulfide as a waste product. Under reducing conditions, microbes reduce the sulfate to sulfide which, combined with Fe2+, forms monosulfides. These are highly reactive and may oxidize during dry periods and leach out into streams during wet periods (Huntington, T.G., 1994). Although groundwater is a dominant source for most streams, waters generally become oxidized once they interact with the atmosphere, by either entering the shallow subsurface or flowing out a spring.

In reduced environments, a sulfurous odor is likely to be present in the waters and in the immediate areas. For the most part, no sulfurous odors were detected within the study area. On some sampling days, there was a mild sulfurous odor at Hogback Spring, and only when the face is very close to the muddy ground next to the stream. The other was next to the corundum granofels blocks within the Spring Hill landslide. Although the

area is largely oxidative, there are likely smaller localized areas of reduction. Overall, it appears unlikely that this is the main source of the elevated sulfate.

The second type of environmental sulfate source is precipitation from environmentally impacted areas or inflow from contaminated areas. With respect to the former, this occurs in areas with poor air quality (e.g., smog). Sulfur dioxide in the atmosphere reacts with water vapor and oxygen to form sulfuric acid, outlined in formula 1) below. Water droplets with sulfuric acid, in addition to carbonic acid from CO_2 in the atmosphere, fall to earth as acid rain. When the acidic rainwater falls into the surface waters, it becomes sulfate, as outlined in formula 2) below.

$$1)\ 2SO_2 + 2H_2O + O_2 \rightarrow 2H_2SO_4$$

$$2)\ H_2SO_4 + 2H_2O \rightarrow 2H_3O + SO_4$$

In these cases, water samples throughout the watershed will show higher sulfate concentrations of about >10 mg/L during large rain events. Although most samples show higher sulfate concentrations during the wet season, there does not appear to be a distinct increase during each storm event across all samples. In addition to this, some sulfate may be taken up by the abundant plant life, as sulfur is a required nutrient for plants. To support this, the elevated sulfate exists in one area instead of uniformly throughout the watershed. With respect to the latter, although there are some abandoned mines in the upper Cascade Canyon (Figure 7), the exact inflow from these mines is unclear. Further study is needed to determine if any mines exist in the vicinity of the corundum granofels unit as well as their sulfate output.

The third type of environmental sulfate source is from geochemical reactions with the local rocks. The sulfur is immobile due to being locked up in the rocks. The two most

common sulfur minerals include gypsum and pyrite, but the former is not found within the study area (Soto, 2015). The latter, along with minerals like graphite, is often associated with reducing environments. Although no pyrite was observed in the thin sections, it could still be present in some samples. With respect to graphite, it can be found in some rocks within the upper watershed area.

Pyrite weathering is known to be a source of sulfate in surface waters. When a body of water interacts with sulfide minerals in the rocks, it will form sulfide or sulfate depending on the redox conditions of the water, along with abundant oxidized iron. As stated previously, sulfate is far more mobile in water than iron since the latter prefers to sorb the nearby rocks, leaving a distinct red-orange coating of iron oxide. This coating can be seen in many streamchannel rocks throughout the watershed and helps support that the local geology is the most likely source for the elevated sulfate.

From water sample data, it is clear that the elevated sulfate originated from the Cascade Canyon area, more specifically in the upper canyon area (Figures 21, 22, and 23). The rock unit containing the most sulfate is the corundum granofels unit (Figure 17), which outcrops near the ridge above Cascade Canyon and as blocks in the Spring Hill landslide deposit within the Barrett-Cascade canyon area (Figure 5). As previously mentioned, this unit has a distinct sulfurous odor with a yellow to orange coating, with some blocks stained black from a previous wildfire. The biotite gneisses were second highest in sulfate concentration and outcrop mostly on the western side of the canyon. The marbles and undifferentiated metasediments are third highest in sulfate concentration and outcrop in great quantities throughout the northeast and southwest part of the watershed.

Although two outcrops from the Cascade Canyon are oriented S75°W/52°NW (AY19-06) and S84°W/84°NW (AY19-07), most units in the area dip to the NE and have shallower dips, indicating folding in the area. The sulfur-rich units in or near the upper Cascade Canyon may be supplying the bulk of the sulfate to Cascade Creek, as well as a decent amount to the South Fork Barrett Creek. North Fork Barrett Canyon may be too far upsection to be influenced by the elevated sulfate zone, despite the Barrett-Cascade area being mostly geologically similar (Figure 20).

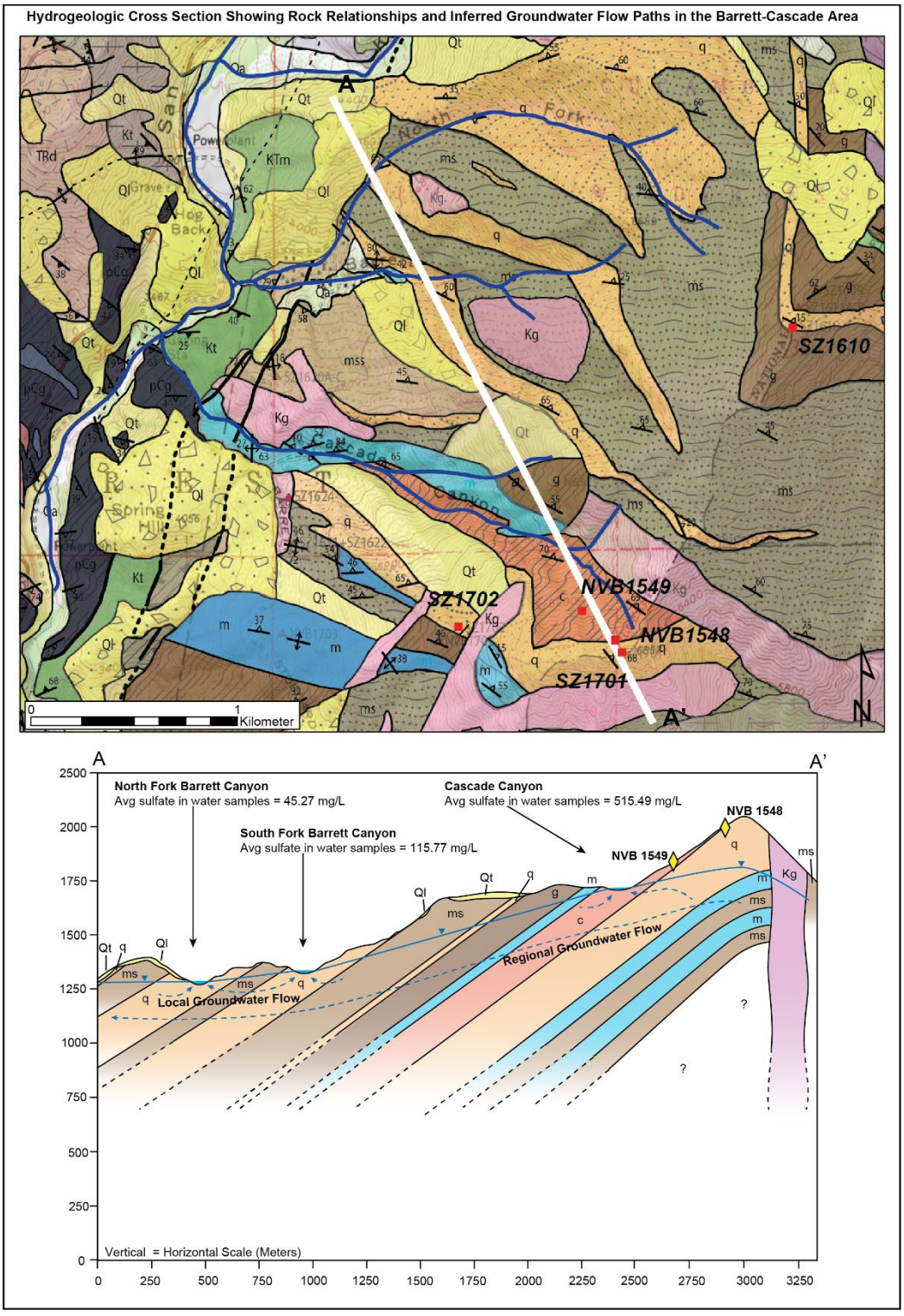

***Figure 20**: Geologic map and cross section of the upper Cascade and Barrett canyons, modified from (Zylstra, 2017). Relevant map units as follows: m=marble, c=corundum hornfels, q=quartzite, g=biotite gneiss, ms=undifferentiated phyllite or schist, Kg=granite, Qt= talus, Qls=landslide, Qa= alluvium. Transect A-A' is shown in addition to streams (blue lines). Cross section includes the water table (blue line with blue triangles), inferred flow paths (blue dashed lines with arrows), two nearby rock samples (yellow diamonds), and the average sulfate within the water samples from each area.*

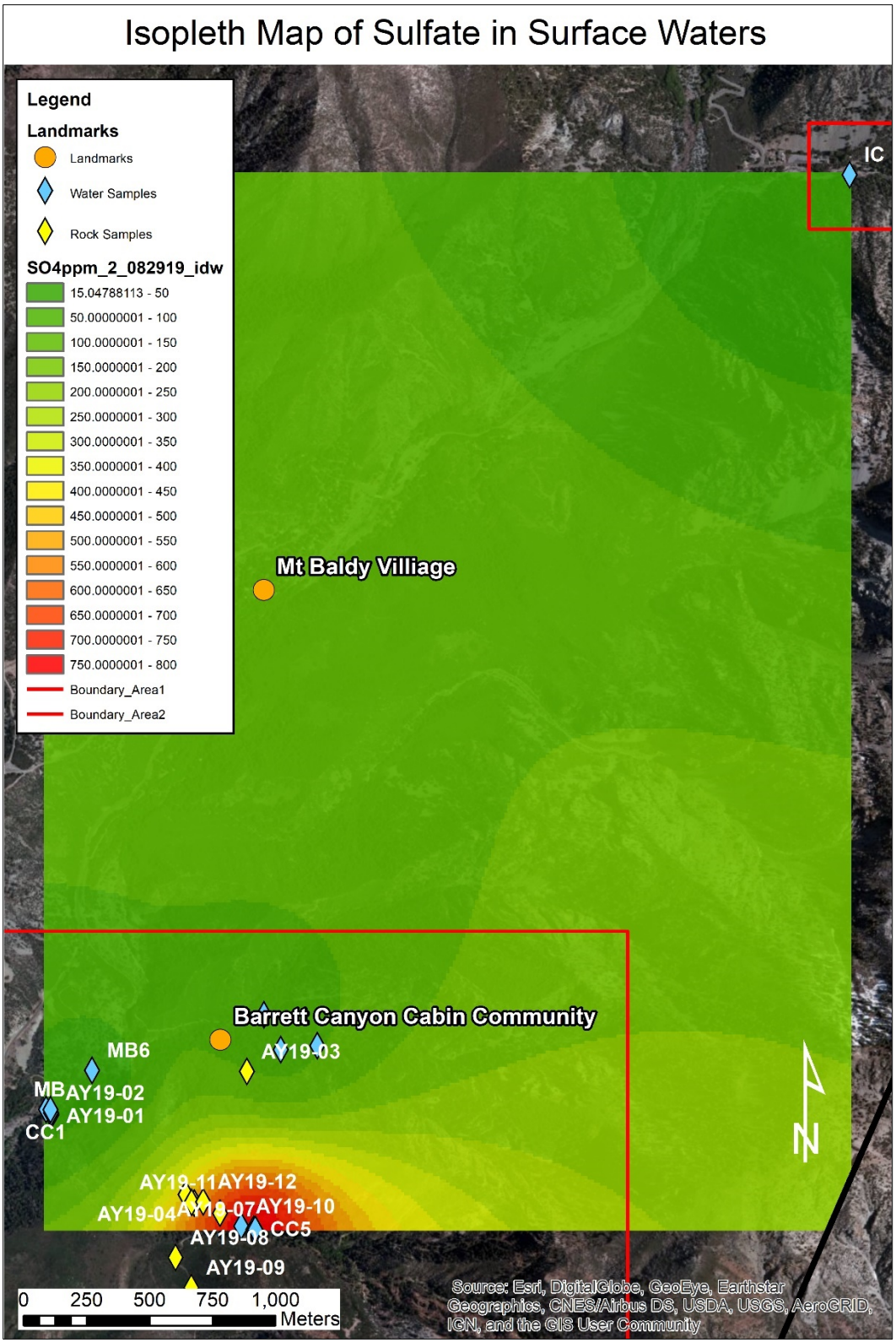

Figure 21: *Isopleth map showing sulfate concentrations in the upper watershed area for water samples collected on 08/29/19, with red indicating the high values and green indicating the lows.*

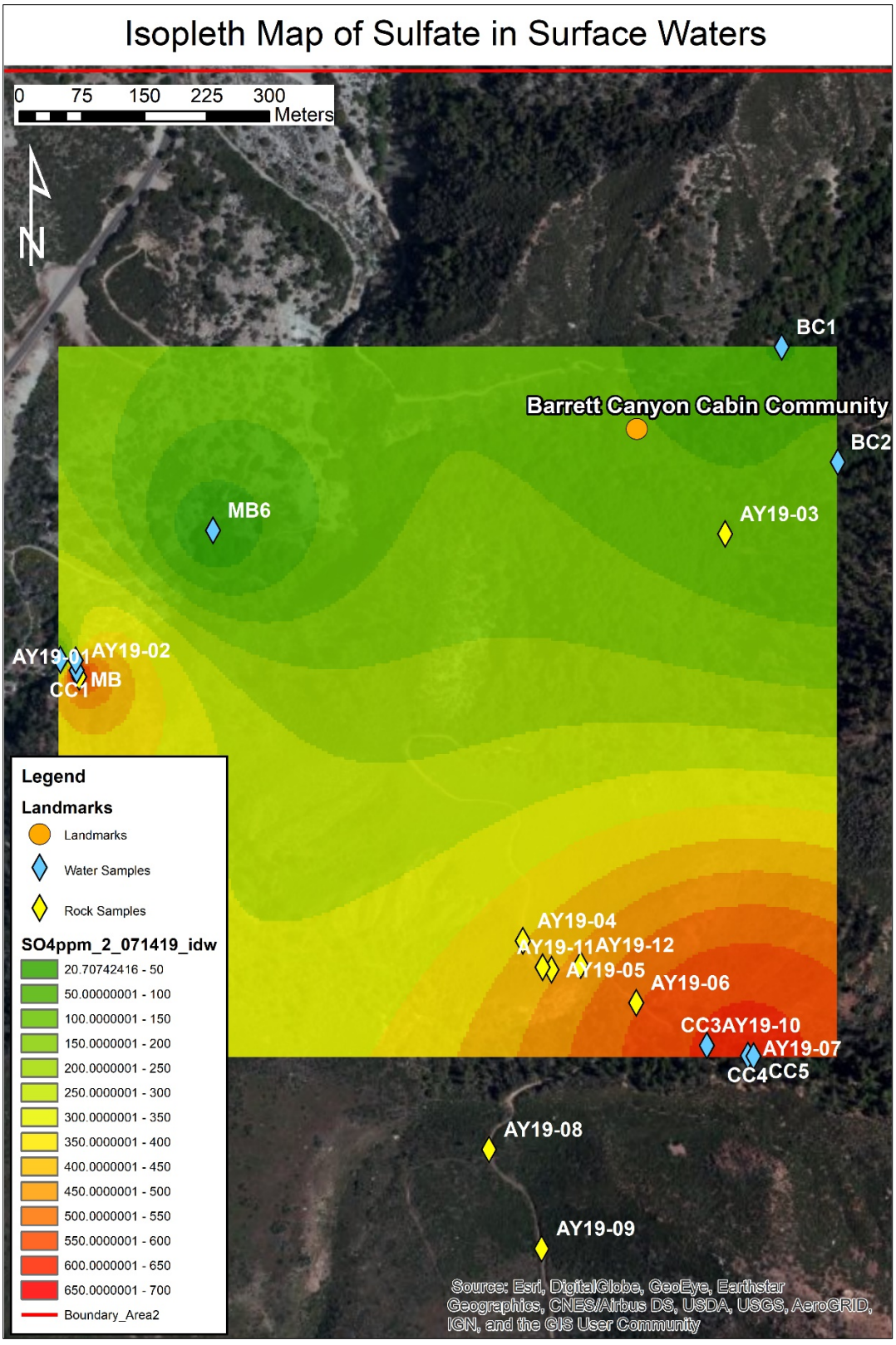

Figure 22: *Isopleth map showing sulfate concentrations in the Barrett-Cascade area for water samples collected on 07/14/2019, with red indicating the high values and green indicating the lows.*

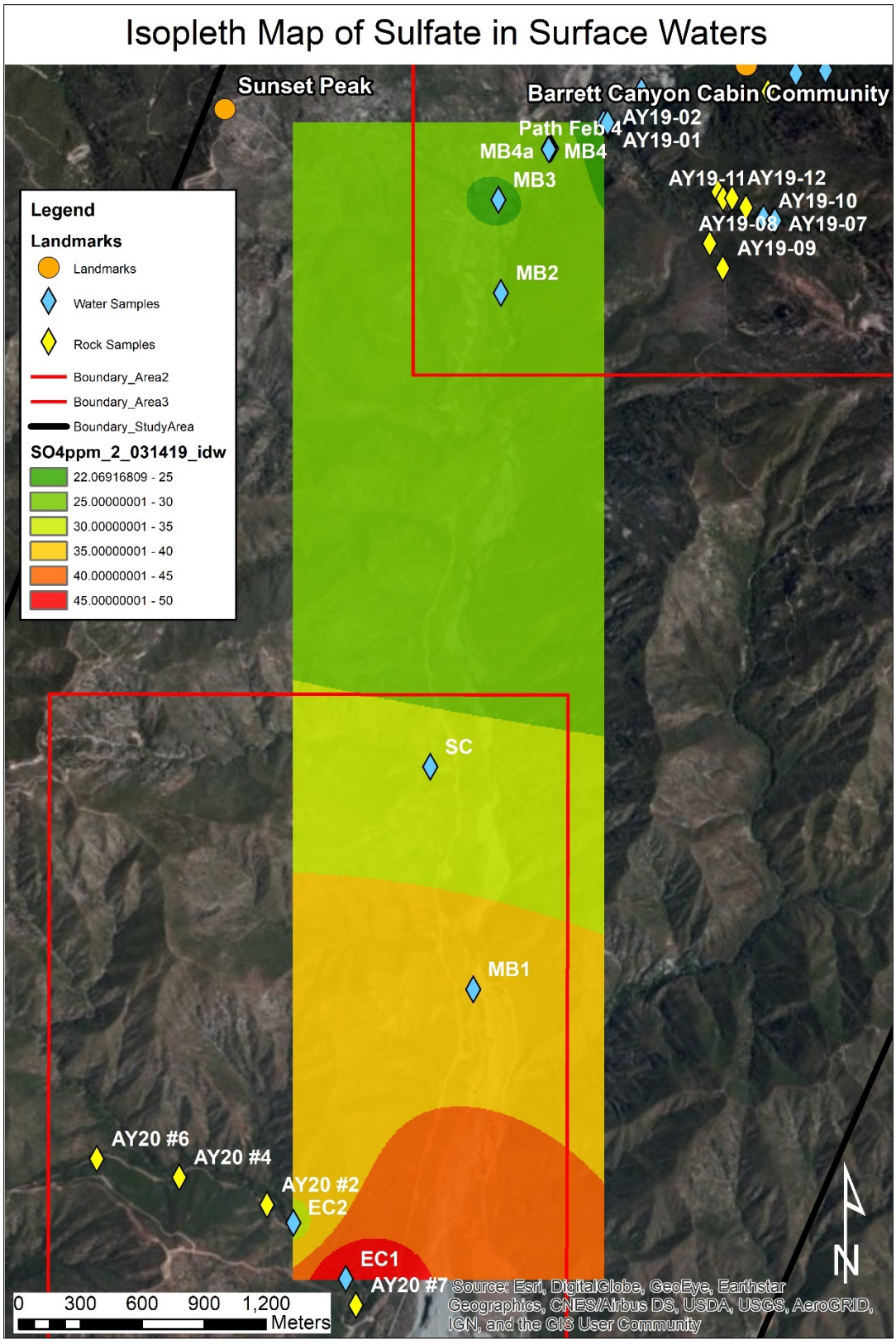

Figure 23: *Isopleth map showing sulfate concentrations in the Evey Canyon and Pond area for water samples collected on 03/14/19, with red indicating the high values and green indicating the lows.*

With respect to iron, concentrations across the rock samples are variable, but units containing the most iron include the biotite gneiss, alluvium, and marble (Figure 18). The granodiorite and quartzite samples contained the lowest iron concentrations, which is to be expected from quartzite. A significant amount of iron was expected for the corundum granofels/schist samples, but they fell on the lower part of the total range. It is unclear why the sample with the most sulfate is among those lowest in iron.

The pH of waters in the watershed is higher than expected from an area with elevated sulfate. The local geology can explain this, since the areas is dominantly granitoids, intrusives, and metasediments. Bedrock tends to raise the pH of groundwater and act as a buffer to acidic inputs, so this may explain why the pH doesn't change much.

Sulfate Leaching

Although significant data could not be obtained, the likelihood that there is measurable down-gradient leaching from the sulfur-rich bedrock, landslide deposits, or sulfur-rich stream sediments cannot be ruled out. One alluvial sample from the Spring Hill landslide, within the vicinity of the corundum granofels blocks, contained 0.11 ppm of sulfate while the other from that area was nondetect. There were no alluvial samples collected from the Hogback Spring or Hogback Landslide. Based on the sulfate from water samples, the Hogback Spring appears to have some leaching, as it is derived from the Hogback Landslide and shows similar seasonal trends to most other sites. However, further studies are needed to determine if any significant sulfate leaching is taking place.

Potential Health Hazards of Elevated Sulfate

This project is important not only for general research, but for human and environmental health. The area is used extensively for residential and recreational uses, with many hiking trails and campgrounds to choose from. Nearby streams and springs are a source of water for visitors, residents, and the local biota. The ecosystem also has its own environmental quality requirements, and human interactions can impact these requirements. When hikers refrain from cleaning up after themselves or their pets, the waste often introduces bacteria or other contaminants into the water or soil.

Access to clean and safe water is an essential need, and due to its frequency of use, is imperative not only to the locals but to those downgradient. This is because water quality in one area may potentially impact the water quality downgradient. There are about 36 cabins in the Barrett-Stoddard Canyon area, all of which obtain their water directly from local streams via pipes or buckets. The quality of these surface waters is more important for them than the other stakeholders downgradient. This is because their water is mostly unfiltered, while the people in Las Angeles get their water already filtered and cleaned. To avoid possible illness, many residents filter and boil their water before use. Boiling kills bacteria and pathogens but may not always remove all dissolved substances.

High concentrations of sulfate above are not immediately harmful to people, aside from a laxative effect, a bitter taste, or possibly an unpleasant rotten egg type odor (EPA, 2019 and EPA, 2003). Some studies were conducted to determine if drinking water with elevated sulfate affected pregnant mothers who planned to breastfeed, and later, their children, but more studies are needed to confirm this (EPA, 1999, WHO 2004, and EPA,

2003). However, there were some cases of diarrhea in infants, so anyone with intestinal sensitivities may be more at risk.

CONCLUSIONS

Based on this project, a series of conclusions can be made. 1) An elevated sulfate anomaly was identified in surface waters within the South Fork Barrett and Cascade Canyons, ranging from 86.65 mg/L to 836.23 mg/L, with a minor anomaly in Evey Canyon, ranging from 30.02 mg/L to 58.28 mg/L. This anomaly is relative to baseline values shown in Icehouse Canyon and lower San Antonio Creek, with ranges of 11.94 mg/L to 15.48 mg/L and 23.28 mg/L to 37.96 mg/L, respectively. 2) A seasonal increase in sulfate during the wet season was observed in most areas and may be due to increased water infiltration into the subsurface catalyzing the pyrite-oxidation reactions, or a seasonal "flushing out" of sulfates that accumulated during the dry season. Cascade Canyon oppositely shows an increase of sulfate during the dry season, which may be due to the elevated water table in that area. There may also be a transition between a mixture of meteoric waters during the wet season to purely groundwater during the dry season. 3) The source of the sulfate anomaly is likely bedrock exposed in the Barrett-Cascade Canyon area as well as the upper Evey Canyon area, from which groundwater is apparently leaching sulfate. These units are similar but have been displaced by the San Antonio Canyon and Evey Canyon faults. The primary bedrock source is likely the sulfurous-smelling, corundum-bearing unit, which outcrops in the upper Cascade Canyon, with additional blocks within the Spring Hill landslide in parts of the South Fork Barret-Cascade Canyon area. Units in Cascade Canyon are dipping to the NW and may

project into the South Fork Barrett Canyon, but North Fork Barrett Canyon may be too far upsection to show any effect. 4) Most Cascade Canyon samples exceeded the EPA secondary standard for sulfate in drinking water, 250 mg/L (EPA, 2019), but the rest of the water samples were below it. Drinking water that is well above the EPA secondary standard for sulfate can cause diarrhea in infants and people with intestinal sensitivities, so people drinking water in the Barrett-Cascade region should filter and test their water regularly for potential issues.

FUTURE RESEARCH

Possible future research projects could include using stable oxygen and sulfur isotopes to distinguish between different types of water sources and if the anomalous sulfate concentrations are caused by pyrite oxidation, longer sampling duration to include a wet year and a dry year (e.g., both an el nino and a la nina cycle) and including a larger sample size for both rock and water samples. Soil analysis could be conducted to determine the pH and sulfur concentrations present within the soil. The soils may provide sulfate to the system.

REFERENCES

Agunwah, R.I., 2020, Geology and Fracture Geometry in Source Region of Hog Back Landslide, Eastern San Gabriel Mountains, with Implications for Failure Mechanisms: [Thesis]: Pomona, California Polytechnic University.

Andrews, J.E., et al. 2004, An Introduction to Environmental Chemistry -2nd ed: Cornwall, Blackwell Science Ltd.

Basin AMD Chemistry, Enviro Sci Inquiry, http://www.ei.lehigh.edu/envirosci/enviroissue/amd/links/science2.html.

Bloom, C.S., 2012, Investigation of Base Flow Recession of Lower San Antonio Creek and Surrounding Springs: [Thesis]: Pomona, California Polytechnic University.

Bowell, R. J. (2004): A review of sulphate removal options for mine waters. – In: Jarvis, A. P., Dudgeon, B. A. & Younger, P. L. (eds): mine water 2004 – Proceedings International Mine Water Association Symposium 2. – p. 75-91, 6 fig., 7 tab.; Newcastle upon Tyne (University of Newcastle).

Boyd, C.E., and , 2020, Typical chemical characteristics of full-strength seawater - responsible seafood advocate: Global Seafood Alliance, https://www.globalseafood.org/advocate/typical-chemical-characteristics-of-full-strength-seawater/ (accessed December 2021).

Christophersen, N. and Seip, H.M., 1982, A Model for Streamwater Chemistry at Birkenes, Norway: Water Resources Research, v.18, p.977-996, doi: 10.1029/WR018i004p00977.

Cravotta, C.A., 2006, Relations Among PH, Sulfate, and Metals Concentrations in Anthracite and Bituminous Coal-Mine Discharges, Pennsylvania: Journal

American Society of Mining and Reclamation, v. 2006, p. 378–408, doi: 10.21000/jasmr06020378.

EPA, 2003, Drinking Water Advisory: Consumer Acceptability Advice and Health Effects Analysis on Sulfate, p.1-23.

EPA, 1999, Health Effects from Exposure to High Levels of Sulfate in Drinking Water Study, p.2-19.

EPA, 2019, Secondary Drinking Water Standards: Guidance for Nuisance Chemicals, https://www.epa.gov/dwstandardsregulations/secondary-drinking-water-standards-guidance-nuisance-chemicals (accessed June 2019).

Faure, G. 1998, Principals and Applications of Geochemistry: A Comprehensive Textbook for Geology Students-2nd ed. New Jersey, Ohio State University, Prentice Hall.

Garrels, R.M., and Mackenzie, F.T., 1967, Origin of the Chemical Compositions of Some Springs and Lakes: Advances in Chemistry Equilibrium Concepts in Natural Water Systems, p. 222–242, doi: 10.1021/ba-1967-0067.ch010. Gray, D. 2000, The History of Barrett Canyon. Print.

Harrison, R.B., Johnson, D.W., and Todd, D.E., 1989, Sulfate Adsorption and Desorption Reversibility in a Variety of Forest Soils: Journal of Environment Quality, v. 18, p. 419, doi: 10.2134/jeq1989.00472425001800040004x.

Heaton, 2008, Comparison of Late Cretaceous Plutonic rocks across the San Antonio Canyon Fault, San Gabriel Mountains [Thesis]: Pomona, California Polytechnic University.

Hem, J.D., 1985, study and interpretation of the chemical characteristics of natural water: US Geological Survey water-supply paper 2254.

Hem, J.D., and Cropper, W.H., 1959, Survey of Ferrous-Ferric Chemical Equilibria and Redox Potentials: US Geological Survey water-supply paper 1459-A

Huntington, T.G., Hooper, R.P., and Aulenbach, B.T., 1994, Hydrologic processes controlling sulfate mobility in a small forested watershed: Water Resources Research, v. 30, p. 283–295, doi: 10.1029/93wr02950.

Edwards, P. J. (1998). Sulfur cycling, retention, and mobility in soils: A review. https://doi.org/10.2737/ne-gtr-250

Johnson, D., and Cole, D., 1977, Sulfate mobility in an outwash soil in Western Washington: Water, Air, and Soil Pollution, v. 7, p. 489-495, doi: 10.1007/bf00285547.

Kurashige, J.K., 2012, Water Quality of Natural Springs in San Antonio Canyon [Thesis]: Pomona, California Polytechnic University.

Lenhert, L., and Soto, P.M., et al., 2015, Discharge and Oxygen-Hydrogen Isotopic Characteristics of Fault Zone-Sourced Springs in Evey and Palmer Canyons, Eastern San Gabriel Mountains, California [Poster]: Pomona, California Polytechnic University.

Labotka D.M., 2016, A sulfate conundrum: Dissolved sulfates of deep-saline brines and carbonate-associated sulfates. v. 190, p. 53-71, https://doi.org/10.1016/j.gca.2016.06.033.

Lynch, J.A.; Corbett, E.S. 1989. Hydrologic control of sulfate mobility in a forested watershed. Water Resources Research. 25:1695-1703.

Mahood, T., The History of David Buel's East Fork Flume, San Gabriel Canyon: http://www.otherhand.org/home-page/archaeology/dave-buels-east-fork-flume-san-gabriel-canyon/the-history-of-david-buels-east-fork-flume-san-gabriel-canyon/ (accessed August 2019).

Mayer, B., Shanley, J., Bailey, S., and Mitchell, M., 2010, Identifying sources of stream water sulfate after a summer drought in the Sleepers River watershed (Vermont, USA) using hydrological, chemical, and isotopic techniques: Applied Geochemistry, v. 25, p. 747–754, doi: 10.1016/j.apgeochem.2010.02.007.

Miao Z., et al., 2012, Sulfate Reduction in Groundwater: Characterization and Applications for Remediation: Environmental Geochemistry Health p. 359-550. doi: 10.1007/s10653-011-9423-1.

Miranda, D., 2018, Response of Streamflow and Spring Discharge from Precipitation Recharge Events In Icehouse Canyon Watershed, Eastern San Gabriel Mountains, California [Thesis]: Pomona, California Polytechnic University.

Missy, The East Fork Saga: http://angelesadventures.com/mines/ (accessed August 2019).

Morse J.W., Millero, F.J., CORNWELL, J.C., 1987, Rickard, D., The Chemistry of the Hydrogen Sulfide and Iron Sulfide Systems in Natural Waters: Earth-Science Reviews, v. 24, p. 1-42. doi: 10.1016/0012-8252(87)90046-8.

MPCA, 1999, Sulfate in Minnesota's Groundwater. https://www.pca.state.mn.us/sites/default/files/sulfate7.pdf (accessed July 2019).

Nourse, J.A., Acosta, R.G., Stahl, E.R., and Chuang, M.K., 1998, Basement geology of the 7.5 minute Mt. Baldy and Glendora quadrangles, San Gabriel Mountains, California, GSA Abstracts with Programs, v. 30, no. 5, p. 56.

Nourse, J.A., Carey, L.R., Bautz, M., Reilly, J., 2010, Hydrogeology of Icehouse Canyon, Contrasted with Upper San Antonio Watershed, San Gabriel Mountains, California, [Paper] Pomona, California Polytechnic University.

Nourse, J.A., 2002. Middle Miocene reconstruction of the central and eastern San Gabriel Mountains, southern California, with implications for evolution of the San Gabriel Fault and Los Angeles basin. Special Paper 365: Contributions to Crustal Evolution of the Southwestern United States: Vol. 365, No. 0 pp. 161–185

Nourse, J.A., 2013, Unpublished data.

Ober, J.A, 2002, Materials Flow of Sulfur, Reston, VA, U.S. Geological Survey Open-File Report 02-298.

Osborn, S.G., 2012, Unpublished data.

Parra, A., 2013, Eldoradoville: The Forgotten Boom Town of the San Gabriels: https://www.kcet.org/shows/departures/eldoradoville-the-forgotten-boom-town-of-the-san-gabriels (accessed August 2019).

Perez, S.L., 2015 A Gis Investigation of Paired Watersheds: Icehouse Canyon and Upper San Antonio Canyon, Eastern San Gabriel Mountains [Thesis]: Pomona, California Polytechnic University.

Rare Gold Nuggets, 2017, Gold Mining in the San Gabriel Mountains of California: http://raregoldnuggets.com/?p=4646 (accessed August 2019).

Santos E., Silva J., and Duarte H., 2016, Pyrite Oxidation Mechanism by Oxygen in Aqueous Medium: Journal of Physical Chemistry C, p. 2760-2768, https://doi.org/10.1021/acs.jpcc.5b10949.

Soto, P.M., 2015, Discharge and Geochemical Characteristics of Evey Canyon and Icehouse Canyon Springs, San Gabriel Mountains, During Extended Drought [Thesis]: Pomona, California Polytechnic University.

Soto, P.M., Lenhert, L., et al., 2015, Discharge and Geochemical Characteristics of Evey Canyon and Icehouse Canyon Springs, San Gabriel Mountains, During Extended Drought [Poster]: Pomona, California Polytechnic University.

Shannon1. (2019, March 29). *Santa Ana River*. Wikimedia Commons. Retrieved November 25, 2021, from https://commons.wikimedia.org/wiki/Category:Santa_Ana_River.

The Diggings, Map of mining claims in The United States, https://thediggings.com/usa/map (accessed August 2021).

USDA-NRCS Web Soil Survey, https://websoilsurvey.sc.egov.usda.gov/App/HomePage.htm.

USGS Water Data for USA, 2021, USGS water data for the nation, https://waterdata.usgs.gov/nwis (accessed December 2021).

Yaralian, D., 2017, Arsenic and Sulfate Contamination within Metamorphosed Units in the Lower San Antonio Canyon [Poster]: Pomona, California Polytechnic University.

WHO, 2004, Sulfate in Drinking-water: Background document for development of WHO Guidelines for Drinking-water Quality, p.1-6.

Wicks, L., 2014, Hydrogeologic and Geochemical Investigation of Robust Spring Discharge at Wingate Ranch, Eastern San Gabriel Mountains California [Thesis]: Pomona, California Polytechnic University.

Wire, N., 2021, Bulk Rock and Single-Crystal Geochemistry of Corundum-Bearing Rocks at Cascade Canyon, CA [Poster]: Pomona College.

Zylstra, S., 2017, Late Cretaceous Plutonic and Metamorphic Overprint of Proterozoic Metasediments of Ontario Ridge, Eastern San Gabriel Mountains, California [Thesis]: Pomona, California Polytechnic University.

APPENDICES

Appendix A: Method for using the Ion Chromatograph

Rules and Notes

- Samples **must not** have acid in them.
- Samples **must** be filtered.
- The suppressor **must** be kept wet, otherwise it will overload the machine.
- *If the valve is closed, the pressure will shoot up and overload the machine.
- Only run up to 10 samples at a time.
- Running 10 samples takes about 600 mL of eluent and about 6 hours (with 15 minutes per sample).
- Prepare each sample one at a time to avoid mistakes. Double check each before proceeding.

Preparations

- Ask sample owner(s) about rules 1 & 2 (clarify tape colors or other forms of identification).
- Make sure there is enough eluent to run the samples. The eluent is a sodium bicarb solution that helps keep ions from precipitating out. The bottle on the top is filled with about 2 Liters of eluent. Replace about once a week and make sure to prime the tubes after each eluent change (see **Eluent**).
- Standards are used to calibrate the IC and make sure it's running correctly. Get them out of the refrigerator and make sure there is enough to run the samples (see **Standards**).

- Open the IC program (Chromeleon 7) on the computer. For now, only the Data and Instrument tabs are needed. If disconnected (the little green button is dark green), click on the button (it will turn light green).
- Go to the Data tab. Save the old "recipe" as a new file. (File > Save As > Graduate Students > Full Name > Last Name + Date). The new file's status show read "idle" for all samples.

Starting up the IC

- *Running the pumps only:* no need to prime or open valves. Just click "on" and watch the pressure. It should show a nice continuous ramping up and level off at **1800 - 2000 psi**. If it gets erratic, shut it down.
- Priming must be done to clear the lines of air bubbles. The pumps are the two black knobs located near the bottom of the unit. *Open the **left** one by turning the knob a few turns. As needed, place some paper towel or a small beaker underneath to catch any stray leaks.
- Go to the Instrument tab. Click "prime" on the program. A warning will pop up, click ok. Wait 5-10 minutes. Pressure may fluctuate but should stay at 0. If it ramps up, check the valve to make sure it is open enough. If the pressure is still ramping up after doing so, **quickly shut it down** and notify the lab owner.
- **This step must be done in quick succession:** Click "off" in the program and close the valve on the unit.
- Turn pumps on using the program. Pressure should show a nice continuous ramping up and level off at **1800 - 2000 psi**. If it gets erratic, shut it down. If running normally, let run about 5 minutes.

- Type in **31 mA** under "suppressor" and turn it on. The suppressor filters out the noise, so the data can be easily seen. Units are µS, same as electrical conductivity (EC). The signal should go down to about **19-20 µS**.

Preparing the Samples

- Go to the Data tab. Insert or delete rows as needed and make sure the position numbers are sequential.
- *Loading the Cartridges (see figure below):* Place the cartridges on the table with the **dots to the right**. Always load the vials from right to left, but not in a snake pattern.

Filling the Cartridges

					Slot 19: Mid Std	●
Slot 18: Blank	Slot 17: Sample 10	Slot 16: Sample 9	Slot 15: Sample 8	Slot 14: Sample 7	Slot 13: Sample 6	●
Slot 12: Mid Std	Slot 11: Blank	Slot 10: Sample 5	Slot 9: Sample 4	Slot 8: Sample 3	Slot 7: Sample 2	●
Slot 6: Sample 1	Slot 5: Blank	Slot 4: High Std	Slot 3: Mid Std	Slot 2: Low Std	Slot 1: Blank	●

- *Filling the Vials (see figure below)*: Each vial has a faint fill line. Marking a small dot on the fill line will make this task easier. Fill with the required liquid (sample, standard, or blank). For better control when pouring, extend your middle and ring fingers and rest the bottle against them. Take care to fill **just to the dot or slightly below**, but not above. After it is filled, place a stopper, white dot downwards, onto the vial and push down with finger to secure. Use the little cylindrical tool to align it and make it flush with the vial (use one end to align and the other end to make flush).

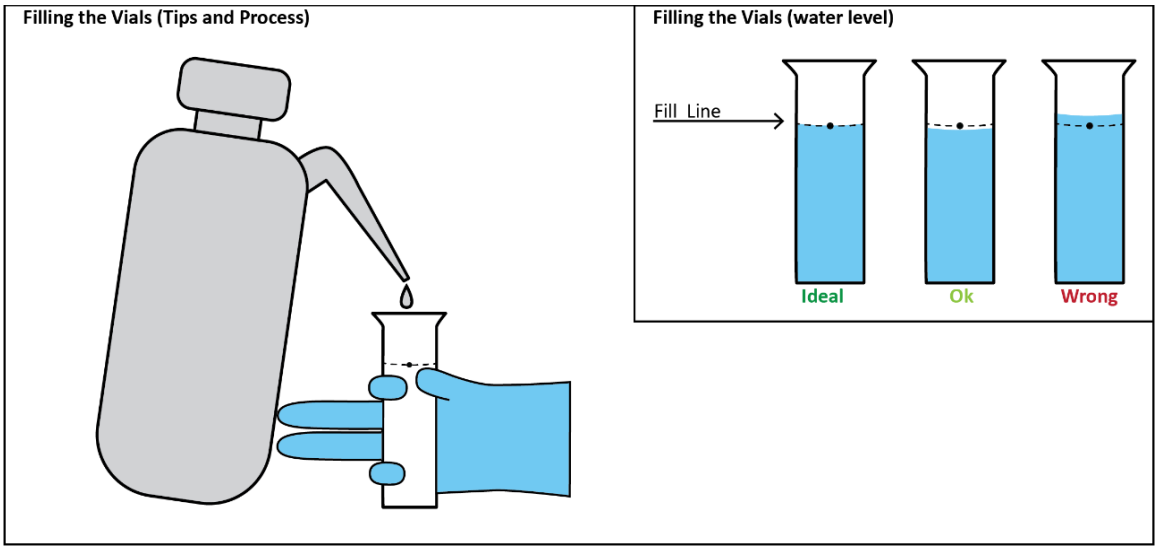

- Close up the used bottle and set aside. Place vial in the cartridge and check the program to make sure it is in the correct position and has the correct name (sample ID/blank/std).
- *Checking the standard values:* Click on the tab for observing the standards. Make sure the high/mid/low concentration values for the standards are correct. Refer to the standards logbook you created. This can be done now or after the run.

Running the Samples

- Place the cartridges into the auto-loader. **Do not change the order of the cartridges**. Just pick up and move as a whole. The auto-loader has a little conveyer belt that brings the samples to the machine. Place the cartridges so the ridges are on the same side as the conveyer belt.

- Click “Start” on the program and then “ok”. Wait for the first 5 samples to be tested (standards and blanks) to make sure the instrument is running properly. Check the process method screen (File > Open > process method) to make sure that the standards follow a straight line and the R^2 values are 0.99.
- A peak should show when an ion is detected. If a peak is detected before/after the program expects an ion to show up, then the computer cannot assign it a name. If you are confident in what the peak is, then you can make it name the peak.
- If more samples need to be run, go back to Data tab, and save the old “recipe” as a new file, but skip priming.
- If all samples are completed for the day, shut the machine down. These **MUST BE TURNED OFF IN ORDER**. Suppressor > pump > tower/console. Keep autosampler on.
- Save the data. File/logo > Export > Excel > IC Results > grad thesis (or whatever applies) > ok. Plug in the USB and the save to it.

Appendix B: Method for creating eluent for the Ion Chromatograph

- Remove cap of eluent container. To avoid contamination, make sure the little tip of the hose does not touch anything. Dispose of old eluent solution into the sink.
- Add 10 mL of bicarbonate solution (Dionex AS22 Eluent Concentrate) to a clean 1.0 L Erlenmeyer flask. Fill to the I L mark with Milli-W water.
- Pour new eluent into the container. If making more than 1 L, repeat step 2 and pour in the second liter. Close the lid.
- Go to the Instrument tab and input the correct volume of eluent added (ex: 1.000 for 1,000 mL).

Appendix C: Method for making standards for the Ion Chromatograph

- The standards are made by weight and include known concentrations. Clean and label the three standard bottles with High/Mid/Low Standard, the creator's name or initials, and the date it was made.
- Create a new table in the logbook. Follow previous layout. See below.

Ion	Ideal ppm (g/mL)	Ideal Wt (g)	Actual Wt (g)	High Std (g/mL)	Mid Std (g/mL)	Low Std (g/mL)
F	20	2				
Cl	100	10				
Br	20	2				
NO3	50	5				
SO4	100	10				
MQ	710	71		-	-	-
Total	-	-		Wt (wo lid)	Wt (wo lid)	Wt (wo lid)

- Take the standard sources out of the fridge and set them, with the standard bottles, next to the scale. Weigh the bottles without the lids. Record weight. Place the high standard bottle on the scale and tare.
- To determine how much of each standard source to add, refer to the ideal weight (since the standards are mostly water, volume and weight are 1:1). Add that volume to the standard bottle, using the pipettes. Record the number in the actual weight column. Tare after each addition.
    - Using the Pipettes (Eppendorf Research Plus): Turn the dial to the correct volume (go to the next 0.010, ex: 2.010). Put a new tip (tapered plastic cap) on it. Push in button to the first click. Insert the pipette into the standard source bottle. Slowly release the button. Without tilting the pipette, position it over the high standard bottle. Push to the first click

until all the liquid is out, then push button all the way. Release the button. If finished with the source, throw away the pipette tip.

- Close the bottle and invert a few times to allow solutions to mix. Calculate the total actual weight (sum of actual weight column).
- Calculate the high standard concentration using the formula below.

$$\text{High Standard} = \frac{(\text{Actual Weight}) \times (\text{Concentration of source Std})}{\text{Total Actual Weight}} \times 1000$$

- For mid and low standards, add in the appropriate volumes of high standard. Always dilute high to medium, then high to low. **never** medium to low. Record all values. Mid Standard is **1:5** ratio, so measure out **20 g** of high standard and add **80 g** of water. Low Standard is **1:150** ratio, so measure out **0.660** g of high standard and add **99 g** of water.
- Calculate the Dilution Factor and determine the concentrations of mid and low standards using the formulas below.

$$\text{Dilution Factor} = \frac{\text{High standard added}}{\text{Total volume (high standard added + MQ added)}}$$

$$\text{Concentration of Standard (Mid and Low)} = \text{High Standard Conc.} \times \text{Dilution Factor}$$

Appendix D: Method for making rock pellets for the XRF

Crushing the rock

- Unfold the C-fold plywood and set it up.
- Lay out a piece of butcher paper on the floor. Lay down the rubber mat, then another sheet of paper. Make sure the iron plate is clean (no white specks) before putting it on top.
- Take the mallet and make sure it is clean as well. Put on safety glasses and earmuffs.
- Crush the sample to about 0.5 cm pieces. Tare a weighing boat on the microbalance and put crushed pieces in the weighing boat. Record the weight.
- Dry out the sample in the oven overnight (75°C) in a glass beaker or thick sample bag, **not the weighing boats**. If the temperature is increased to 175°C, use a glass beaker and put a note to display the temperature change.

Cleaning up the rock crushing station

- Tilt the plate so the sample rolls onto the paper. Throw out the paper with the sample and get a new piece of paper.
- Clean the metal plate. Use the green power brush, vacuum with the shop vac, and wipe it down with isopropyl alcohol until the paper towel comes off light gray rather than black. If more samples need to be crushed, replace the iron plate.
- Clean the mallet. Put the wire brush on the floor and hold it with foot. Hold the mallet about 6 inches from the head to avoid injury from the metal brush. Wipe the mallet across the brush for about 30 seconds. Check to see that there is no more white dust. Wipe with isopropyl alcohol until clean.

- Rinse off the mat in the sink with water and put on the drying rack. Fold up the plywood and put away. Sweep up the area using the broom and dustpan. Use the shop vac to clean the area.

Milling the sample

- Get the mill out of the cupboard in the next room. It is expensive, so **be careful**. The two little balls inside (as well as the container itself) are delicate and cannot survive a fall to the ground. The threads are aluminum and can be cross threaded easily.
- Pour in enough crushed sample to cover the balls, but no more than halfway full. Close the mill to just **finger tight**, but not too hard.
- Put the mill in the shaker. Screw it in and wiggle it around a bit to make sure it is secured. Tighten the little metal lever **as tight as possible**. The little muddler/wood stick can be used to assist in this.
- Put the dial for 30 mins and push the white button. Set a timer since the dial itself does not count down. If there is a problem and you need to turn it off, turn off the power strip button.

Making the pellet mixture

- Place a sheet of printer paper on the table and place a piece of weighing paper on top. Take the mill out of the shaker. Screw off the lid and dump out the milled sample onto the weighing paper. **Watch for the little balls.** Be prepared to catch them if they roll away. If the balls are in the sample pile, remove the little balls with the fingers and place them on a weighing boat. Tap the mill on the weighing paper to get out any stuck dust. Place the mill on the corner of the printer paper.

- Locate the cellulose, which is used as a binder. The ratio must be precise and round to exactly **6.00 g of sample and 1.20 g of cellulose**! Tare a weighing boat on the microbalance. Use a little weighing paper to scoop the sample into the boat. Add cellulose using a little scoop (one can be made from a dropper in a pinch).
- Wipe out the mill using a paper towel to remove the residual dust. Wipe out under the gasket as well. Put onto a clean paper.
- Add the sample and cellulose mixture back into the mill, but without the balls. Place it into the shaker for 3 minutes.

Cleaning the mill

- Unscrew both sides off and wipe off with paper towel. Clean using isopropyl alcohol. If needed, you can blast the inside of the lid a bit to clean off the dust. Rinse the gasket with water. Blow it off with air gun from the lab.
- If it is still gunky, reassemble and pour in some sand, put it into the shaker for 10 minutes, and clean out again. **Do not blow off the balls**. Reassemble and put back away.

Making the pellets

- Place a sheet of printer paper next to the press to set up the die. Take out all the components and place them on the paper.
- Locate the base and put the sleeve on top of it. **Make sure they are correctly lined up** and check throughout the process that they stay this way.
- Place in one of the two small discs, shiny side towards sample. Place in a sample cup from drawer, open side up. Set in the funnel. Dump out sample onto a

weighing paper and pour it into the funnel. Gently put the plunger in (to avoid dust) and gently press down a bit.

- Lift (using a back-and-forth twisting motion) both the plunger and the funnel. Place the second small disc in, shiny side towards the sample. Place in the large cylinder, **beveled side down**.
- Make sure the top part on the press is high enough, unscrew on the top to adjust. Hold the die by the base and place it into the press. It will be heavy, so be careful. Center it in the press. Turn the top crank until it touches the top of the die. Double-check it centering.
- Tighten the little black knob on the side to finger tight. Crank the large handle in short fast rhythm until 15 tons is reached. Wait for 1 minute. If the pressure falls, crank a little to get the pressure back up. Loosen the black knob (if not, pressurized oil will go all over the place).
- Pick the sleeve up from the base and place it on the printer paper. This must be done quickly since the little disc will fall out about 5 seconds after.
- The pellet will often be stuck inside, so the press will have to be used again to get it out. Place a piece of weighing paper in the press and place the sleeve on top and centered. Repeat the press procedure. Press until the sample becomes unstuck.
- Press on the center of the die with the thumb so all the parts come up as one. Take the sleeve up over the sample and put it on the printer paper with the base.
- Take out the pellet **touching only the sides**, and gently clean the dust off the pellet. The sample container has grooves, which can be cleaned with the

fingernails, but the top is cleaned by folding a kimwipe a bit and gently brushing off the top.

- Write the sample name on the bottom with a sharpie/marker and store in a dry, airtight container, like a Tupperware.

Cleaning the Die and Press

- Clean all the pieces using isopropyl alcohol and a paper towel. If black residue comes off, repeat until light gray.
- Once clean, do not place them back on the dirty printer paper. Put them in their glass storage container.
- Wipe down the press handle and working space.

Appendix E: Raw Anion Data of Water Samples

Sample ID	pH	Alkalinity	F	Cl	NO3	Br	SO4
Site ID-Date-Sample#		*mg/L*	*mg/L*	*mg/L*	*mg/L*	*mg/L*	*mg/L*
BC1-010519-24	7.35	111.5005	0.3879	0.9527	0.0646	0.0782	49.6592
BC1-011819-29	7.42	76.1940	0.3541	1.3458	1.2174	0.0962	45.3263
BC1-020119-34	7.75	99.3882	0.4051	1.1928	0.2020	0.0865	49.8696
BC1-022319-41	7.32	83.6754	0.3066	1.2279	0.7122	0.0170	35.8428
BC1-031619-48	8.06	84.5052	0.3049	1.1817	0.5733	0.0500	35.1453
BC1-040819-54	7.28	91.0805	0.3936	1.3647	0.5657	0.0767	42.6641
BC1-050319-64	8.12	99.3366	0.3208	0.9959	0.2694	0.1958	39.8723
BC1-052419-70	8.12	115.0471	0.3353	0.9231	0.3355	0.0201	39.2585
BC1-060719-74	7.91	102.7551	0.3745	1.0328	0.5818	0.1028	41.6712
BC1-071419-83	8.02	108.9121	0.4286	1.1832	0.2660	0.2473	48.7678
BC1-080819-89	8.00	111.5338	0.3979	1.1662	0.2059	0.0430	51.3367
BC1-082919-95	8.01	99.4995	0.4067	1.0675	0.1774	0.2052	50.3364
BC1-112418-08	8.02	111.1304	0.4072	0.9285	0.0578	0.1942	50.9739
BC1-113018-15	7.67	174.7869	0.3304	0.9551	0.1516	0.0336	53.5263
BC1-122218-19	7.70	110.6986	0.3299	0.8552	0.3343	0.0088	44.7489
BC2-010519-25	8.05	123.5265	0.4317	1.0077	0.7623	0.2043	89.2660
BC2-011819-30	7.60	69.6339	0.3459	1.3494	1.8669	0.2227	164.1298
BC2-020119-35	8.24	115.7611	0.4186	1.4069	2.1366	0.0725	158.4101
BC2-022319-42	8.18	103.3303	0.3929	1.4415	1.2794	0.0877	145.5052
BC2-031619-49	7.49	107.3671	0.4685	1.6008	1.2190	0.0399	161.5088
BC2-040819-53	8.39	114.3661	0.5147	1.5474	0.9413	0.0190	129.7280
BC2-050319-65	8.38	111.9867	0.3679	1.0749	0.5485	0.1428	103.0570
BC2-052419-69	8.23	112.7261	0.4466	1.2052	0.7473	0.0415	121.1449
BC2-060719-73	8.32	112.3413	0.3923	1.1572	0.5194	0.0409	110.5734
BC2-071419-82	8.34	114.4859	0.5223	1.2451	0.7110	0.0432	109.0888
BC2-080819-88	8.37	115.1090	0.5011	1.3533	0.5410	0.0936	100.1622
BC2-082919-94	8.32	117.9615	0.5181	1.1980	0.7481	0.3755	89.8603
BC2-112418-09	7.56	148.8361	0.5179	1.0617	0.3631	0.0845	86.6585
BC2-113018-16	7.32	158.0451	0.3832	1.0481	1.1284	0.0735	106.4352
BC2-122218-20	7.40	125.5417	0.3979	0.9622	0.4533	0.0543	88.5969
CC1-050319-60	8.12	180.5404	0.6493	2.6311	0.1571	0.0587	503.7215
CC1-052419-67	8.30	188.3427	0.8422	2.9404	0.9905	0.0445	548.1989
CC1-060719-77	8.23	190.2313	0.6565	2.3077	0.3772	0.1128	463.3979
CC1-062419-80	8.23	207.3109	0.7089	2.4332	0.0596	0.0714	505.7134
CC1-071419-86	8.06	225.6906	0.8641	3.3521	0.1347	0.0428	662.0206
CC3-011819-31	7.28	92.8604	0.3720	1.6256	0.6696	0.0235	229.9939
CC3-020119-38	7.37	132.2367	0.4918	2.0395	0.1866	0.0586	360.1024
CC3-022319-43	7.68	130.6070	0.4657	2.7776	0.3787	0.0534	430.0687
CC3-031619-50	8.28	143.1818	0.4069	2.2221	0.0075	0.2257	375.5292
CC3-041919-57	8.18	173.1819	0.5989	3.1221	0.3299	0.0100	615.2385
CC3-052419-68	8.09	186.4392	0.6284	2.8959	1.3228	0.0695	526.5611
CC3-060719-71	8.01	183.8490	0.4800	2.1503	0.2589	0.0730	484.9037
CC4-020119-36	7.76	137.4453	0.4242	2.4468	0.1867	0.0699	369.9948
CC4-020119-37	7.95	129.3299	0.4329	2.1226	0.2568	0.0336	365.5425
CC4-041919-56	8.01	178.9037	0.6449	2.9781	0.2380	0.0619	597.6138
CC4-060719-72	8.10	181.4920	0.4991	2.3884	0.1282	0.0255	550.8704
CC4-071419-81	8.00	219.9413	0.4932	2.4787	0.7966	0.0660	614.4784

Sample ID	**pH**	**Alkalinity**	**F**	**Cl**	**NO3**	**Br**	**SO4**
Site ID-Date-Sample#		*mg/L*	*mg/L*	*mg/L*	*mg/L*	*mg/L*	*mg/L*
CC4-080819-87	7.88	248.2977	0.6384	3.5822	5.3712	0.0799	836.2271
CC4-082919-93	7.70	269.5629	0.5598	3.2313	0.0432	0.0222	797.9916
CC4-122218-21	7.75	178.9713	0.5384	2.5557	0.2206	0.0700	494.7740
CC5-041919-55	8.01	168.0991	0.4733	2.2015	0.6750	0.1045	492.2830
EC1-010419-19	8.19	218.2512	1.6197	8.7684	0.0477	0.0368	47.7235
EC1-021919-30	8.30	223.3607	1.5637	10.4762	2.1773	0.1015	58.2840
EC1-031419-36	8.34	227.5886	1.5410	9.0541	2.6852	0.0903	49.2252
EC1-041119-43	8.39	219.7492	1.5733	7.9566	1.1509	0.1469	42.7181
EC1-050219-49	8.32	238.8663	1.5885	7.8379	0.7694	0.1585	41.9407
EC1-053019-55	8.27	225.6157	1.5054	7.6240	1.0980	0.1445	40.6807
EC1-061619-61	8.34	213.5976	1.8112	8.3446	1.1932	0.1204	44.8667
EC1-063019-67	8.26	228.3169	1.7987	8.5588	2.5832	0.1191	46.6131
EC1-071319-73	8.35	226.0954	1.6856	7.7884	0.0725	0.1702	42.0710
EC1-081119-79	8.16	212.9985	1.7344	7.4238	0.7917	0.0528	40.6617
EC1-082619-85	8.28	224.3913	1.3739	5.9487	0.4920	0.1509	32.8026
EC1-110918-01	6.61	236.1035	1.7060	6.1993	0.3784	0.1888	35.1946
EC1-121918-14	8.10	241.2925	1.7335	8.9605	0.1126	0.0183	54.7108
EC2-010419-20	8.10	218.4554	1.5534	6.4607	0.5335	0.1963	38.3387
EC2-012519-25	8.16	231.4228	1.5676	9.1545	0.8612	0.1277	50.9823
EC2-021919-31	8.35	223.5587	1.5654	8.6988	2.7423	0.0969	40.0468
EC2-031419-37	8.35	224.7792	1.5165	7.0028	5.0930	0.1229	34.0570
EC2-041119-44	8.34	228.7658	1.4761	6.4354	2.4153	0.1281	32.0038
EC2-050219-50	8.21	199.3573	1.5314	6.1592	1.7596	0.0787	31.4811
EC2-053019-56	8.25	209.3702	1.4624	6.7302	1.8899	0.2179	32.3200
EC2-061619-62	8.22	213.4558	1.7754	7.3336	1.9162	0.2604	37.1550
EC2-063019-68	8.18	212.2717	1.8401	7.5473	4.9206	0.0872	38.7623
EC2-071319-74	8.14	210.2473	1.7137	7.0748	3.1832	0.3451	35.8705
EC2-081119-80	8.30	221.0362	1.6013	5.9608	1.6835	0.0253	33.6922
EC2-082619-86	8.04	214.0539	1.3896	5.3062	1.5081	0.1562	30.0206
EC2-110918-02	7.44	252.0434	1.8618	7.9219	0.0554	0.0436	45.1666
EC2-121918-15	8.02	224.4646	1.6219	6.9205	0.5396	0.1381	40.9782
IC-041919-58	7.88	109.4112	0.1726	0.7388	0.4823	0.1886	11.9434
IC-050319-63	8.30	103.0706	0.2259	0.9432	0.5627	0.1079	12.6021
IC-082919-92	8.25	93.2716	0.2191	0.7569	0.2310	0.0894	15.0470
MB-010519-23	7.52	151.2195	0.4337	1.2602	0.2409	0.0669	77.7646
MB-110918-03	7.41	192.7751	0.4463	1.3676	0.2099	0.1029	58.0193
MB-112418-06	8.01	146.0845	0.3993	1.6247	1.4357	0.0640	74.5559
MB-113018-14	7.46	150.9226	0.3348	1.4611	1.4679	0.0381	72.2767
MB-122218-17	8.24	138.5287	0.3279	1.0504	0.1832	0.0309	64.0615
MB1-041119-42	8.40	147.6828	0.3073	1.5620	2.8945	0.0725	25.9816
MB1-050219-48	8.39	146.0432	0.3423	1.5820	0.8590	0.1791	29.5225
MB1-053019-54	8.39	145.0688	0.3441	1.9507	1.9122	0.1623	34.5006
MB1-061619-60	8.36	159.5303	0.3471	1.5997	0.8959	0.0767	31.8523
MB1-063019-66	8.36	167.2481	0.3970	1.7434	0.8697	0.2341	37.9580
MB1-071319-72	8.38	136.9929	0.3242	1.3769	1.3215	0.1015	23.2841
MB1-081119-78	8.43	179.6751	0.4461	1.8245	1.1005	0.2683	27.2496
MB1-082619-84	8.29	185.4415	0.4483	1.8975	0.8529	0.1408	27.0719
MB2-010419-16	8.00	155.0079	0.3843	1.3136	0.3147	0.0674	69.9143
MB2-012519-21	8.42	175.4188	0.3117	1.4809	1.9502	0.0402	37.1263

Sample ID	pH	Alkalinity	F	Cl	NO3	Br	SO4
Site ID-Date-Sample#		*mg/L*	*mg/L*	*mg/L*	*mg/L*	*mg/L*	*mg/L*
MB2-021919-26	8.40	167.9122	0.2460	1.5882	2.0640	0.0686	25.3284
MB2-031419-32	8.48	179.7189	0.2575	11.2488	1.8703	0.3172	26.1877
MB2-041119-38	8.46	138.5266	0.3168	1.5820	1.0531	0.1107	29.3188
MB2-050219-45	8.41	173.7441	0.3020	1.4065	1.0863	0.1384	32.5093
MB2-053019-51	8.37	174.6036	0.3287	2.1194	1.5769	0.1316	38.6233
MB2-061619-57	8.35	150.9899	0.3273	1.3100	0.7826	0.0463	35.7690
MB2-063019-63	8.30	147.8707	0.3223	1.2515	2.9719	0.0971	42.2158
MB2-071319-69	8.25	151.2119	0.3932	1.3756	0.7100	0.0828	44.9656
MB2-081119-75	8.24	155.8653	0.3328	1.8286	1.1049	0.0975	37.5096
MB2-082619-81	8.17	159.6381	0.3584	1.3462	0.6547	0.0545	37.7361
MB2-113018-11	7.30	169.0487	0.3287	1.6575	1.3501	n.a	75.4008
MB3-011819-26	8.45	199.4943	0.4363	3.6894	4.6744	0.0651	28.5508
MB3-021919-27	8.59	204.8277	0.3866	3.6946	2.8673	0.1571	23.5306
MB3-031419-33	8.62	212.2139	0.4275	3.6377	2.5056	0.1025	24.7411
MB3-031619-44	8.67	220.2712	0.3618	3.2750	2.9360	0.1270	22.2429
MB3-041119-39	8.59	236.3392	0.4450	3.7661	11.9926	0.0382	30.7850
MB4-010419-17	7.84	179.4094	0.3698	1.4698	0.7683	0.1256	30.8708
MB4-012519-22	7.61	194.4950	0.3596	1.8694	1.1804	0.0573	32.7046
MB4-021919-28	7.53	187.2746	0.3927	2.0626	2.4498	0.0762	27.6078
MB4-031419-34	8.00	189.5436	0.4349	1.9068	2.0487	0.0833	27.1358
MB4-041119-40	7.52	186.3600	0.4646	1.9206	2.2040	0.0774	28.6926
MB4-050219-46	7.55	184.9514	0.4453	1.8583	1.8696	0.0646	28.7368
MB4-053019-52	7.69	192.2581	0.3806	2.0934	1.5395	0.1162	26.7961
MB4-061619-58	7.68	185.0087	0.3890	1.7958	1.4574	0.1951	26.4295
MB4-063019-64	7.73	187.0467	0.4072	1.8712	1.2031	0.1169	27.2226
MB4-071319-70	7.51	185.5058	0.3602	1.9807	1.7225	0.0512	24.4158
MB4-081119-76	7.62	156.7688	0.4160	1.5948	1.6269	0.1596	24.7509
MB4-082619-82	7.51	181.2345	0.3786	1.6632	1.1225	0.0289	25.5135
MB4-112418-04	7.57	216.1237	0.4043	1.5369	0.9548	0.0190	30.7507
MB4-113018-12	7.22	189.7433	0.3491	1.5350	2.2820	0.0473	29.4504
MB4a-031619-45	7.44	136.4381	0.3656	4.3303	34.9378	0.1150	16.6523
MB5-010419-18	8.28	146.9505	0.4005	1.1476	0.1102	0.0379	73.4198
MB5-011819-27	7.77	133.4929	0.3726	1.4054	3.1117	0.0821	50.2587
MB5-012519-23	8.45	152.8459	0.2788	1.4554	1.8320	0.1050	27.3332
MB5-020119-32	8.37	153.9711	0.2908	1.3734	3.0540	0.0277	27.7322
MB5-021919-29	8.45	148.6481	0.2283	1.6335	2.1441	0.1716	21.3713
MB5-022319-39	8.28	121.6744	0.2356	1.5982	2.2027	0.0371	23.0520
MB5-031419-35	8.66	148.4749	0.2710	1.7391	1.8640	0.0503	22.0688
MB5-031619-46	8.43	147.9670	0.2064	1.3050	1.6925	0.0594	18.9577
MB5-040819-51	8.48	149.7407	0.2122	1.2118	1.1763	0.0800	23.3913
MB5-041119-41	8.16	137.2752	0.2720	1.5387	2.0990	0.2210	24.3814
MB5-050219-47	8.43	135.2868	0.3042	1.2729	0.9956	0.1121	26.6386
MB5-050319-59	8.26	141.2339	0.2759	1.1259	1.1118	0.1052	25.2436
MB5-052419-66	8.20	136.0561	0.3107	1.2552	1.4513	0.0843	39.0819
MB5-053019-53	8.12	134.9404	0.3285	1.9030	2.5446	0.3346	36.6727
MB5-060719-76	8.42	141.5835	0.2846	1.3017	1.8307	0.0900	32.4416
MB5-061619-59	8.23	143.9488	0.3524	1.3238	4.1030	0.0559	34.8849
MB5-062419-79	8.36	141.8947	0.2718	1.0882	0.6934	0.0318	31.7022

Sample ID	pH	Alkalinity	F	Cl	NO3	Br	SO4
Site ID-Date-Sample#		*mg/L*	*mg/L*	*mg/L*	*mg/L*	*mg/L*	*mg/L*
MB5-063019-65	8.30	137.9079	0.3736	1.4006	1.1123	0.1675	47.3283
MB5-071319-71	8.35	137.3949	0.3555	1.6962	20.8600	n.a.	42.8374
MB5-071419-85	8.41	139.3546	0.3106	1.2773	0.6544	0.0400	38.0584
MB5-080819-91	8.49	109.9801	0.3554	1.1380	0.6321	0.2807	36.8335
MB5-081119-77	7.90	138.8140	0.4411	1.3696	0.9961	0.4489	41.4359
MB5-082619-83	8.37	140.9043	0.4180	1.9506	2.8303	0.0242	49.0145
MB5-082919-97	8.44	140.6278	0.3154	1.1453	1.7965	0.1487	41.0605
MB5-121918-13	8.14	141.8727	0.3496	1.2485	0.4131	0.1842	78.0795
MB6-010519-22	7.60	201.4496	0.3605	1.3614	1.2851	0.0562	25.2058
MB6-011819-28	7.17	181.8770	0.2994	1.4279	1.5693	0.0754	24.3473
MB6-020119-33	7.64	186.1834	0.3314	1.5699	1.6387	0.0491	26.8523
MB6-022319-40	7.68	217.9571	0.3095	1.4860	3.2935	0.0346	20.9260
MB6-031619-47	7.35	166.3443	0.2765	1.4130	2.1504	0.0850	21.6775
MB6-040819-52	7.77	182.7749	0.2755	1.3264	2.1799	0.1576	21.0233
MB6-050319-61	7.79	183.9270	0.2648	1.9922	2.9965	0.1364	23.9714
MB6-060719-75	7.75	182.0383	0.2668	1.5854	2.1192	0.0479	22.3680
MB6-062419-78	7.60	183.7649	0.3084	1.4003	2.0240	0.0882	19.9557
MB6-071419-84	7.73	184.2584	0.3356	1.6269	1.9649	0.0630	20.6710
MB6-080819-90	7.62	174.8094	0.3575	1.7949	3.6293	0.1280	21.6334
MB6-082919-96	7.84	172.9863	0.3053	1.3961	1.6636	0.0579	19.8605
MB6-112418-07	7.80	241.7888	0.3320	2.7638	2.8045	0.0431	24.5486
MB6-113018-13	7.30	193.7872	0.2951	1.2454	1.0330	0.0384	24.0361
MB6-122218-18	7.57	235.1236	0.2725	1.1551	1.1709	0.0370	22.8890
SC-050319-62	8.09	250.1459	0.3940	3.7713	1.4620	0.0509	33.3173
SF1-112418-10	7.54	133.1499	0.4984	1.1354	0.7356	0.0747	88.2267

Appendix F: Raw Cation Data of Water Samples

Sample ID	Ca	Mg	Na	K	Sr	As
Site ID-Date-Sample#	*mg/L*	*mg/L*	*mg/L*	*mg/L*	*mg/L*	*mg/L*
BC2-010519-25	62.4510	26.1310	3.0290	1.6044	0.2444	0.0000
BC2-011819-30	55.0790	22.8490	5.1017	3.6319	0.2028	0.0000
BC2-020119-35	76.5510	28.5250	1.7980	1.4527	0.3057	0.0000
BC2-022319-42	68.2510	27.5880	0.4489	1.1487	0.2665	0.0000
BC2-031619-49	70.4640	29.1310	0.6261	1.3332	0.2867	0.0000
BC2-040819-53	68.5230	29.8930	0.7766	1.3332	0.2589	0.0000
BC2-050319-65	67.2850	26.7210	0.4831	1.1058	0.2615	0.0019
BC2-052419-69	66.1030	24.4520	1.5671	1.6361	0.2696	0.0000
BC2-060719-73	62.0780	27.7340	1.7831	1.6644	0.2565	0.0000
BC2-071419-82	62.9810	24.1480	4.4479	2.2094	0.3088	0.0000
BC2-080819-88	63.8760	24.1700	0.7712	1.2529	0.2535	0.0000
BC2-082919-94	63.7060	25.3210	0.9918	1.3721	0.2543	0.0000
BC2-112418-09	68.7380	24.2070	3.7383	1.9652	0.2355	0.0000
BC2-113018-16	70.8970	29.9540	5.2160	3.9380	0.2607	0.0000
BC2-122218-20	66.3160	26.9920	1.8734	1.6164	0.2561	0.0000
CC1-050319-60	116.1890	72.5180	26.5208	8.6016	0.8165	0.0000
CC1-052419-67	181.2160	79.3480	3.3840	3.6100	1.0059	0.0000
CC1-060719-77	121.0190	68.8340	28.5188	8.7485	0.8247	0.0000
CC1-062419-80	145.3180	70.7970	27.2990	7.9220	1.0355	0.0000
CC1-071419-86	209.1850	82.4320	19.0120	8.0720	1.1746	0.0000
CC3-011819-31	71.7460	38.6850	3.2970	3.5690	0.4591	0.0000
CC3-020119-38	96.3090	61.6160	13.7935	5.1996	0.6405	0.0000
CC3-022319-43	134.7090	63.3280	2.2600	2.8030	0.6051	0.0000
CC3-031619-50	115.0150	70.4850	24.7155	8.5090	1.2097	0.0000
CC3-041919-57	196.9750	77.0670	3.4130	3.5900	0.8570	0.0000
CC3-052419-68	137.6790	76.3290	27.5060	9.6460	0.6622	0.0000
CC3-060719-71	141.1700	63.4708	27.5580	8.9051	0.7830	0.0000
CC4-020119-36	91.3596	44.5530	1.5840	2.2008	0.6879	0.0000
CC4-020119-37	87.8955	43.3431	1.1852	1.8833	0.6426	0.0000
CC4-041919-56	99.6609	62.4094	26.0922	8.3632	0.7446	0.0000
CC4-060719-72	102.1977	60.3165	27.3453	8.8862	0.7783	0.0000
CC4-071419-81	131.4394	73.0737	8.1574	4.6813	1.1591	0.0000
CC4-080819-87	137.3809	81.3150	39.8994	11.5080	1.0794	0.0000
CC4-082919-93	166.9593	90.7891	8.8423	5.1681	1.4799	0.0000
CC4-122218-21	102.2841	53.9454	12.9869	5.3021	0.8566	0.0000
CC5-041919-55	96.6549	61.0389	25.2479	8.2061	0.7219	0.0000

Sample ID	B	Ba	Bi	Cd	Co	Cu
Site ID-Date-Sample#	*mg/L*	*mg/L*	*mg/L*	*mg/L*	*mg/L*	*mg/L*
BC2-010519-25	0.0383	0.0000	0.0303	0.0000	0.0000	0.0000
BC2-011819-30	0.0455	0.0000	0.0412	0.0000	0.0000	0.0000
BC2-020119-35	0.0371	0.0000	0.0264	0.0000	0.0000	0.0000
BC2-022319-42	0.0363	0.0000	0.0344	0.0000	0.0000	0.0000
BC2-031619-49	0.0369	0.0000	0.0296	0.0000	0.0000	0.0000
BC2-040819-53	0.0418	0.0000	0.0295	0.0000	0.0000	0.0000
BC2-050319-65	0.0378	0.0000	0.0334	0.0000	0.0000	0.0000
BC2-052419-69	0.0386	0.0000	0.0336	0.0000	0.0000	0.0000
BC2-060719-73	0.0441	0.0000	0.0335	0.0000	0.0000	0.0000
BC2-071419-82	0.0431	0.0567	0.0356	0.0000	0.0000	0.0000
BC2-080819-88	0.0379	0.0000	0.0314	0.0000	0.0000	0.0000
BC2-082919-94	0.0384	0.0000	0.0334	0.0000	0.0000	0.0000
BC2-112418-09	0.0422	0.0000	0.0277	0.0000	0.0000	0.0041
BC2-113018-16	0.0428	0.0000	0.0251	0.0000	0.0000	0.0000
BC2-122218-20	0.0383	0.0000	0.0315	0.0000	0.0000	0.0000
CC1-050319-60	0.0754	0.0281	0.0502	0.0000	0.0000	0.0000
CC1-052419-67	0.0535	0.0000	0.0389	0.0000	0.0000	0.0000
CC1-060719-77	0.0786	0.0218	0.0472	0.0000	0.0000	0.0000
CC1-062419-80	0.0749	0.0062	0.0355	0.0000	0.0000	0.0000
CC1-071419-86	0.0857	0.0121	0.0308	0.0000	0.0000	0.0000
CC3-011819-31	0.0418	0.0000	0.0275	0.0000	0.0000	0.0000
CC3-020119-38	0.0535	0.0000	0.0355	0.0000	0.0000	0.0000
CC3-022319-43	0.0423	0.0000	0.0357	0.0000	0.0000	0.0000
CC3-031619-50	0.1100	0.0266	0.0790	0.0000	0.0000	0.0000
CC3-041919-57	0.0522	0.0000	0.0455	0.0000	0.0000	0.0000
CC3-052419-68	0.0646	0.0040	0.0465	0.0000	0.0000	0.0000
CC3-060719-71	0.0716	0.0205	0.0423	0.0000	0.0000	0.0000
CC4-020119-36	0.0432	0.0000	0.0304	0.0000	0.0000	0.0000
CC4-020119-37	0.0444	0.0000	0.0316	0.0000	0.0000	0.0000
CC4-041919-56	0.0667	0.0230	0.0416	0.0000	0.0000	0.0000
CC4-060719-72	0.0717	0.0216	0.0420	0.0000	0.0000	0.0000
CC4-071419-81	0.0698	0.0000	0.0518	0.0000	0.0000	0.0000
CC4-080819-87	0.0815	0.0384	0.0402	0.0000	0.0000	0.0000
CC4-082919-93	0.0560	0.0000	0.0337	0.0000	0.0000	0.0000
CC4-122218-21	0.0548	0.0000	0.0296	0.0000	0.0000	0.0000
CC5-041919-55	0.0661	0.0216	0.0383	0.0000	0.0000	0.0000

Sample ID	Fe	Mn	Mo	Ni	Pb	Pd
Site ID-Date-Sample#	*mg/L*	*mg/L*	*mg/L*	*mg/L*	*mg/L*	*mg/L*
BC2-010519-25	0.0000	0.0000	0.0294	0.0000	0.0000	0.0040
BC2-011819-30	0.0302	0.0000	0.0304	0.0000	0.0000	0.0027
BC2-020119-35	0.0274	0.0000	0.0288	0.0000	0.0000	0.0039
BC2-022319-42	0.0193	0.0000	0.0276	0.0000	0.0000	0.0037
BC2-031619-49	0.0059	0.0000	0.0288	0.0000	0.0000	0.0035
BC2-040819-53	0.0022	0.0000	0.0306	0.0000	0.0000	0.0030
BC2-050319-65	0.0439	0.0000	0.0290	0.0000	0.0000	0.0052
BC2-052419-69	0.0516	0.0000	0.0285	0.0000	0.0000	0.0032
BC2-060719-73	0.0384	0.0000	0.0304	0.0000	0.0000	0.0045
BC2-071419-82	0.0433	0.0000	0.0305	0.0000	0.0000	0.0036
BC2-080819-88	0.0000	0.0000	0.0287	0.0000	0.0000	0.0037
BC2-082919-94	0.0018	0.0000	0.0287	0.0000	0.0000	0.0035
BC2-112418-09	0.0000	0.0000	0.0287	0.0000	0.0000	0.0025
BC2-113018-16	0.0000	0.0000	0.0299	0.0000	0.0000	0.0039
BC2-122218-20	0.0000	0.0000	0.0291	0.0000	0.0000	0.0038
CC1-050319-60	0.1602	0.0000	0.0295	0.0000	0.0000	0.0000
CC1-052419-67	0.0488	0.0000	0.0278	0.0000	0.0000	0.0022
CC1-060719-77	0.0270	0.0000	0.0288	0.0000	0.0000	0.0005
CC1-062419-80	0.0000	0.0000	0.0278	0.0000	0.0000	0.0012
CC1-071419-86	0.0000	0.0000	0.0289	0.0000	0.0000	0.0000
CC3-011819-31	0.0000	0.0000	0.0281	0.0000	0.0000	0.0024
CC3-020119-38	0.0083	0.0000	0.0284	0.0000	0.0000	0.0015
CC3-022319-43	0.0370	0.0000	0.0279	0.0000	0.0000	0.0027
CC3-031619-50	0.0303	0.0000	0.0571	0.0000	0.0000	0.0059
CC3-041919-57	0.0000	0.0000	0.0276	0.0000	0.0000	0.0026
CC3-052419-68	0.0000	0.0000	0.0429	0.0000	0.0000	0.0031
CC3-060719-71	0.0586	0.0000	0.0288	0.0000	0.0000	0.0000
CC4-020119-36	0.0263	0.0000	0.0282	0.0000	0.0000	0.0030
CC4-020119-37	0.1237	0.0000	0.0276	0.0000	0.0000	0.0038
CC4-041919-56	0.0319	0.0000	0.0282	0.0000	0.0000	0.0006
CC4-060719-72	0.0286	0.0000	0.0301	0.0000	0.0000	0.0025
CC4-071419-81	0.0000	0.0000	0.0320	0.0000	0.0000	0.0000
CC4-080819-87	0.0000	0.0000	0.0262	0.0000	0.0000	0.0019
CC4-082919-93	0.0085	0.0000	0.0286	0.0000	0.0000	0.0019
CC4-122218-21	0.0000	0.0000	0.0293	0.0000	0.0000	0.0028
CC5-041919-55	0.0017	0.0000	0.0286	0.0000	0.0000	0.0020

Sample ID	Rb	Si	Ti	V	W	Zn	Zr
Site ID-Date-Sample#	*mg/L*	*mg/L*	*mg/L*	*mg/L*	*mg/L*	*mg/L*	*mg/L*
BC2-010519-25	0.0000	9.5041	0.0235	0.0294	0.0692	0.0000	0.0289
BC2-011819-30	0.0000	10.2707	0.0246	0.0067	0.0300	0.0000	0.0349
BC2-020119-35	0.0000	10.4923	0.0244	0.0406	0.0735	0.0062	0.0284
BC2-022319-42	0.0000	10.5304	0.0237	0.0387	0.0669	0.0000	0.0279
BC2-031619-49	0.0000	11.2010	0.0234	0.0423	0.0714	0.0000	0.0284
BC2-040819-53	0.0000	10.1038	0.0237	0.0292	0.0677	0.0000	0.0294
BC2-050319-65	0.0000	10.4920	0.0256	0.0353	0.0705	0.0154	0.0280
BC2-052419-69	0.0000	10.3742	0.0249	0.0348	0.0703	0.0000	0.0287
BC2-060719-73	0.0000	10.3031	0.0261	0.0234	0.0576	0.0000	0.0308
BC2-071419-82	0.0000	9.9907	0.0242	0.0216	0.0608	0.0000	0.0313
BC2-080819-88	0.0000	10.4406	0.0235	0.0320	0.0704	0.0000	0.0279
BC2-082919-94	0.0000	10.6442	0.0238	0.0292	0.0693	0.0000	0.0280
BC2-112418-09	0.0000	9.5726	0.0233	0.0232	0.0646	0.0000	0.0304
BC2-113018-16	0.0000	9.5011	0.0231	0.0241	0.0608	0.0000	0.0313
BC2-122218-20	0.0000	9.8366	0.0233	0.0305	0.0700	0.0000	0.0288
CC1-050319-60	0.0000	15.2470	0.0306	0.0252	0.0299	0.0000	0.0394
CC1-052419-67	0.0000	16.6996	0.0233	0.0778	0.0700	0.0000	0.0302
CC1-060719-77	0.0000	16.6373	0.0252	0.0277	0.0233	0.0000	0.0391
CC1-062419-80	0.0000	16.5095	0.0221	0.0561	0.0590	0.0000	0.0350
CC1-071419-86	0.0000	17.9519	0.0221	0.0548	0.0568	0.0000	0.0353
CC3-011819-31	0.0000	12.1039	0.0229	0.0487	0.0707	0.0000	0.0288
CC3-020119-38	0.0000	12.7244	0.0236	0.0428	0.0562	0.0000	0.0336
CC3-022319-43	0.0000	13.3732	0.0239	0.0614	0.0718	0.0000	0.0297
CC3-031619-50	0.0000	27.7063	0.0478	0.0494	0.0693	0.0000	0.0728
CC3-041919-57	0.0000	14.9261	0.0219	0.0661	0.0679	0.0000	0.0311
CC3-052419-68	0.0000	14.8492	0.0223	0.0230	0.0325	0.0000	0.0385
CC3-060719-71	0.0000	16.2748	0.0264	0.0247	0.0284	0.0069	0.0391
CC4-020119-36	0.0000	14.4196	0.0236	0.0665	0.0698	0.0000	0.0293
CC4-020119-37	0.0000	13.9236	0.0267	0.0606	0.0669	0.0310	0.0294
CC4-041919-56	0.0000	15.5976	0.0243	0.0264	0.0292	0.0000	0.0392
CC4-060719-72	0.0000	15.7127	0.0248	0.0257	0.0296	0.0000	0.0392
CC4-071419-81	0.0000	17.8242	0.0216	0.0663	0.0676	0.0000	0.0339
CC4-080819-87	0.0000	18.9699	0.0219	0.0290	0.0272	0.0000	0.0404
CC4-082919-93	0.0000	20.0660	0.0211	0.0928	0.0721	0.0000	0.0317
CC4-122218-21	0.0000	14.1766	0.0221	0.0616	0.0638	0.0000	0.0331
CC5-041919-55	0.0000	15.2627	0.0230	0.0225	0.0301	0.0000	0.0389

Appendix G: Additional Figures

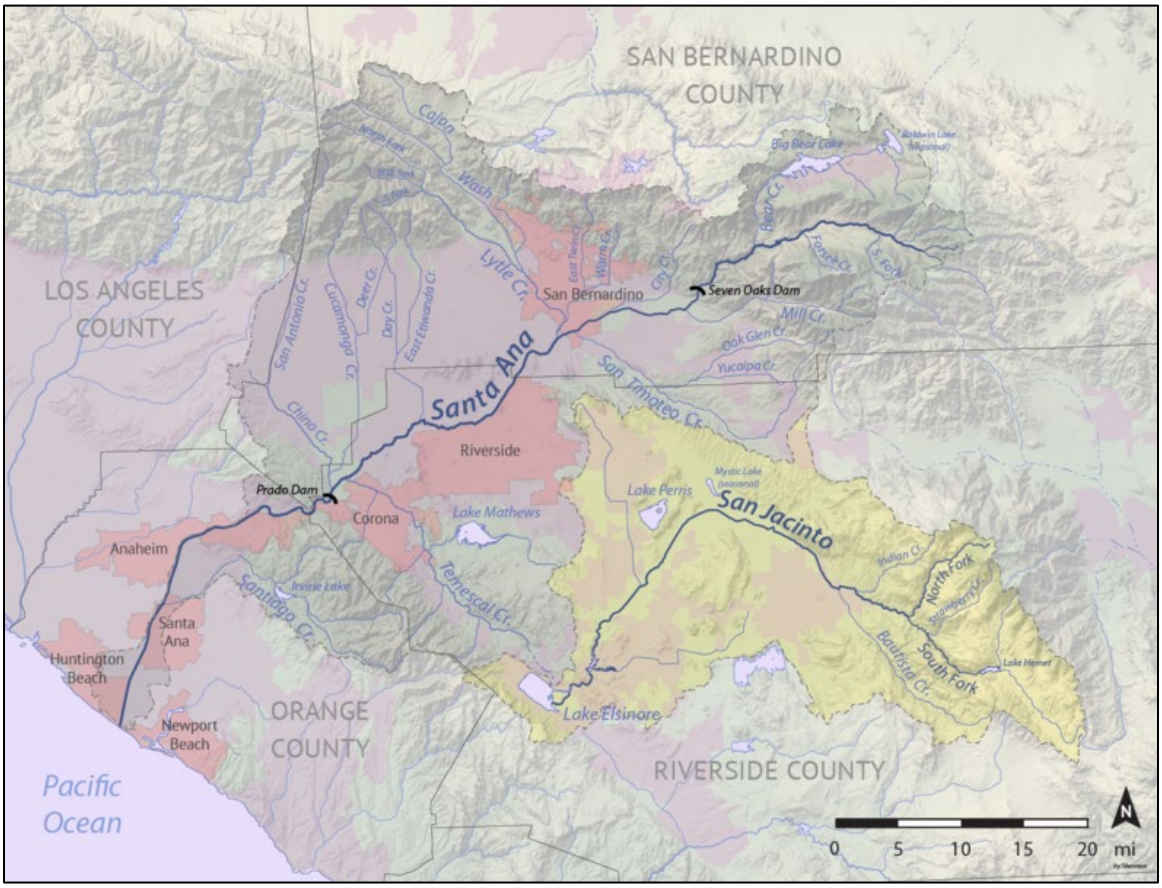

G1: *Santa Ana River Drainage Basin (Source: Wikipedia)*

G2: *Pictures of the water sampling process showing a-b) collecting the water sample, c) filling the sample bottles, d) recording the sample number and writing field notes, and e) taking measurements of the stream and recording the data.*